NASA/TM—2007-214409 ARL–TR–3878

Passive Endwall Treatments for Enhancing Stability

Michael D. Hathaway
U.S. Army Research Laboratory, Glenn Research Center, Cleveland, Ohio

July 2007

NASA STI Program . . . in Profile

Since its founding, NASA has been dedicated to the advancement of aeronautics and space science. The NASA Scientific and Technical Information (STI) program plays a key part in helping NASA maintain this important role.

The NASA STI Program operates under the auspices of the Agency Chief Information Officer. It collects, organizes, provides for archiving, and disseminates NASA's STI. The NASA STI program provides access to the NASA Aeronautics and Space Database and its public interface, the NASA Technical Reports Server, thus providing one of the largest collections of aeronautical and space science STI in the world. Results are published in both non-NASA channels and by NASA in the NASA STI Report Series, which includes the following report types:

- TECHNICAL PUBLICATION. Reports of completed research or a major significant phase of research that present the results of NASA programs and include extensive data or theoretical analysis. Includes compilations of significant scientific and technical data and information deemed to be of continuing reference value. NASA counterpart of peer-reviewed formal professional papers but has less stringent limitations on manuscript length and extent of graphic presentations.

- TECHNICAL MEMORANDUM. Scientific and technical findings that are preliminary or of specialized interest, e.g., quick release reports, working papers, and bibliographies that contain minimal annotation. Does not contain extensive analysis.

- CONTRACTOR REPORT. Scientific and technical findings by NASA-sponsored contractors and grantees.

- CONFERENCE PUBLICATION. Collected papers from scientific and technical conferences, symposia, seminars, or other meetings sponsored or cosponsored by NASA.

- SPECIAL PUBLICATION. Scientific, technical, or historical information from NASA programs, projects, and missions, often concerned with subjects having substantial public interest.

- TECHNICAL TRANSLATION. English-language translations of foreign scientific and technical material pertinent to NASA's mission.

Specialized services also include creating custom thesauri, building customized databases, organizing and publishing research results.

For more information about the NASA STI program, see the following:

- Access the NASA STI program home page at *http://www.sti.nasa.gov*

- E-mail your question via the Internet to *help@sti.nasa.gov*

- Fax your question to the NASA STI Help Desk at 301–621–0134

- Telephone the NASA STI Help Desk at 301–621–0390

- Write to:
  NASA STI Help Desk
  NASA Center for AeroSpace Information
  7121 Standard Drive
  Hanover, MD 21076–1320

NASA/TM—2007-214409 ARL–TR–3878

Passive Endwall Treatments for Enhancing Stability

Michael D. Hathaway
U.S. Army Research Laboratory, Glenn Research Center, Cleveland, Ohio

Prepared for
Advances in Axial Compressor Aerodynamics
sponsored by the von Karman Institute for Fluid Dynamics
Brussels, Belgium, May 15–18, 2006

National Aeronautics and
Space Administration

Glenn Research Center
Cleveland, Ohio 44135

July 2007

Acknowledgments

I am indebted to Dr. Anthony J. Strazisar, Chief Scientist at NASA Glenn Research Center, for the opportunity to prepare these notes and give a lecture at the von Karmon Institute. Dr. Strazisar was the principal driving force responsible for initiating, advocating, and technical leadership of the NASA Stall Control Program over the past decade. Much of the technical accomplishments on tip injection and recirculation stall control technologies reported in the Recent Advancements Section of these notes were due to his personal research contributions. Numerous other individuals either actively involved in various facets of or vicariously involved through many helpful discussions and interactions also contributed greatly to the successful accomplishments achieved under the NASA Stall Control Program. I would like to acknowledge their efforts including Drs. John Adamczyk, Kenneth L. Suder, Michelle Bright, Aamir Shabbir, Ed Greitzer, Choon Tan, Nicholas Cumptsy, Frank Marble, Pete Tramm, Zoltan Spakovszky, Harold Weigl, Ms. Sonia Ensenat, and no doubt others to whom I apologize for their unintended omission herein. I would also like to acknowledge Drs. Yuan Dong, Vinod Nangia, Nick Nolcheff, Milt Ortiz, and Aspi Wadia for providing information regarding the application of passive endwall treatments in production engines.

Level of Review: This material has been technically reviewed by technical management.

Available from

NASA Center for Aerospace Information
7121 Standard Drive
Hanover, MD 21076–1320

National Technical Information Service
5285 Port Royal Road
Springfield, VA 22161

Available electronically at http://gltrs.grc.nasa.gov

Passive Endwall Treatments for Enhancing Stability

Michael D. Hathaway
U.S. Army Research Laboratory
Glenn Research Center
Cleveland, Ohio 44135

1. Introduction

The operational envelope of gas turbine engines is constrained by the stability limit of the compression system for which there are grievous consequences if exceeded: Potential engine failure leading to possible loss of aircraft or crew. To avoid such failures, compressor designs must provide adequate stability (stall) margin to accommodate inlet distortions, degradation due to wear, throttle transients, and other factors that reduce compressor stability from the original design intent (fig. 1). Assuring adequate stall margin is a critically important design constraint that may require, among other options, increased solidity, number of stages, bleed flows, additional variable geometry stages, or possibly allowing the compressor operating line to fall below the maximum efficiency potential of the compression system.

The stability of compression systems has thus been a challenging problem for turbomachinery designers since the advent of the gas turbine engine, and successful management of such remains critical for achieving successful gas turbine engines. The stability limit is an inherent characteristic of compression systems, discussed in detail in the lecture notes of this series given by Dr. Ira Day. Suffice it to say herein, a compression system must impart sufficient energy to increase the momentum of the air as required to meet the static pressure rise demand, while at the same time assuring that there is sufficient momentum throughout to maintain the adverse pressure gradient that the compressor necessarily produces. Where low momentum fluid exists in the compression system there exists the potential for an unstable balance between the low momentum fluid, the shear forces, and the adverse pressure gradient. The areas of low momentum fluid typically associated with the viscous layers and leakage flows can be adversely impacted by the aerodynamic blockages produced from such. For typical well-designed modern compression systems the most critical region of low momentum fluid is located in the rotor tip clearance region, primarily associated with the tip leakage vortex. The lecture notes in this series of Professor Choon Tan provide an extensive overview of the flow features in the rotor endwall that limit the stability of tip critical rotors. Cumpsty (ref. 1) and Lakshiminaryana (ref. 2) also provide overviews of the flow physics in the tip region of axial compressors and the influence of such on the compressor stability limit, and cite numerous references on this subject.

Given the potential catastrophic consequences of compressor stall, there is considerable incentive for developing technologies that can extend the stable operating range of compressors without undue performance degradation. These lecture notes provide a fairly extensive overview of what's been learned from numerous investigations of various passive casing endwall technologies that have been proposed for alleviating the stall limiting physics associated with the compressor endwall flow field.

My personal comments or opinions are written in italicized text where given in the lecture notes.

2. Historical Overview

2.1 Infancy of Endwall Treatments—1950 Through Late 1960

Numerous passive casing endwall treatment technologies have been proposed almost from the outset of the first gas turbine engines. The earliest reported concept (ref. 3) for improving endwall flow conditions to enhance compressor stability while also addressing part speed operability was a 1950 patent filing by Geoffrey Wilde of Rolls Royce Limited which proposed aft stage bleeds that fed flow upstream of the IGV's to be injected along the casing ahead of the IGV's. The patent included provisions for

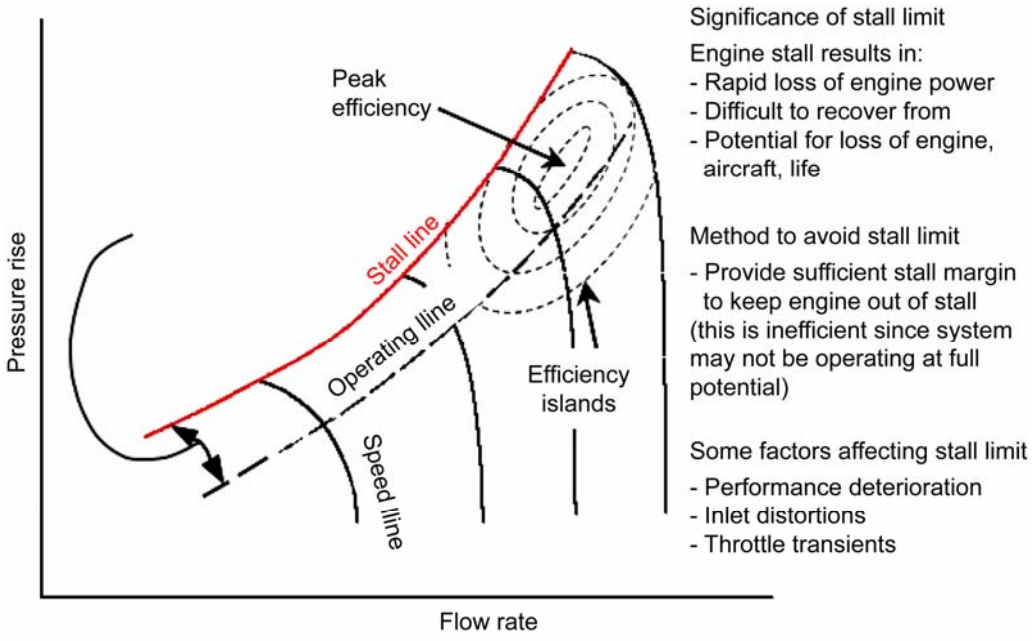

Figure 1.—Compressor stall concerns.

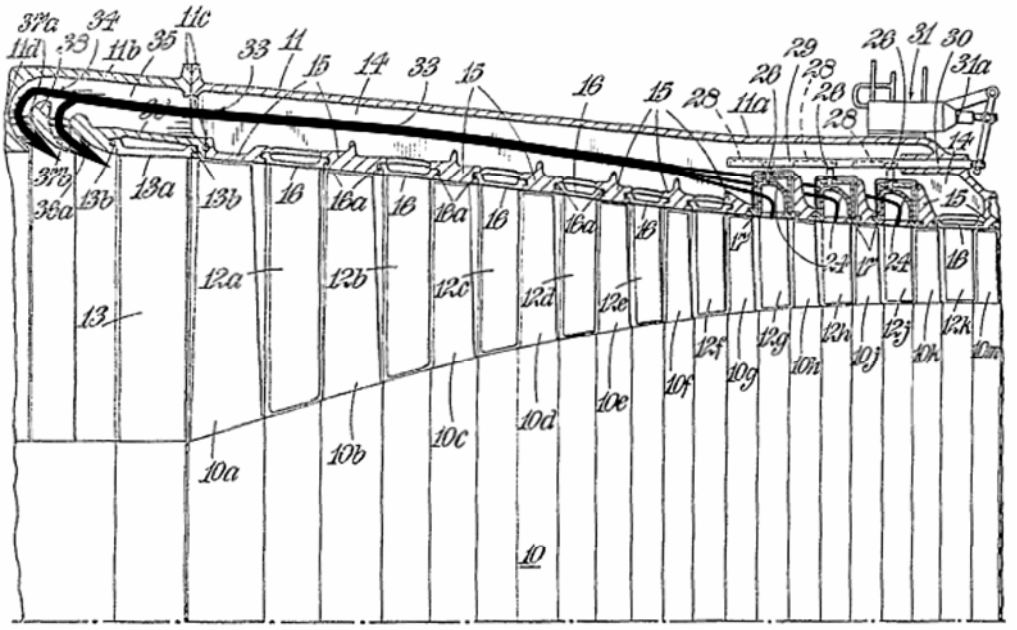

Figure 2.—A1950 patent (ref. 3) proposed recirculating engine speed-modulated air forward from aft stages to inject ahead of the first stage rotor in order to improve the rotor tip velocity triangle, and therefore provide stability improvement.

controlling the amount of bleed flow according to the rotor speed in order to maintain favorable endwall incidence angles with rotor speed, and for controlling the IGV blade angle setting according to rotor speed (fig. 2). A 1955 patent filing (ref. 4) by Ronald Turner of Power Jets Limited proposed incorporating holes and slots in the rotor and stator endwall shrouds to promote turbulence and thereby energize the low energy endwall flow to improve performance. However the earliest reported experimental investigations of concepts for improving the stall limiting aerodynamics associated with the rotor tip region was initiated in the early 1960 by the NASA Lewis Research Center.

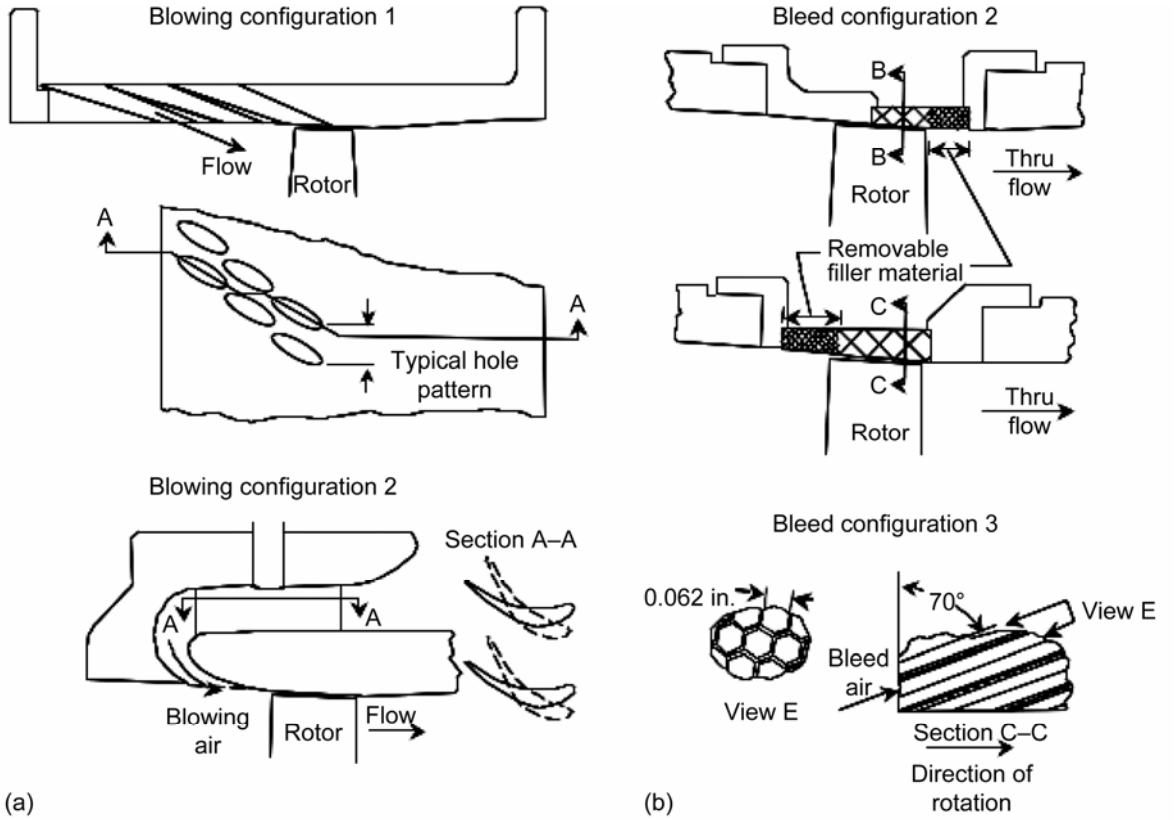

Figure 3.—NASA/GE Bleed/Blowing Studies (refs. 8 to 12). (a) Blowing configurations. (b) Bleed configurations.

Motivated by the successful use of boundary layer control in delaying flow breakdown in cascade tunnels (ref. 5) and inlets (refs. 6 and 7) and the potential for realizing similar benefits by controlling the end wall boundary layer in the compressor rotor tip region, the NASA Lewis Research Center contracted the then Flight Propulsion Division of the General Electric Company in the early 1960 to conduct tests of a high-speed single stage axial compressor rotor with different casing blowing and bleeding configurations (refs. 8 to 13) (fig. 3). For this part-span shrouded rotor, rotating stall was initiated at mid-span which had not been expected. With inlet distortion, however, stall did originate at the rotor tip.

For the distorted inlet conditions where the rotor tip controlled stall, both blowing and bleeding (configuration nos. 1 and 3, respectively (fig. 3) at the tip improved the stall range, with blowing being more effective than bleeding. Casing bleed had an adverse impact on stall range with undistorted inlet flow conditions where stall occurred at the mid-span, *probably as a result of reducing the mid-span flow moving it closer to stall*. For this case, blowing improved the stall range, but only slightly more so than provided by the blowing insert without blowing. It was determined that, even without blowing or bleeding, the outer porous casings used in the blowing and bleeding configurations improved the stall range as compared to the smooth casing configuration. The mechanism that produced these results was not determined. The flow phenomena hypothesized by the authors to be responsible for the improved flow range of the porous casing treatments alone were that the wall porosity or some resonance condition in the cavities acted to stabilize the endwall, or perhaps the roughness of the endwall, or possible flow recirculation acted to thicken the casing boundary layer which thereby reduced the rotor tip diffusion factors.

Bailey and Voit (ref. 14) subsequently further investigated the benefits of similar porous casing treatments, but without external suction or blowing (fig. 4). They tested both the tapered holes and the honeycomb casing treatments as had been previously tested with external blowing and bleeding, and also tested radial hole casing treatments. In addition, they used baffles to prevent axial or circumferential flow

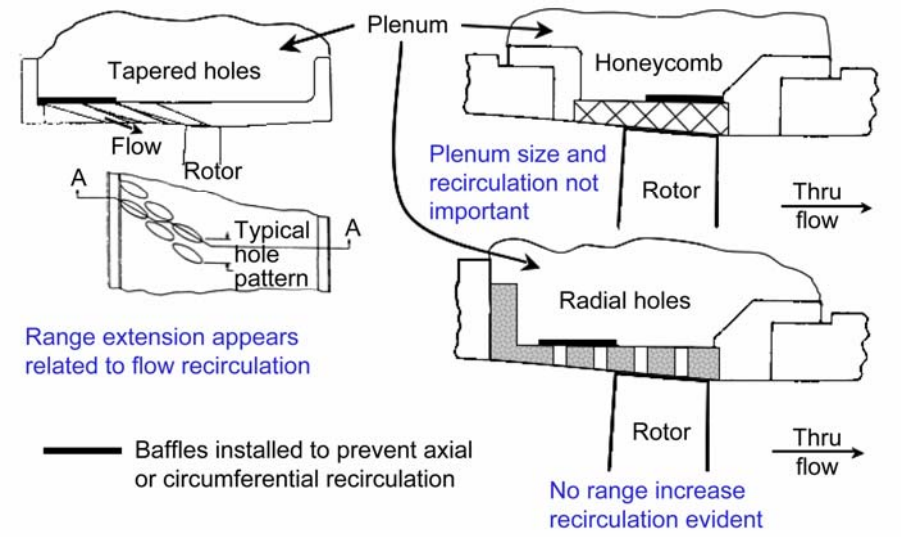

Figure 4.—Early porous casing treatments tested without suction or blowing (ref. 14).

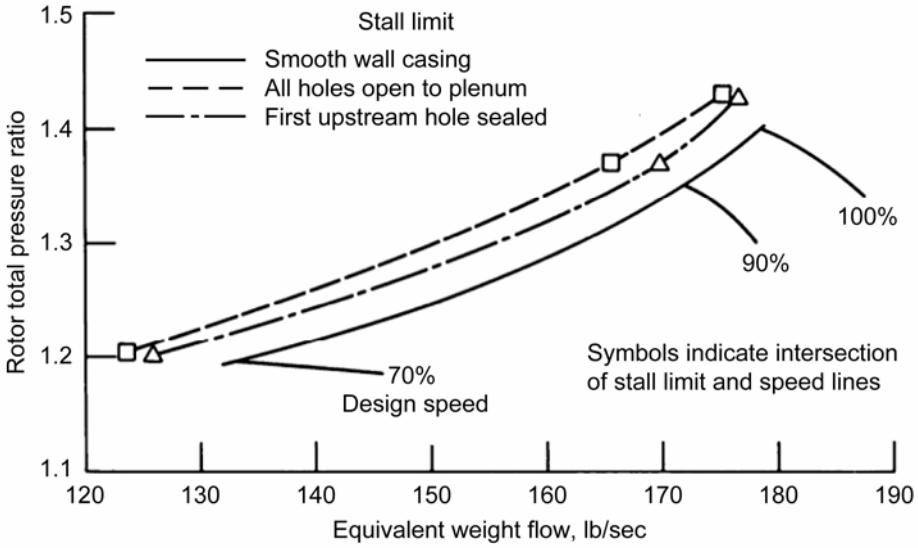

Figure 5.—Importance of axial flow recirculation for tapered holes casing treatment (ref. 14).

recirculation in order to assess its importance for range extension. Their investigations showed that for the tapered holes range extension was dependent on flow recirculation, (fig. 5), which was found not important for honeycomb casing treatments. Though recirculation was evident for the radial drilled holes no range increase was provided. The evidence from the tapered holes with different arrangements of baffles indicates that the initial pressure rise increase imparted by the rotor can be effectively used to provide stall range increase by allowing air to recirculate forward for reinjection ahead of the rotor tip to alleviate the endwall weakness which limits the rotor stability. These results though among the first investigations of endwall casing treatments are consistent with future findings, which will be reported in the next section on Recent Advancements.

2.2 Exploring Porous Endwall Treatments—Early to Mid-1970s

The success of the earliest investigations launched a series of additional experimental investigations through the mid-1970 (refs. 15 to 22) of numerous porous-wall casing treatments (fig. 6). The objectives of these mostly parametric investigations were to better understand the effective mechanism of porous-wall casing treatments. Among the questions that they endeavored to answer with regard to the effectiveness of casing treatments were:

- Does acoustical tuning play a significant role?
- Is porosity (i.e., percentage of open area) an important parameter?
- Are deeper treatments better than shallow treatments?
- What axial coverage is most effective?
- Does recirculation play a significant role?
- How effective are they in the presence of inlet distortions, radial or circumferential?
- What is the underlying mechanism for effectiveness?

To answer these questions numerous types and configurations of casing treatments were tested. Among the different types of casing treatments tested were: honeycomb, radial holes, perforated, axial slots, skewed slots, blade angled slots, and circumferential grooves. Among the different configurations tested were: axial length of treatments, extending beyond or shorter than the rotor tip chord, deep as well as shallow treatment depths, and also acoustically tuned to a perceived "suitable" fraction of the rotor

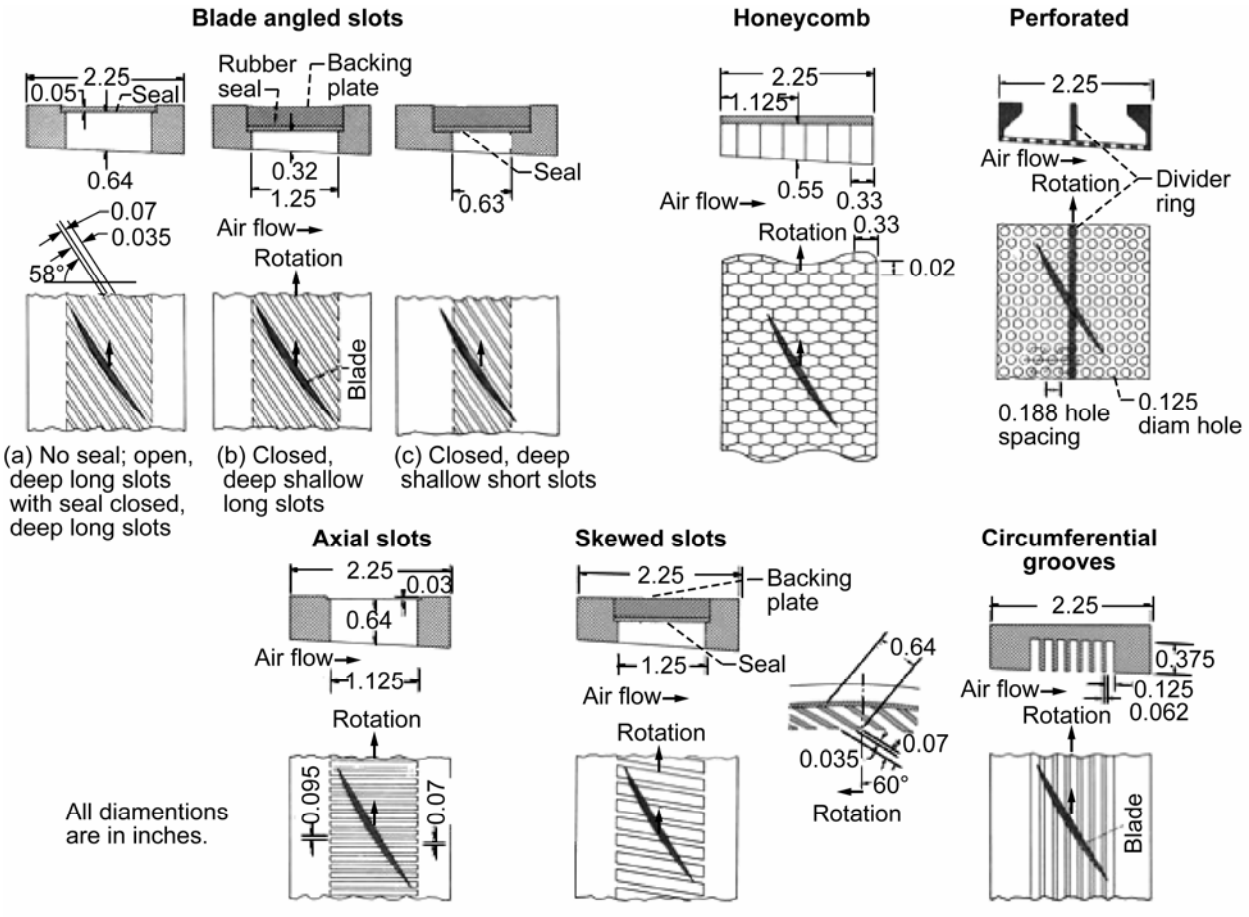

Figure 6.—Examples of various porous-wall casing treatments investigated in the 1970's, (refs. 15 to 22).

blade passing frequency, differing number of holes, slots, or grooves, testing with or without a plenum and with different plenum sizes, and including baffles or seals to prevent circumferential or axial flow recirculation. However, due to various circumstances; differences of treatment configurations, limited experimental capabilities, inadequate instrumentation, non tip-critical blades, *different blade loading profiles*, isolated rotor tests versus single or multistage, etc. there are considerable inconsistencies reported between the various investigations from the early 1960 through the mid-1970s, *after which there appears to more consistency of the reported data*. The remainder of this section will therefore attempt to establish what we've learned, with the benefit of hindsight, about porous casing treatments from these past experimental investigations before proceeding to discuss recent advancements in the next section. Since the chronological order of events is less important than understanding what's been learned the lecture notes will focus on the latter rather than the accuracy of the historical record.

For the most part, all of the tested porous casing treatments provided range extension, especially if definitively found to be tip critical (refs. 8 to 20) (figs. 7 and 8) for example. Some early investigations even indicated the potential for minimal efficiency decrement, though the measured loss was reported to be less than the smooth wall case (fig. 8). Some casing treatments drastically degraded both pressure ratio and efficiency. *If is certainly apparent that though range extension may be achievable for tip critical rotors it is difficult to maintain performance without clear understanding of the fundamental mechanism of casing treatment effectiveness*.

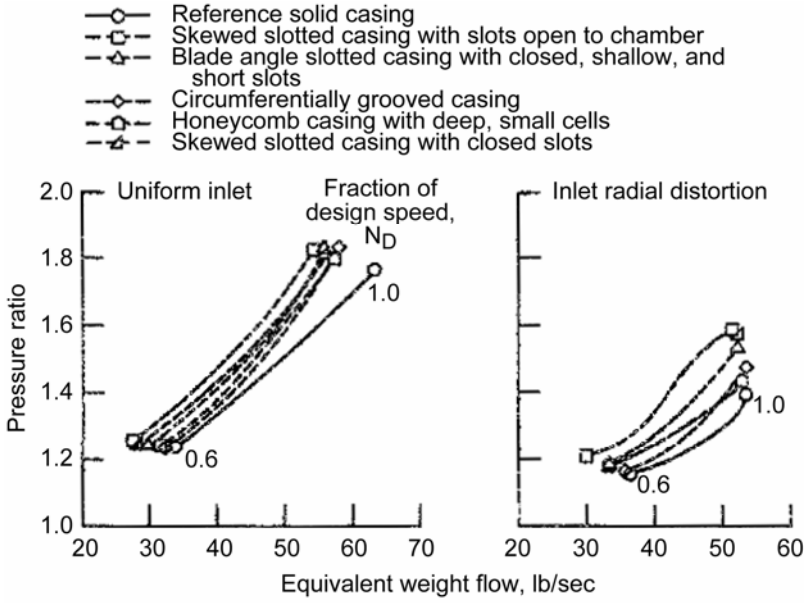

Figure 7.—Typical stall range extension benefits of porous-wall casing treatments (ref. 15).

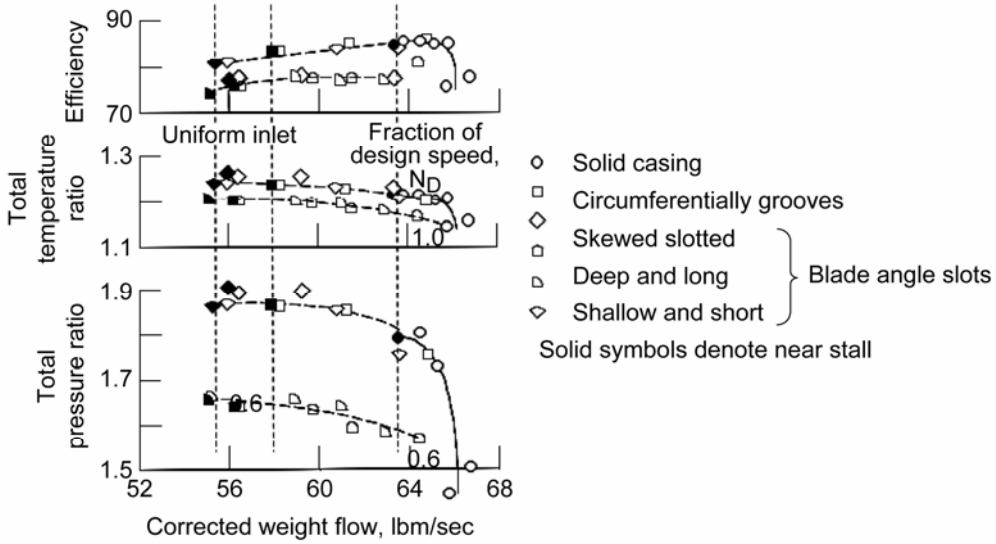

Figure 8.—Measured performance potential of porous-wall casing treatments (ref. 16).

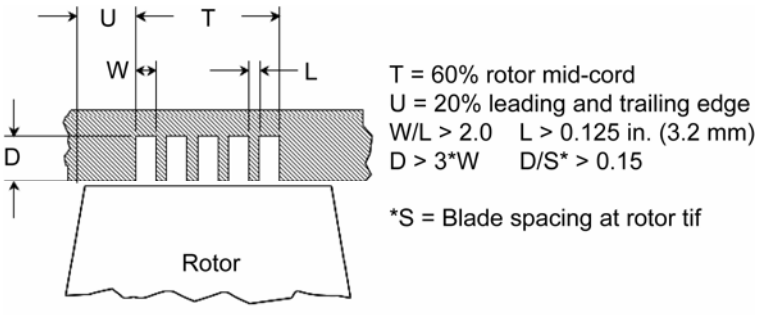

Figure 9.—"Rules of thumb" for circumferential groove design (ref. 21).

Prince, et al. (ref. 20) initiated the first reported attempts to take a comprehensive, physics based approach to understanding the mechanism of casing treatment effectiveness. Based on a comprehensive survey of the past research through the early 1970 they posed a number of clearly elucidated questions that they desired to answer, with what they felt to be a suitable arrangement of test configurations. They had extensive instrumentation including hot-wire surveys in the casing treatment slots and grooves, and they also initiated comprehensive analyses to provide insight and to aid interpretation and understanding of the data. Their tests of different configurations of circumferential grooves, skewed slots, and blade-angled slot casing treatments were found to be consistent with previously reported findings. They confirmed that compressibility effects and cavity resonance were not essentially requirements for effectiveness of casing treatments. The improved stall margin correlated with measurements of increased static pressures on the rotor blade pressure surface in the tip region and increased diffusion on the suction surface relative to the smooth wall. However, they were unable to arrive at a definitive understanding of the mechanism of casing treatment effectiveness.

Based on a survey of the results of Prince, et al. (ref. 20) and previous investigators (refs. 14 to 18), Wisler and Hilvers (ref. 21) subsequently outlined some design "rules of thumb" for circumferential-grooved casing treatments. The "rules of thumb" (fig. 9) for designing circumferential grooved casing treatments are as follows:

1. Most stall range improvement comes from treating the middle 60 percent of projected rotor axial chord. Treating first/last 20 percent of leading/trailing edges is ineffective (refs. 14 to 18 and 20).
2. Most successful treatments have 65 to 75 percent open area of treated surface. For circumferential grooves, therefore, assure that cavity width/land width >2.0 (ref. 20).
3. Cavity depth should be at least three times cavity width (ref. 18).
4. Ratio of cavity depth to blade spacing should be >0.15 (ref. 20).
5. For mechanical reasons, a minimum land width of 0.125 in. *Sufficient land width must also be available to provide adequate bonding of abradable material used for the rotor tip rub strip.*

Despite the inconsistencies of the early investigations through the mid-1970s what appears to be generally supportable from the early literature are the following:

- ***Acoustical tuning does not appear to be a significant factor*** (refs. 14, 15, and 20).
- ***Flow recirculation can be beneficial or detrimental*** as evidenced by the following examples tested with or without a plenum and with or without seals or baffles.
    - ✓ Bailey and Voit (ref. 14) showed strong evidence of the importance of axial recirculation for tapered holes. With three tapered holes, two upstream and one downstream of the rotor trailing edge, range extension depended on having at least one upstream hole in communication via a plenum with the single hole downstream of the rotor leading edge. With the downstream hole sealed from the plenum or both upstream holes sealed there was no range extension. *With benefit of hindsight we can hypothesize that axial flow communication was facilitated by the increased pressure at the downstream hole which pumped fluid forward where it was reinjected upstream of the rotor, presumably improving the endwall flow physics, and thus extending the stable operating range of the compressor.* Bailey and Voit noted that range extension was directly related to the amount of flow recirculated (fig. 5).
    - ✓ Other investigators (refs. 16 to 18) showed that including a plenum to allow flow recirculation did not improve range, but *it should be recognized that these casing treatments were not of the type tested by Bailey and Voit and perhaps are therefore are not benefited by the presence of a plenum to enhance flow recirculation. It should also be recognized that all treatments are themselves potential loss mechanisms and therefore must alleviate an equal or greater loss mechanism, presumably associated with the rotor tip stall mechanism, to prevent performance decrements or realize a net gain in performance.*
    - ✓ Tesch (ref. 17) and later Prince (ref. 20) tested skewed slots with a mid-slot axial baffle to prevent axial flow recirculation. Their results showed an improvement in efficiency of the skewed slots with the presence of the mid-slot baffle. Prince (ref. 20) also tested circumferential grooves with baffles installed in the grooves to prevent circumferential flow recirculation. He reported an increase in stall range, but a reduction in efficiency with the baffles installed.
- ***Compressibility is not essential for understanding the mechanism of casing treatment effectiveness*** as noted by general agreement of low speed compressor tests of casing treatments (refs. 20 and 21) with past experimental findings.
- ***Performance is degraded when the treatment extends beyond the blade chord***, at least for the types of porous casing treatments tested. *Recent concepts to be discussed in the following section on Recent Advancements will show that this is not a general rule for all types of casing treatments.*
- ***Radial holes or perforated endwall treatments provide no range benefit***.
- ***Porous casing treatments are more effective with inlet distortions***.
- ***Efficiency, and in some cases pressure rise, is reduced with casing treatments***.

2.3 Emergence of Cohesive Results and Trends—Late 1970 Through Early 1990

Jumping ahead about a decade later to the mid-1980s Fujita and Takata (ref. 23) tested different configurations of axial, skewed, and circumferential groove casing treatments which had been shown by previous investigators to have the greatest stall range potential or exhibited the least efficiency decrement. Their results, consistent with past measurements, clearly show that the more effective the casing treatment is in extending the stable operating range of the compressor the greater the efficiency penalty (fig. 10(a)). Those casing treatments that are most efficient also provide the least stall range increase. They also observed from their measurements another potential benefit of casing treatments, that they appeared to be effective in desensitizing the impact of tip clearance on range and efficiency (fig. 10(b)). The axial and skewed casing treatments, AV–4C and SV–4C, respectively, showed little change in stall range or efficiency with increasing tip clearance. The circumferential groove casing treatment, CV–3C, provided stall range increase, but followed the same trend with increasing tip clearance as with the smooth wall. *The ability of casing treatments to desensitize the detrimental impact of tip clearance increase is a potentially very useful aspect of casing treatments for mitigating the detrimental impact of blade tip clearance increase due to erosion, tip rubs, and normal wear.*

Noting the diversity of results reported in the literature Greitzer, et al. (ref. 24) recognized a need for fundamental understanding of the mechanism for casing treatment effectiveness to provide design guidance or a useful criterion for application of rotor casing treatment. Based on an assessment of the reported results from prior investigations of casing treatments, and from detailed investigations of flow in the endwall region Greitzer, et al. observed two possible modes in which a compressor could stall. The first was due to “blade stall” where a significant portion of the span would have thick suction side wakes. The second was due to “wall stall” associated with the low momentum “boundary layer” fluid along the compressor endwall. They hypothesized that the effectiveness of casing treatments was dependent on the compressor stall being limited by a “wall stall” condition. To test their hypothesis they setup an experimental program in which two types of blade rows were designed; a high solidity case that would be expected to exhibit a wall stall, and a low solidity case that would be expected to exhibit a blade stall. If their hypothesis were correct they had expected that the effectiveness of the skewed slot casing treatments would be greatest for the high solidity case, and minimally effective or ineffective for the low solidity case.

The measured one-dimensional performance for the high and low solidity cases is shown in figure 11. The results clearly show a higher measured peak static pressure rise was achieved for the high solidity case, which also did not roll over until the flow rate was much lower than the low solidity case. This is consistent with the expected lower flow angle deviation for the high solidity case, which thus achieved greater turning, less deviation, and consequently higher peak static pressure than the low solidity case. What is of greater significance though is the difference in the measured stall points with and without casing treatment for the high and low solidity cases. For the high solidity case the casing treatment was very effective, substantially increasing the stable operating range of the rotor by ~14 percent (change in the stalling mass flow rate), and also producing an ~8 percent increase in the peak pressure rise capability relative to the smooth wall case. However, for the low solidity case the casing treatment was only minimally effective, ~1 percent change in the stalling mass flow rate.

They also made detailed measurements to better support their hypothesis that casing treatment effectiveness was dependent on the rotor exhibiting an endwall stall that limited rotor stability, For the low solidity case they measured significant blade stall where the casing treatment was shown to be ineffective in extending the stable operating range of the rotor, see the low solidity cases of figure 11. With the high solidity blades they measured significant endwall stall with relatively narrow wakes consistent with attached (i.e., unstalled) blade boundary layers, see high solidity cases of figure 11. The results reported by Greizer, et al. support their hypothesis that the fundamental criterion for application of endwall casing treatments requires that the rotor stability be limited by a “wall stall” condition.

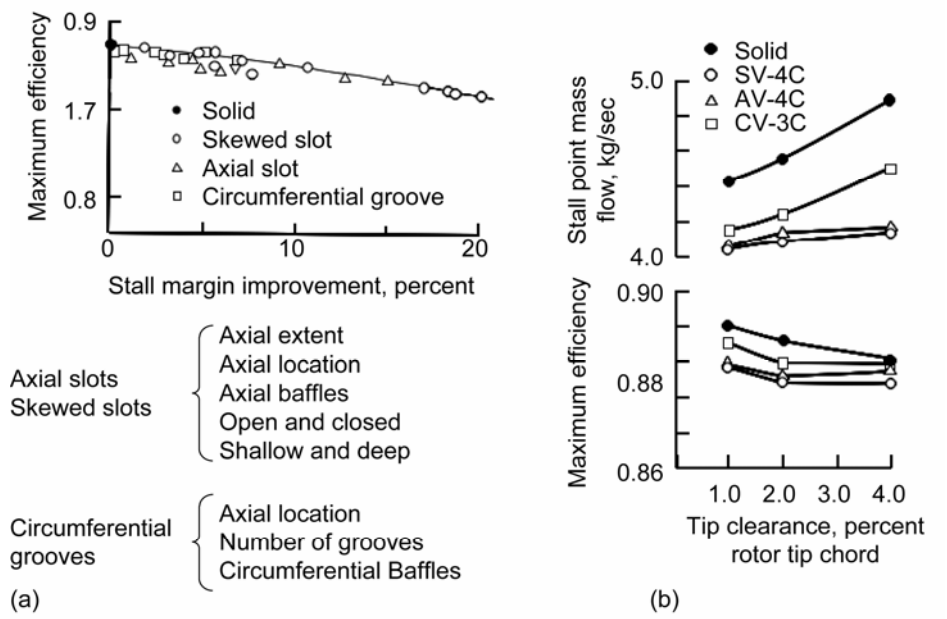

Figure 10.—Typical measured trend of decreasing efficiency with increasing stall range. (a) Efficiency trend with stall range improvement. Desensitization of tip clearance increase due to casing treatments. (b) Sensitivity to tip clearance variation. (ref. 23).

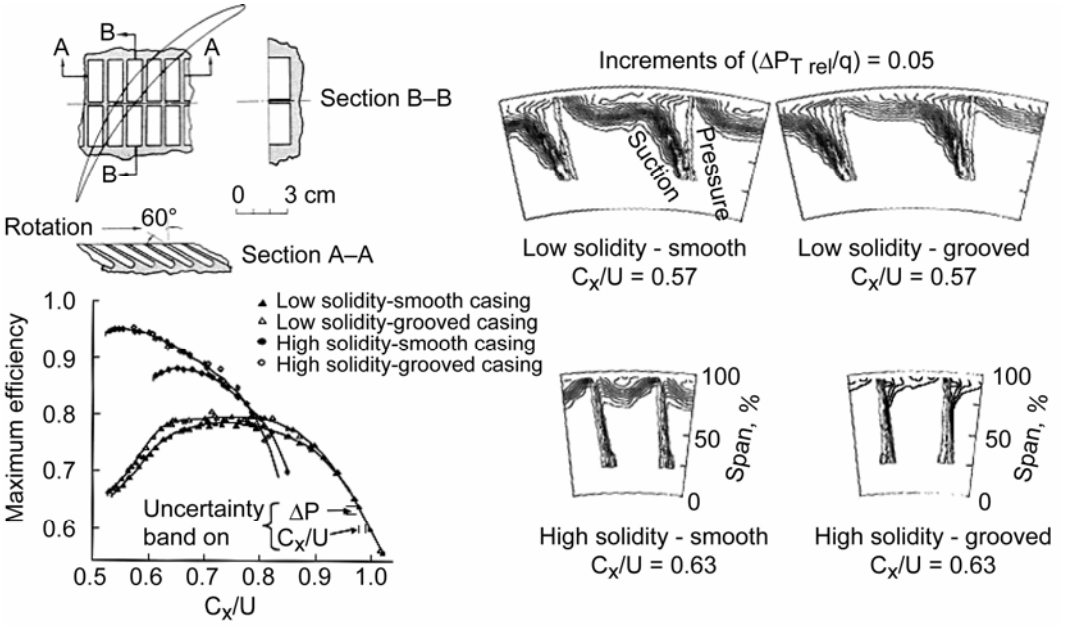

Figure 11.—Effectiveness of endwall casing treatment for conditions of blade stall, low solidity case, versus wall stall, high solidity case (ref. 24).

Backing up to the late 1970 beginning with the investigations of Takata and Tsukuda (ref. 25), there appears to be greater consistency in the reported findings of the various investigators with each adding to our understanding of casing treatments for stall range enhancements. Most of the investigations of casing treatments in the late 1970 through the early 1990 focused on understanding the fundamental mechanism of skewed slot casing treatments since this casing treatment had been shown by early investigators to

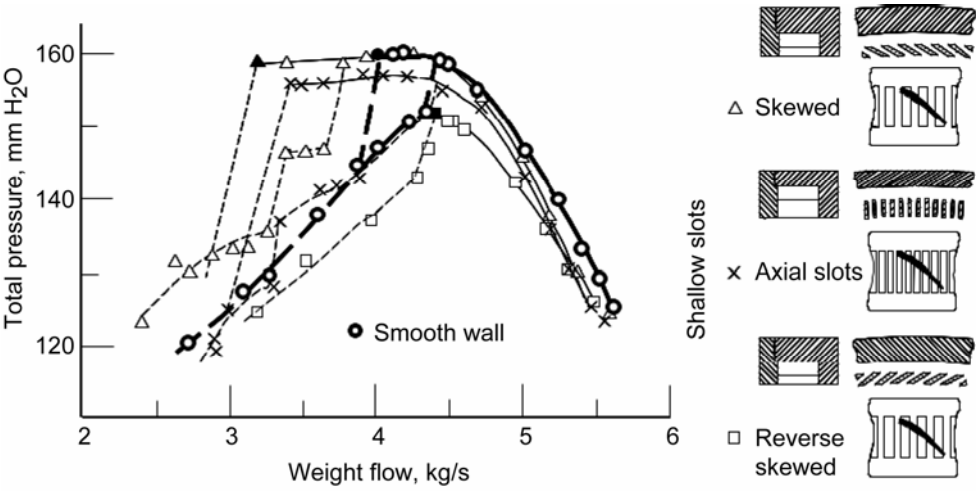

Figure 12.—Impact of orientation of skewed slots on stall range and performance (ref. 23).

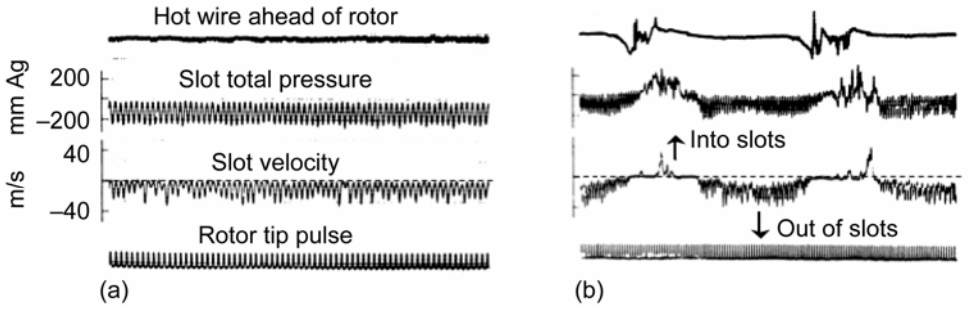

Figure 13.—Hot-wire traces within skewed treatment slots at mid-chord (ref. 23). Flow into slots is positive and out of slots is negative. (a) Design flow rate. (b) Rotating stall.

provide the greatest range extension. Takata and Tsukuda were the first to report clear evidence of the importance of orientation of skewed grooves on stall range and performance (fig. 12). As evidenced from the results of figure 12, the greatest range extension for skewed axial slots is when the slots are skewed opposite to the rotor rotation. The slots oriented in this manner are conducive to allowing the rotor to pump fluid into the slots. The fluid in the slots is then subsequently ejected as the rotor passes by the slot opening. When the slots are oriented radially there is a decrease in stall range extension and also a decrease in pressure rise capability. The worse condition is when the slots are oriented with the rotor rotation, which is much less conducive for enabling fluid to be pumped into the slots. The consequence of this improper orientation of the slots is severe, leading to a reduction in stall range that is less than with the smooth wall. There is also a much more severe drop in pressure rise capability with improper orientation of the skew angle of the casing treatment slots.

Takata and Tsukuda also independently measured the flow in the slot cavities and behind the rotor using hot-wire as was done by Prince, et al. (ref. 20). The results of their hot-wire measurements within the slots clearly show a periodic pumping of flow into the slots near the rotor trailing edge, and a periodic expulsion or jetting of the flow from the slots to the core flow from the rotor leading edge to mid rotor chord. Figure 13 shows time traces of the hot-wire measurements at mid chord for two operating conditions; near design point, and while in rotating stall. For the design flow condition, (fig. 13(a)), we clearly see that the flow is periodically “jetting” from the slots into the core flow. Takata and Tsukuda report that this behavior is exhibited from the rotor leading edge to mid rotor chord. When closer to the rotor trailing edge they measured flow into the slots. When the rotor is in rotating stall, (fig. 13(b)), the hot-wire measurements clearly show flow pumping into the slots as the stall cell moves by, and out of the slots between the stall cells. Takata and Tsukuda hypothesized that the dynamic effect of the high-speed

jet on the main-stream flow facilitates momentum exchange, which they felt was the essential mechanism of the skewed slot casing treatment for stall margin improvement.

Cheng, et al. (ref. 26) provide supporting confirmation of the effectiveness of endwall treatments when "wall stall" limits the stable operating range of the compressor, as indicated by Greitzer, et al. (ref. 24), and also provides supporting confirmation of flow jetting from the axial skewed slots beneficially impacting the near wall flow. For these investigations, however, the authors were interested in investigating whether or not "casing" endwall treatments could also be effective in improving the stall margin when a stator hub stall limits the stable operating range of a compressor. Considering that past experimental evidence has shown that the relative motion between the endwall and blade is an important element of the success of grooves in reducing endwall blockage the authors observed that similar such conditions exist for a cantilevered stator, and as such hub endwall treatments should also be effective in reducing stator endwall blockage. They also felt that if stator hub treatments were similarly effective for tip critical cantilevered stators as casing endwall treatments were for tip critical rotors that the stator geometry would be much more amendable to investigations of the flow details within the blade passages as well as providing a different perspective for understanding the mechanism of casing treatment for stall margin improvement. They were not the first to test the effectiveness of stator hub endwall treatments (refs. 21 and 25). However, for whatever reason, the early investigations did not show any measurable benefit of stator hub endwall treatments.

Cheng, et al. investigated two different stator blades; one with a high blade stagger angle which would be expected to exhibit a "wall stall," and the other with a low blade stagger angle which would be expected to exhibit a "blade stall". The results of their investigation clearly showed that hub endwall treatments were also effective in improving the stability of stators wherein "wall stall" limited the stability of the stator blades, and were essentially ineffective in increasing the stable operating range of low stagger blades wherein "blade stall" limited the stator stability. Detailed measurements of the circumferential variation in total pressure change across the stator at different span locations clearly shows evidence of a jet of high total pressure fluid near the hub along the stator pressure side, as evidence by a "spike" in total pressure for the case with hub treatment (fig. 14). They then proposed a conceptual "picture" of a jet emanating from the groove leading edge region, as first observed by Takata and Tsukuda (ref. 25) based on hot-wire measurements within the casing treatment slots (fig. 15).

Smith and Cumpsty (ref. 27) used an isolated low speed rotor to make detailed measurements of the rotor flow field and within the casing treatment slots to improve understanding of the fundamental flow physics of skewed casing treatments. They employed the same skewed slot casing treatment design as was used by Prince, et al. (ref. 20). Their measurements included detailed surveys of the loss pattern downstream of the rotor using a hot-wire probe, and a rotating frame traversing probe to make measurements within the blade passages and in the treatment slots using hot-wires. As did Fujita and Takata (ref. 25) they also measured the effectiveness of the skewed slots treatment with increasing rotor tip clearance (fig. 16). Their measurements clearly show that up to 6 percent rotor tip clearance the skewed slots casing treatment is providing increase stall range with higher total pressure capability that provided by the smooth wall casing treatment for the same tip clearance. In fact up to 3.5 percent tip clearance the measurements show that the peak pressure rise capability and stall limit are almost identical to the smooth wall case at 1 percent tip clearance. This is consistent with the experimental findings reported by Fujita and Takata (ref. 23).

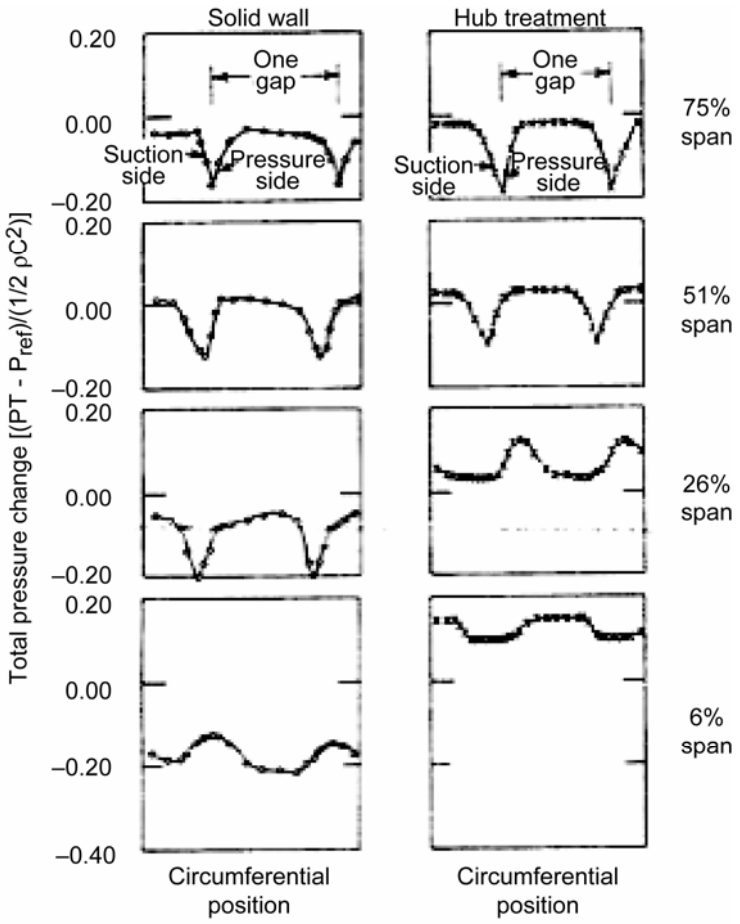

Figure 14.—Measured evidence of pressure side jet of high pressure fluid emanating from skewed stator hub treatment slots (ref. 26).

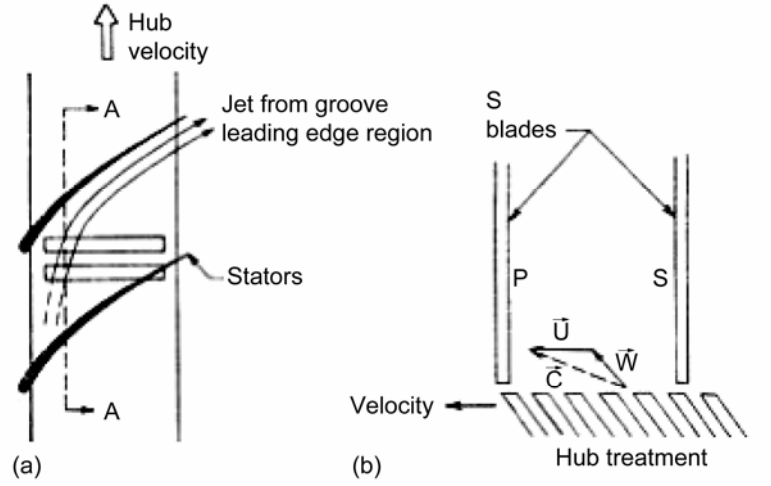

Figure 15.—Measured evidence of pressure side jet of high pressure fluid emanating from skewed stator hub treatment slots (ref. 26). (a) Audial (inward) view. (b) View as Section A–A.

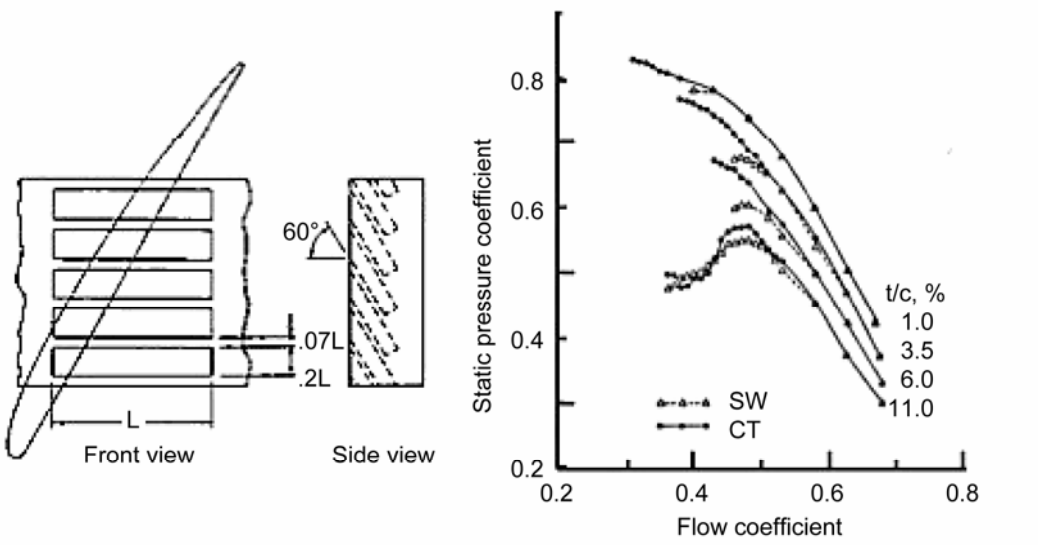

Figure 16.—Effectiveness of skewed slot casing treatment for desensitizing the typical detrimental impact of increasing tip clearance (ref. 27).

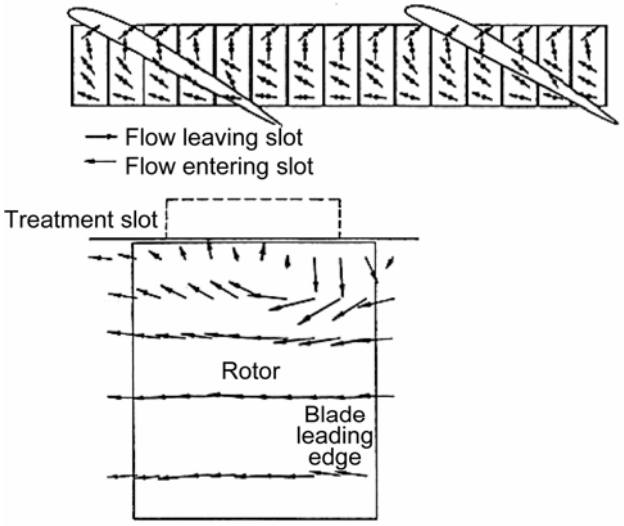

Figure 17.—Velocity vectors 20 percent from the rotor pressure side and at mid-depth in the treatment slots as measured by hot-wire measurements (ref. 27).

Detailed hot-wire measurements within the rotor passage and in the blade slots are shown in figure 17. The measurements clearly show evidence of flow entering the treatment slots towards the blade trailing edge and then emanating from the treatment slots near the blade leading edge. The spanwise extent of flow recirculation, as influenced by flow into and out of the cavity, is indicated by the upper sketch in figure 17. The relative magnitude of the vectors clearly indicates a “jet” of high velocity fluid emanating from the treatment slots near the rotor leading edge which was originally indicated by Takata and Tsukuda (ref. 25) as responsible for momentum exchange which they had hypothesized as the mechanism of stall margin improvement for skewed slot casing treatments. In spite of the measurements supporting this mechanism Smith and Cumpsty admitted that the reason for the casing treatment mechanism was still not well understood. Primarily due to ignorance of the fundamental flow mechanism that ultimately leads to stall. The authors noted that the evidence clearly indicates that a rapid

accumulation of endwall blockage is responsible for initiating the instability, and that the casing treatment provides a path for the high swirl low momentum endwall fluid to enter and be turned by the slots and subsequently reinjected towards the rotor leading edge. They noted that the low momentum fluid that contributes to the endwall blockage is well suited to enter the casing treatment slots, which are then able to effectively utilize that flow to energize the endwall fluid toward the rotor leading edge.

As noted by the authors, Tesch (ref. 17) and Prince, et al. (ref. 20) had previously measured an improvement in efficiency when the skewed slots were divided with the inclusion of a baffle at mid axial slot distance. Smith and Cumpsty considered that though this might seem to preclude the possibility of axial flow from the rear to the front of the blade, with the typical thin highly stagger blades of modern compressors, and with the axial extent of typical casing treatments, there is still ample opportunity for axial flow to occur from pressure surface to suction surface. Smith and Cumpsty considered therefore that the overriding characteristic of casing treatments that provide stall range improvement was the provision of a flow path between the pressure and suction surface. They further considered that for stall margin improvement to be realized the blading must be such that flow blockage accumulates near the blade tip pressure surface. They then interpreted the results of Greitzer, et al. to be consistent with this in that both the low and high solidity blades exhibited flow separation in the endwall. A suction surface/endwall stall was present for the low solidity blades thereby making the casing treatment ineffective for increasing stall range, and a pressure surface/endwall stall was present for the high solidity blades, which is why the casing treatment proved effective for increasing the stall range of the compressor. As had been previously reported (ref. 20) they also concluded that unsteady effects in the slots are of minor importance, the steady flow is what matters for casing treatment effectiveness. Given the measurements indicated the significance of flow recirculation in utilizing the endwall blockage by turning it 180°, they considered that continuously curved passages would be more effective than rectangular passages.

Further substantiation of the fluid physics within skewed casing treatment slots was provided by detailed hot-wire measurement within a stator hub endwall treatment by Johnson and Greitzer (ref. 28). A schematic of the skewed slot casing treatment employed at the hub endwall of a stator row is shown in figure 18 along with the measured performance with and without the hub endwall treatment which clearly shows the considerable stall range benefit and enhanced peak pressure rise capability afforded by the skewed slot treatment. Detailed hot-wire measurements close to the stator hub and within the stator passage clearly show the influence of the skewed slots hub endwall treatment on the stator flow

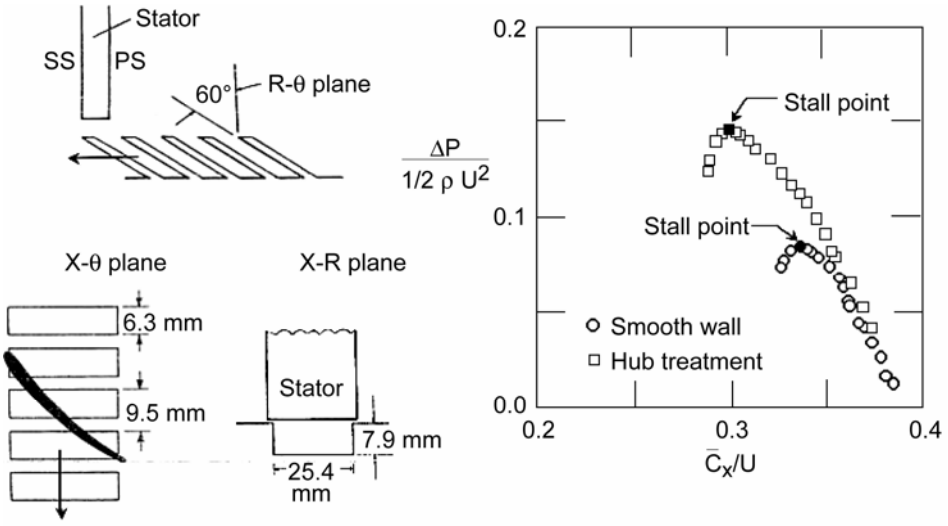

Figure 18.—Skewed slot hub treatment and measured performance with and without the stator hub treatment (ref. 28).

field (figs. 19 and 20). For the smooth wall case the hot-wire measurements at 2 percent span from the hub, upper half of figure 19(a), clearly show a large region of low axial momentum fluid (endwall blockage) beginning from about 40 percent chord near the blade suction surface, moving across the passage to about 60 percent chord near the blade pressure surface, and extending downstream across the passage. This low axial momentum region subsides in extent away from the hub as indicated by the measurements of the smooth wall case at 6 percent span from the hub, upper half of figure 19(b).

The influence of the skewed slot hub treatment is also clearly indicated by the hot-wire measurements. The measurements at 2 percent span from the hub for the case with hub treatment, bottom half of figure 19(a), show spanwise flow into the slots in the approximate vicinity of where the low axial momentum flow existed for the smooth wall case. As suggested by Smith and Cumpsty (ref. 27) based on their measurements of skewed slots casing treatment over a rotor, and supported by the measurements of Johnson and Greitzer (ref. 28) shown in figures 19 and 20, this low axial momentum high swirl fluid is evidently well suited to moving into the skewed slots hub treatment. This further confirms the utility of stator hub endwall treatments for investigating the flow mechanism of casing treatments for stall range improvement. The flow ingested into the slots near the passage trailing edge is shown to be jetting from the slots near the passage leading edge with a strong orientation towards the blade pressure surface, bottom half of figures 19(a) and 20(a), where the injected fluid appears to follow along the pressure surface towards the passage exit apparently never directly impacting the blockage fluid. The influence of the hub endwall treatment is still quite evident at 6 percent span from the hub, bottom half of figure 19(b), where the extent of endwall blockage was much less for the smooth wall case, upper half figure 19(b). Figure 20(b) clearly shows the large spanwise extent of the influence of the skewed slot hub treatment, bottom half of figure 20(b), relative to the blockage measured for the smooth wall case, upper half of figure 20(b). *This implies that perhaps the skewed slot casing treatment was not optimally designed to alleviate the hub endwall blockage with minimal efficiency decrement*. Johnson and Greitzer (ref. 28) show additional evidence to that of Smith and Cumpsty (ref. 27) of the removal of blockage towards the rear of the passage and injection of a high velocity jet towards the leading edge. *The blockage removal is apparently contributing to stall range enhancement as it is the rapid growth of the endwall blockage as a compressor is throttled towards stall, Khalid, et al. (ref. 29), that precipitates stall. However, it is less evident what role the upstream jet injection plays in range enhancement, if any, as it does not appear from the measurements of figures 19 and 20 to have any direct impact on the blockage flow, though it does facilitate the blockage flow removal by providing a path for it to be reinjected into the main stream in a potentially beneficial manner*.

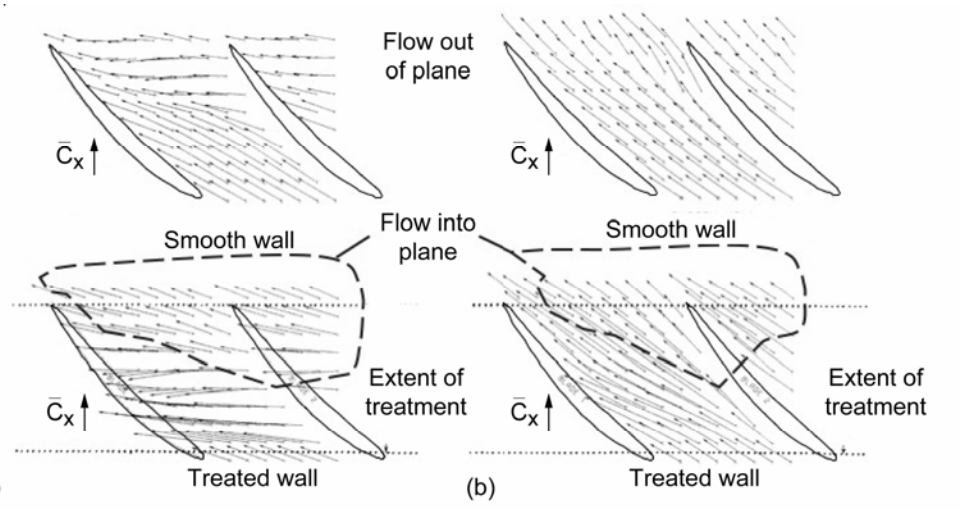

Figure 19.—Hot-wire measurements of velocity vectors, normalized by average freestream axial velocity, at (a) 2 percent and (b) 6 percent span, with and without skewed slots hub treatment.

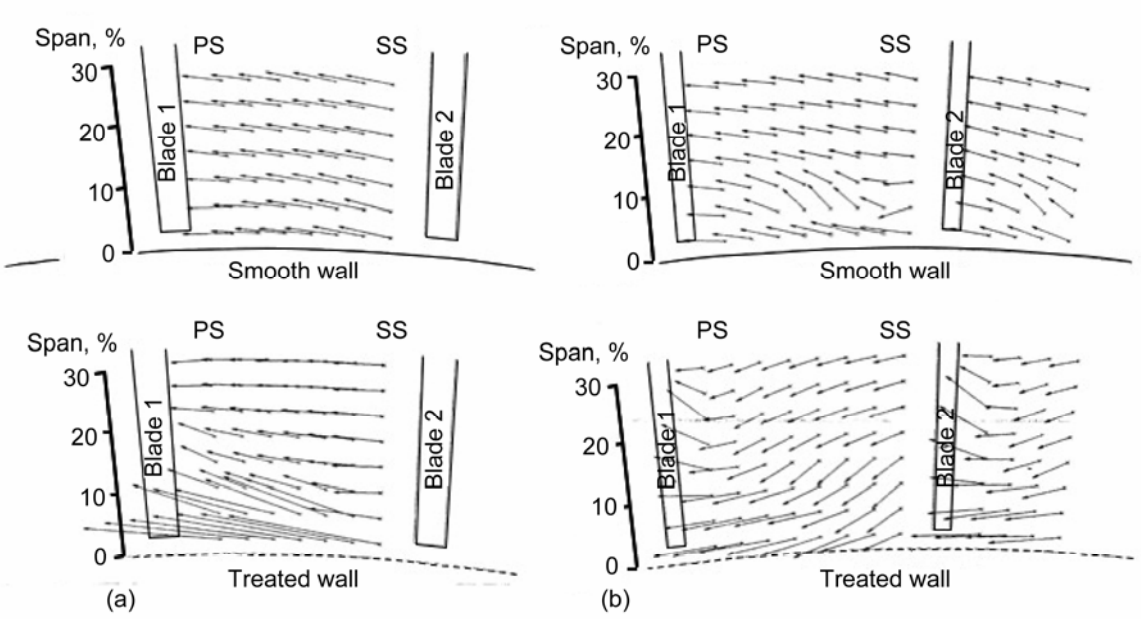

Figure 20.—Hot-wire measurements of velocity vectors, normalized by average freestream axial velocity, (a) at 20 percent and (b) 78 percent axial chord, with and without skewed slots hub treatment.

Given the perceived importance of blockage removal and flow reinjection Lee and Greizer (ref. 30) provided external means, via a plenum below the treatment slots, for augmenting blowing and suction with the primary objective of clarifying the mechanism by which casing treatments, which involve flow removal and injection such as skewed slots casing treatments, suppress stall. They used the same facility and similar endwall treatment as used by Johnson and Greitzer (ref. 28). With the aid of detailed hot-wire measurements the effects of both augmented suction and injection through the treatment slots was investigated for a number of different skewed slot configurations covering differing axial extents and locations relative to the stator hub passage. A schematic of the treatment injection and suction conditions, treatment geometry and configurations are shown in figure 21. The schematic of the treatment (fig. 21(a)), illustrates that the hub incorporating the treatment slot is rotated relative to the stator blades, and that a plenum provided below the hub to which the slots are open provides a mechanism to blow into or suck flow out from the slots. Lee and Greitzer tested several different casing treatment configurations selected to isolate the effects of blowing and suction at different axial locations with smaller or larger slot openings to facilitate or impede axial recirculation. The configurations were selected to independently isolate the benefits of suction, blowing, and axial flow recirculation, and compare those results to conventional skewed slot casing treatment without augmented suction or blowing. As with Johnson and Greitzer (ref. 28) the stator was designed to be highly loaded to assure the stator hub endwall would be limiting the compressor stability.

Figure 22 shows a comparison of hot-wire measurements of velocity vectors acquired at 2 percent span from the stator hub for the smooth wall, and treated wall without suction or blowing, from Johnson and Greitzer (ref. 28), and with blowing from the 22.5 percent front slots treatment configuration (ref. 30). These results show that blowing from the 22.5 percent font slots configuration is comparable to the hub treatment without blowing or suction in that for both there is evidence of a jet emanating from the treatment slot near the blade leading edge and impinging on the pressure surface. Therefore, blowing is seen to reasonably mimic the jet injection from conventional skewed slot treatments.

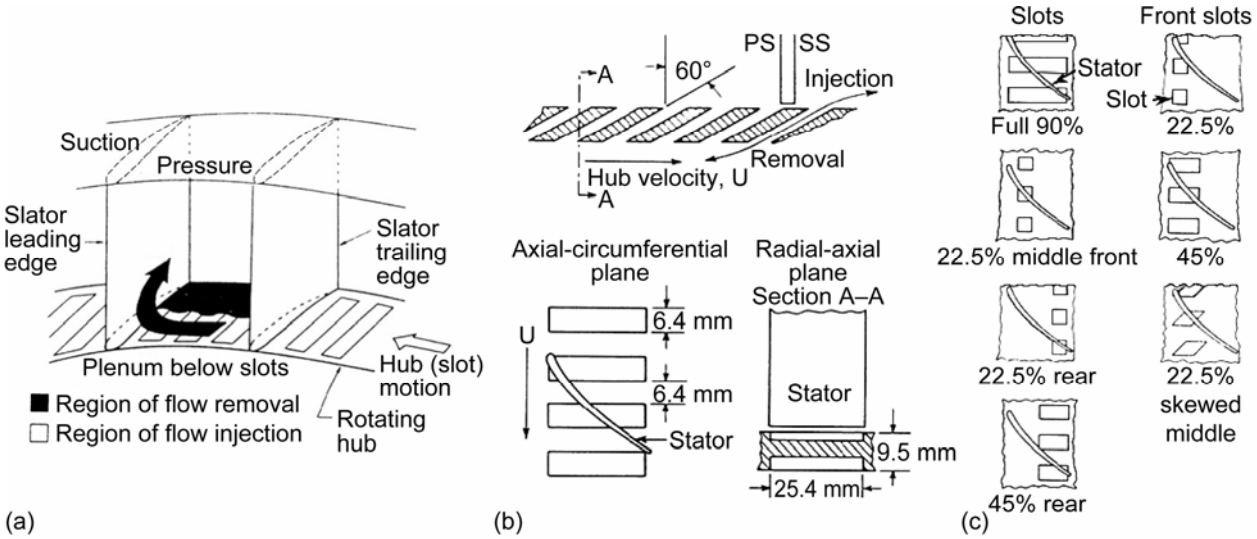

Figure 21.—Skewed slot treatment geometry and configuration for hub blowing and suction investigations of Lee and Greitzer (ref. 30). (a) Schematic of treatment suction/blowing conditions. (b) Treatment geometry. (c) Tested treatment configurations.

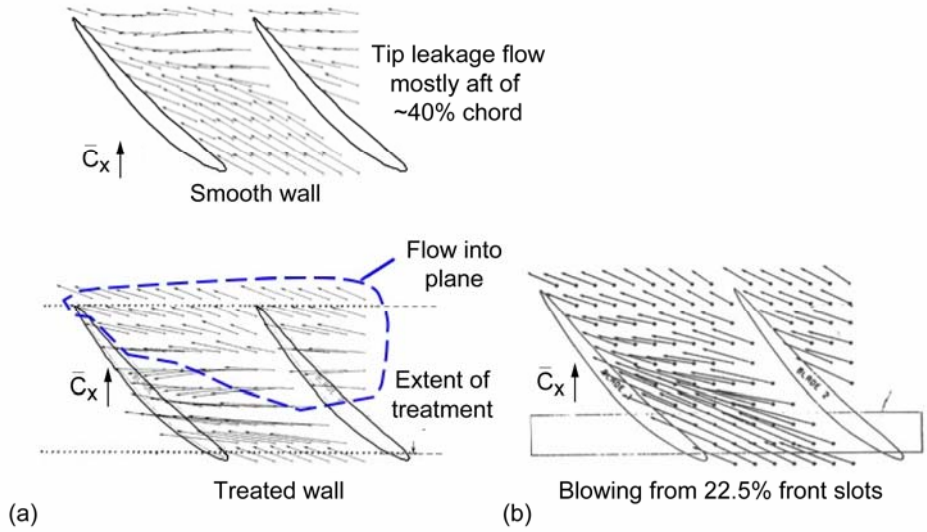

Figure 22.—Comparison of velocity vectors acquired from hot-wire measurements (a) at 2 percent span from hub for smooth and treated wall measurements (Johnson and Greitzer (ref. 28)), and (b) blowing from 22.5 percent front slots (Lee and Greitzer (ref. 30)).

Figure 23 shows the axial development though the stator passage of pitch averaged streamwise velocity profiles near the inner 30 percent span from the hub. These measurements show that at the leading edge the smooth wall, conventional skewed slot treatment, and 22.5 percent front slots with blowing are in agreement, and at 8 percent axial chord both the conventional and 22.5 percent front slots with blowing provide essentially identical increase in streamwise velocity near the hub. Progressing towards mid-axial chord we see the spanwise influence of the 22.5 percent front slots blowing case is smaller than for the conventional hub treatment case, and that the conventional hub treatment begins to roll off toward the hub sooner than for the 22.5 percent front slots blowing case, but not as fast as for the smooth wall case. Both the conventional skewed slot treatment and the 22.5 percent front slots blowing treatment begin to look similar again towards the blade trailing edge. The general shape of the streamwise velocity hub profile is generally fuller for the conventional hub treatment and the 22.5 percent front slot blowing case.

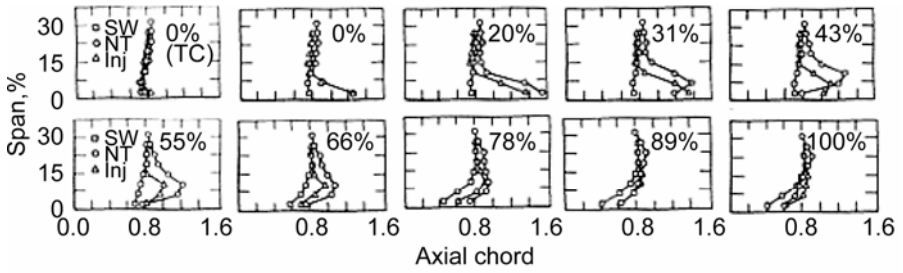

Figure 23.—Development of hot-wire measured pitchwise averaged streamwise velocity profiles through the stator hub for smooth wall (SW), conventional hub treatment (HT), and 22.5 percent front slot injection (INJ) (ref. 30).

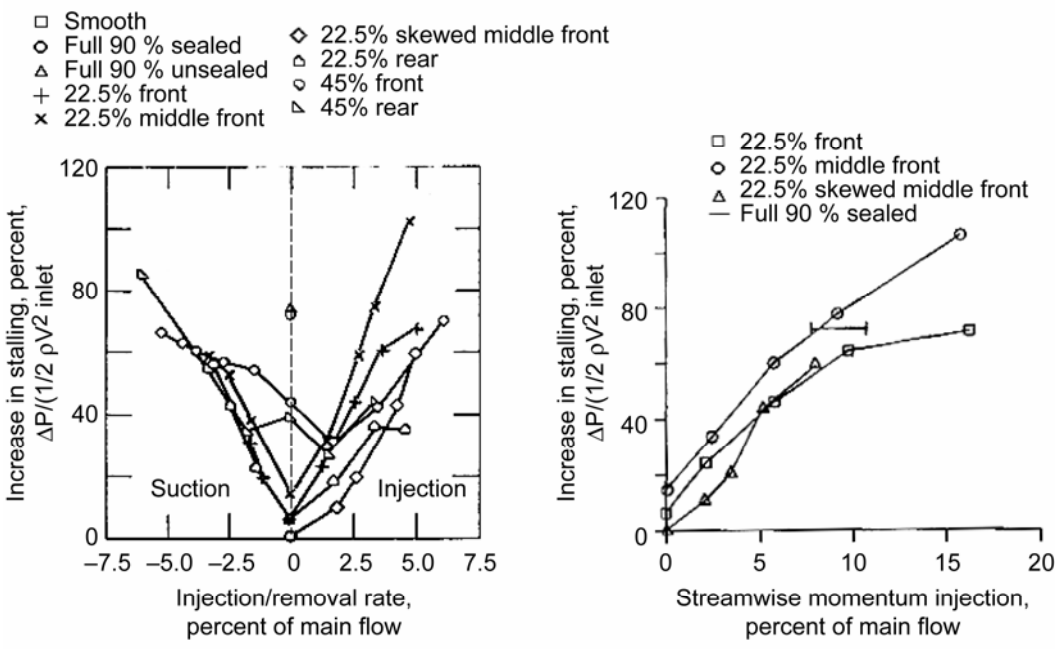

Figure 24.—Increase in stalling pressure rise relative to smooth wall for different slot treatments with differing rates of suction or injection (blowing), and as a function of streamwise momentum of the injected air as a percentage of the main flow (ref. 30).

Lee and Greitzer also tested the different slot configurations with different amounts of blowing and suction to ascertain the influence of injection/blowing amount on effectiveness for increasing the stalling pressure rise capability (fig. 24) which also provided a commensurate stall margin improvement. The measurements clearly show that injection over the 22.5 percent middle front slots is most effective, with 45 percent rear slot suction being the next most effective for increasing the stalling pressure rise capability. For the configurations tested the stall range generally increased as the stalling pressure rise capability increased. The full 90 percent sealed slots reflect the conventional skewed slot treatment that occupied 5 to 95 percent of stator axial chord. Only those cases with greater than about 3 percent injection or 5 percent suction provided greater increases in stalling pressure rise capability than was provided by the conventional skewed slot casing treatment. *Reflecting back on the smooth wall velocity vectors measured by Johnson and Greitzer (ref. 28) (fig. 22), the tip leakage flow was observed to cross over from the pressure surface the suction surface at about 40 percent chord. Examining figure 24 the most effective injection case is where flow is injected from the middle front 22.5 percent slots suggesting perhaps the importance of energizing the leakage flow just upstream of where it crosses the blade tip. Injection from the 22.5 percent front slots was a bit less effective and it's effectiveness decreased for high blowing rates. Blowing from the longer 45 percent front slots initially decreased relative to no blowing*

and then increased the stalling pressure rise capability, perhaps indicating again that where and how strong the jet is are important parameters to consider for optimizing effectiveness of injection. The axial skewed 22.5 percent middle front slot case (fig. 21(c)), did not seem to provide improvement. The effectiveness of the 45 percent rear slots initially drops with suction, relative to no suction, and then increases following essentially, with similar effectiveness, of suction from the 22.5 percent front, or rear slots and only slights less effective, but monotonically increasing with suction parallel to the 22.5 percent middle front slots. The 45 percent front slots are initially more effective with no suction, with their effectiveness increasing with suction, but at a lower rate of improvement relative to the other suction cases. All suction cases cross at about 3.5 percent suction, which is close to that measured for flow into and out of the slots tested by Johnson and Greitzer (ref. 28).

The suction cases were generally independent of where the suction took place with effectiveness monotonically increasing with suction rate, whereas the effectiveness of injection was dependent on where the fluid was injected and exhibited differing rates of improvement with injection flow rate. Also plotted to the right hand side of figure 24 is a comparison of the effectiveness of different injection configurations as a function of streamwise momentum normalized by the main flow momentum. It appears to indicate that injection effectiveness is dependent on the amount of streamwise momentum, and might be an important consideration for design of casing treatments that employ injection.

The first reported computational investigation of endwall treatment effectiveness was reported by Crook, et al. (ref. 31), who employed a steady three-dimensional Navier-Stokes solver to compute the complex flows associated with endwall treatments. They studied the same stator hub treatment case previously tested by Johnson and Greitzer (ref. 28) and Lee and Greitzer (ref. 30) (fig. 21(b)), and modeled the casing treatment suction and injection with a wall boundary condition (fig. 25). Figure 26 shows contour plots of total pressure difference normalized by inlet dynamic pressure. Figure 26(a) shows a high loss region emanating from upstream and moving across the passage towards the pressure surface. The particle path lines clearly identify the low-pressure fluid as that coming from the leakage vortex, *which appears to leave the suction surface approximately at about 30 percent chord*. The treated wall simulation results clearly show that the region associated with the leakage flow is now filled with high total pressure fluid, and that the predominance of the fluid contributing to the increased total pressure is emanating from flow originating near the blade leading edge. The majority of the mid-pitch fluid from the slot model impinges on the blade pressure surface and is essentially wasted in that it does not appear to contribute to alleviating the endwall blockage associated with the leakage vortex. *More careful tailoring of the treatment design may be able to better exploit the potential benefits of the injected air*.

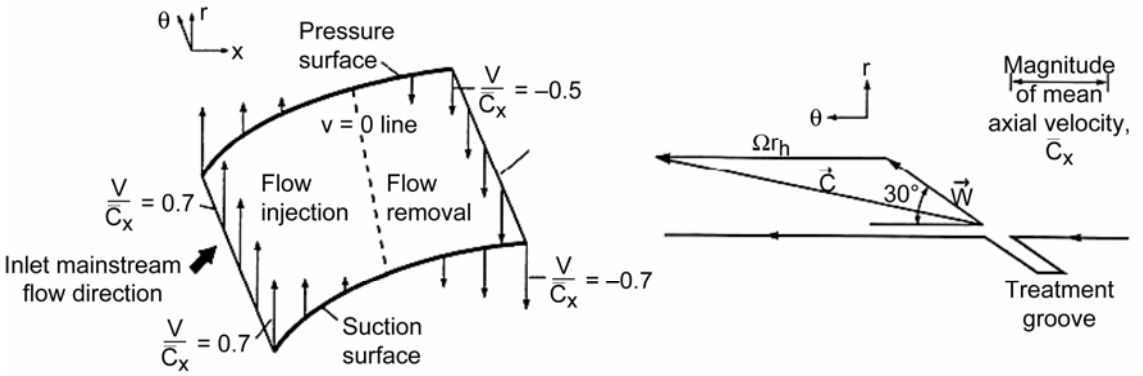

Figure 25.—Computational model of hub treatment radial velocity profile, V denotes radial velocity (ref. 31).

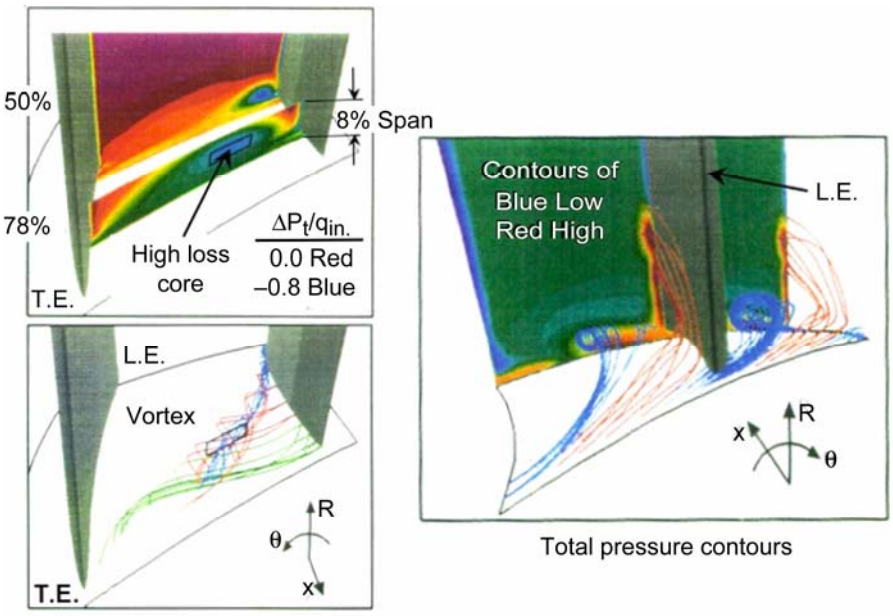

Figure 26.—Contour plots normalized total pressure change and particle traces predicted by simulations for both a smooth and treated hub wall (ref. 31).

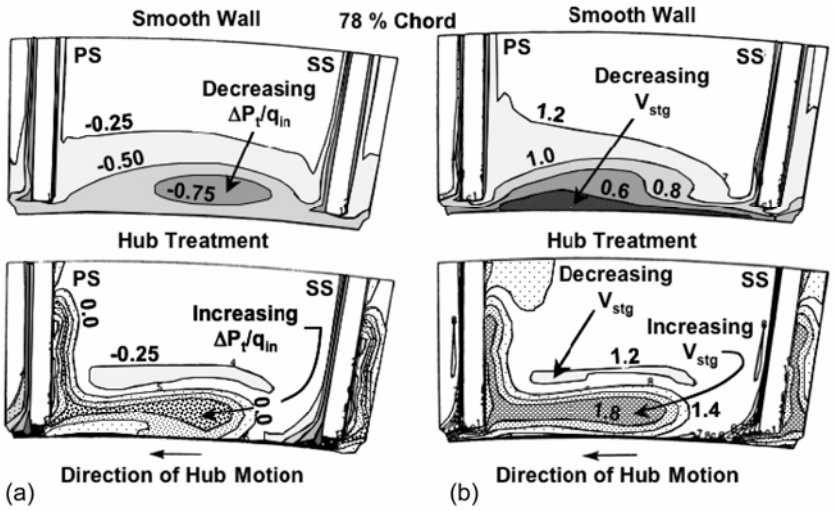

Figure 27.—Contour plots of total pressure change and stagger line velocity at 78 percent stator chord for both the smooth and treated wall cases (ref. 31). (a) Total pressure, $\Delta P/q_{in.}$. (b) Stagger line velocity, V_{stg}/V_x.

Comparisons of contour plots of total pressure change and stagger line (essentially streamwise) velocity at 78 percent stator chord are provided in figure 27 for both the smooth and treated wall cases. The smooth wall predictions shown in figure 27(a) clearly show a deficit in total pressure near the hub and concentrated at about mid-pitch. The stagger-line velocity in this vicinity is also low and decreasing for the smooth wall case (fig. 27(b)). The simulations of the treated wall case, however, show increasingly high positive total pressure in the vicinity of where there was previously a low negative total pressure for the smooth wall case. Similarly there is a predicted high stagger-line velocity for the treated case in the region where the stagger-line velocity was lower for the smooth wall case. The evidence is strong that the flow endwall treatment model is depicting similar physics to what has previously been measured (refs. 28 and 30) and that the hub treatment is effective in removing the low total pressure fluid and replacing it with high total pressure fluid with high streamwise momentum, which had previously been noted as important for effectiveness of injection (ref. 30).

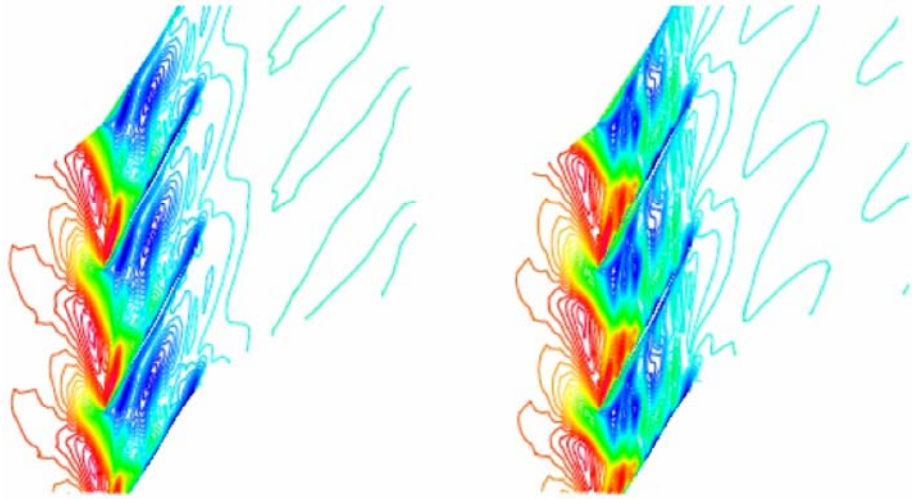

Figure 28.—Comparison of relative Mach contours at teh rotor tip for smooth wall and with circumferential grooves (ref. 33). (a) Smooth wall. (b) Circumferential grooves.

The first reported attempt at a comprehensive computationally based analysis of casing treatments configurations was by Hall, et al. (refs. 32 and 33) who used the ADPAC code to analyze circumferential groove, skewed slots, and a recessed-vane casing treatment (ref. 34) with and without inlet distortion. The computational investigations of Hall, et al. included steady and unsteady simulations of the various casing treatments coupled to different compressor geometries, initially to validate the predictive capability against test cases, and subsequently to investigate the capabilities of the treatments with inlet distortion on a transonic fan stage. The boundary conditions used for the different cases were direct point-to-point coupling, time average, or time-accurate. They concluded that circumferential distortion provided range benefit due to removal of blockage near the endwall as a result of vortex segmentation and blade passage shock repositioning, which they considered to be an essentially steady state process (fig. 28). The time accurate simulations of the skewed slot treatment confirmed removal of low total pressure high swirl fluid from the rear of the passage and subsequent reinjection towards the front of the passage with reduced swirl to energize the fluid in the tip leakage vortex (fig. 29(a)). The injected flow was observed to increase the blade tip loading, but without separation due to the blockage removal towards the rear of the passage (fig. 29(b)). However, due to various issues related to in some cases inadequacy of boundary conditions, or discrepancies of predictions relative to measured results, as well as computational resources limiting the number of time-accurate simulations, they considered that additional development was required before being useful for accurate design analysis. Ensenat (ref. 35), conducted an intensive analysis of the numerous steady state simulations generated, *but due to inconsistencies, inadequacies of boundary conditions for certain treatments, limited cases, and discrepancies relative to measured results or repeated simulations* was unable to draw any useful conclusion for guiding casing treatment design. Ensenat observed that the treated cases, to varying degrees, provided increased tangential velocities downstream of the treatment and increased blockage relative to the smooth wall case, perhaps caused by increased shock/wall boundary layer interaction.

An aspect of endwall treatments not previously reported on was investigated by Cumpsty (ref. 36) who tested the effect of part circumference casing treatments. He tested the same skewed slot casing treatment on the same test rotor as was reported on by Smith and Cumpsty (ref. 27), in this instance using tape to seal off different circumferential extents of the casing treatment. Figure 30 shows the measured characteristics of each of the part circumference casing treatments tested. What's readily apparent from these results is that range extension and pressure rise capability are directly related to circumferential extent of coverage, and furthermore that there is little apparent dependency on which portion of the circumference is covered, as can be seen by the case with continuous 1/2 of the circumference treated

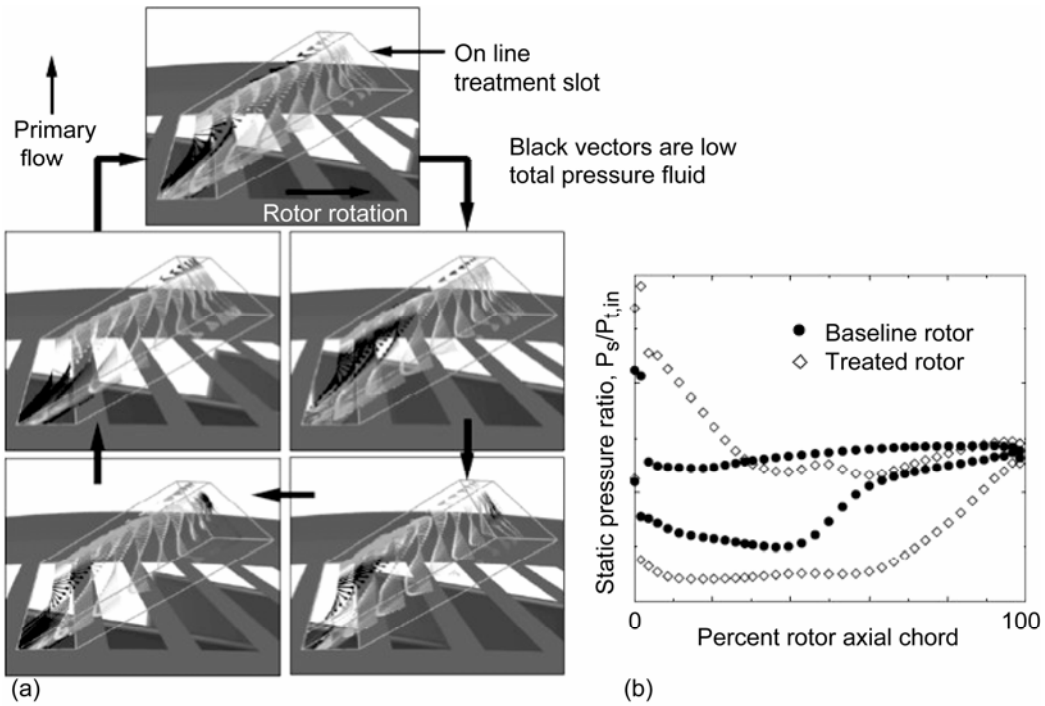

Figure 29.—Time accurate simulation of skewed slot treatment (ref. 33). (a) instantaneous view of flow in skewed slots. (b) Time averaged blade tip loading.

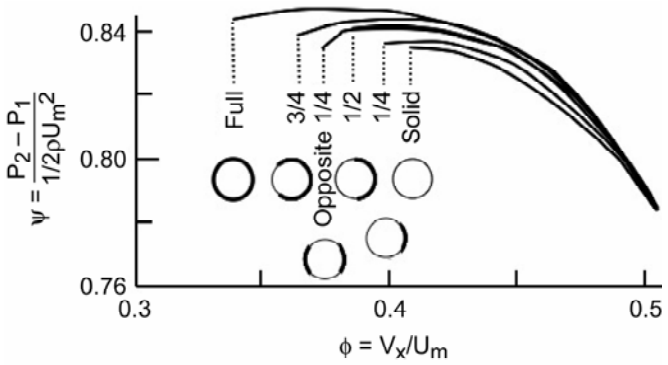

Figure 30.—Effect of part circumference skewed slot casing treatment (ref. 36).

compared to two opposite 1/4 portions of the circumference treated. Both cases exhibit a drop in total pressure at about the same flow rate, though the case of two opposite 1/4 treatments appears to actually stall at a slightly lower flow rate.

From figure 31(a) with 180° of continuous treatment we see that the measured downstream endwall displacement thickness grows in the untreated area, and grows more rapidly as flow is reduced towards stall. The treatment then acts to decrease the downstream endwall displacement thickness returning it to its original magnitude before again entering the untreated region of the circumference. With the 90° opposed treated regions (fig. 31(b)) the lesser circumferential extent of the treated region does not allow as much time for the downstream endwall displacement thickness to return to its original untreated wall value. The 270° treated region follow the 90° opposed treated region, but has remaining time to bring the downstream endwall displacement thickness back to the untreated value. Whereas the 90° opposed treatment is already entering the untreated area before fully recovering to the untreated value of the downstream displacement thickness.

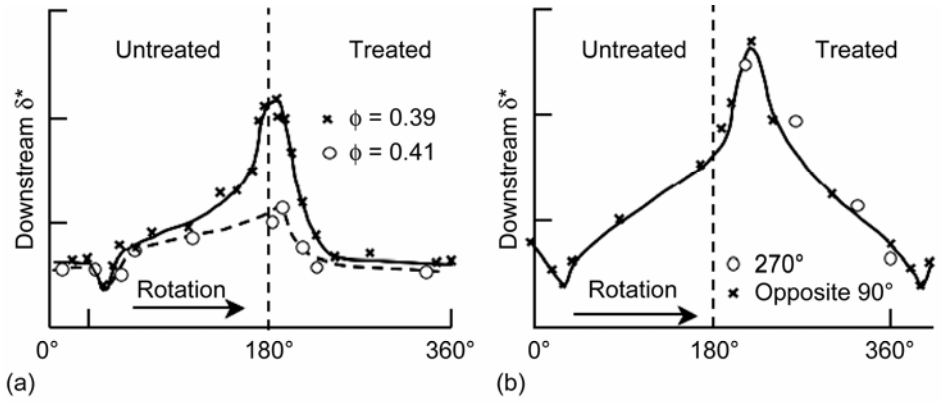

Figure 31.—Growth in downstream displacement thickness across the untreated and treated portions of the circumference for (a) 180° continuous, and (b) two 90° opposed treated regions of the circumference (ref. 36).

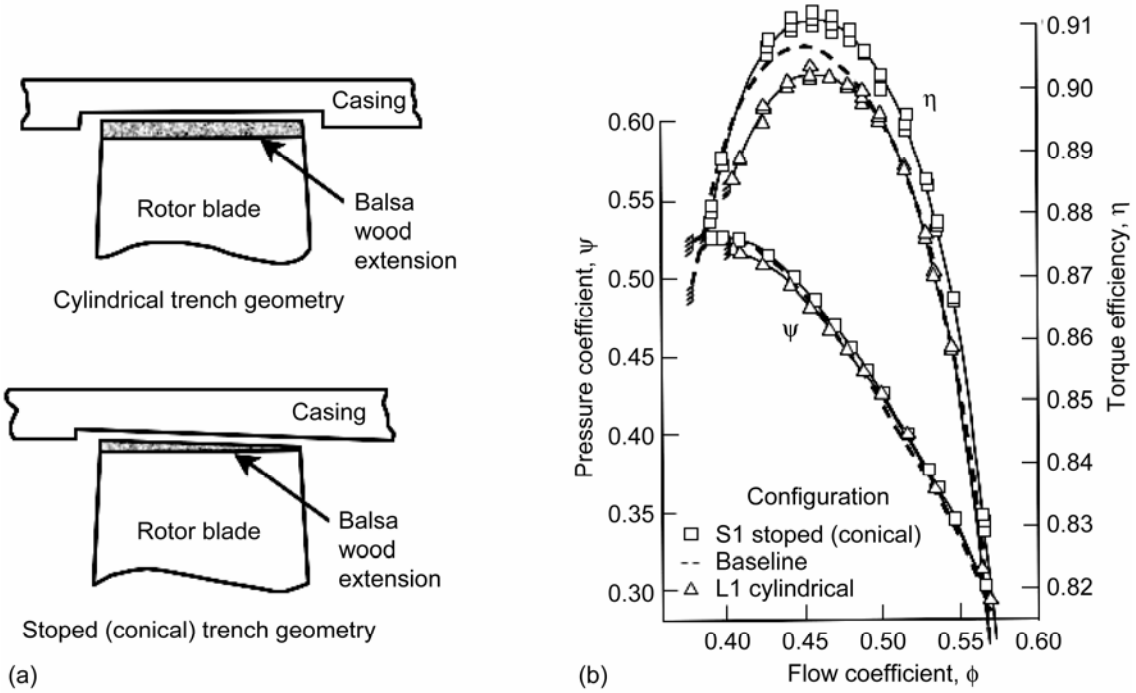

Figure 32.—Measured performance of cylindrical and sloped casing recesses compared with smooth wall for a low speed 4-stage compressor (ref. 39). (a) Cylindrical and sloped recesses. (b) Performance comparison of cylindrical and sloped casing recesses.

A simpler endwall "treatment" for expected performance benefit was proposed in a 1980 patent by Bobideau and Njiler (ref. 37), as an improved blade-tip seal to minimize the detrimental aspects of the rotor tip clearance leakage. Their blade tip seal consisted of a rectangular trench in the casing in which the rotor tip could be partially immersed, *presumably for removing or trapping the tip clearance leakage flow away from the main power stream*. Wisler and Beacher (refs. 38 and 39) recognizing the potentially detrimental aspects of the resultant forward facing step at the downstream end of the recess proposed a sloped trench concept instead and proceeded to test, in a low speed four stage compressor, various arrangements of axial extent of rectangular and sloped casing recesses, as well as extent of immersion of the rotor into the casing recess. They found that the sloped recess endwall treatment with the rotor tip line-on-line with the original casing contour provided the best performance (fig. 32) increasing efficiency

relative to the smooth wall, but without improvement in stall margin. *Though this type of endwall treatment did not prove effective for stall margin improvement it provides additional support that careful management of the endwall leakage flow is important for minimizing the typical efficiency loss of endwall treatments*. Related research investigating the impact of stepped tip gaps was reported by Thompson, et al. (ref. 40).

Based on the research investigations summarized in this section the following aspects of endwall treatments are evident, or necessary for effectiveness in extending the stable operating range of compressors:

- Efficiency decrease is proportional to stall range increase (ref. 23).
- Endwall treatments may desensitize the affects of increasing tip clearance (refs. 23 and 27).
- Endwall or blade tip stall is required for casing treatment effectiveness (refs. 24 and 27)
- Rapid accumulation of endwall blockage leads to stall (ref. 29).
- Improper orientation angle of skewed slots detrimentally impacts range and performance (refs. 25 and 26).
    - Slots must be aligned to facilitate flow entering them.
    - Angle of flow injection is important.
    - Skewed slots promote periodic suction and injection and are well suited for removal of fluid with low axial momentum.
- Slots remove high loss, high swirl flow from the rear, which is turned and reintroduced with lower swirl toward the front (refs. 27, 28, 30 to 33).
- Unsteady effects in slots of minor importance (ref. 27).
- Provision of flow path from pressure to suction surface important (ref. 27).
- Removal of blockage via suction contributes to compressor stability (refs. 30 and 31)
    - Range extension is linearly related to the suction rate with little regard to where in the passage the suction takes place.
    - Removal of blockage from the front of the passage alters the typical linear trend of range extension with rate of suction.
    - Removal of blockage from the rear of the passage is most effective.
- Injection is most effective, but dependent on where the fluid is injected. *Injection just ahead of the leakage flow where it crosses the blade tip appears most effective* (ref. 30).
- Injection appears to correlate with magnitude of streamwise injected momentum (ref. 30).
- Injection and conventional skewed slots treatments improve endwall streamwise velocity profile (ref. 30).
- Injection upstream alleviates leakage vortex by replacing with fluid that has high total pressure, and high streamwise momentum (refs. 25 to 28, 30 to 31).
- Conventional skewed endwall treatments are more effective than with augmented blowing or suction except for the high rates of suction (>5 percent) or blowing (>3 percent) (ref. 31).
- Circumferential grooves provide volume to accommodate endwall leakage flow, reducing blockage in segmented fashion (refs. 32 and 33)

To summarize:

- Enhancing compressor stability remains of considerable interest.
- Most endwall treatment provide range, but with a consequent reduction in performance commensurate with the amount of range extension.
    - *Endwall treatments are inherently a loss producing mechanism, and therefore for performance retention with range extension the treatment must reduce or eliminate a greater loss mechanism.*
    - *Careful design of casing treatments for optimum performance is essential.*
- Injection or suction can be effective means for range extension.
    - *Important to know where and how much to inject and suck.*

- *Removing fluid from the power stream is detrimental to overall engine performance, and therefore should be avoided or minimized.*

- *It's important to understand precise phenomena of stall or essential physics that limit stall range.*
- *It's important to understand the precise mechanism of endwall treatments for stall range improvement with minimum performance loss.*
- Computational analysis can be helpful for understanding fundamental physics.

2.4 Endwall Blowing/Suction and Flow Recirculation Revisited

Before proceeding to the section on Recent Advancements of casing treatments, I will briefly review some of the numerous ideas for casing treatment configurations that attempt to exploit the potential benefits of flow suction and blowing (injection). Recall that the first reported endwall treatments started off with the idea of using suction and blowing to improve the endwall condition that was responsible for setting the stall limit of tip critical compressors (figs. 2 and 3) (refs. 3, 9 to 14). In the 1990 numerous individuals began revisiting similar concepts that attempt to exploit flow removal and reinjestion (refs. 41 to 45). Most are patented ideas that to the best of my knowledge have not been reported in the open literature. Several variants of some recirculating casing treatment concepts that have been patented (refs. 41 to 43, and 45) are provided in figures 33. It's evident that characteristics of beneficial aspects of casing treatments summarized in this and the preceding section have influenced the patent concepts. Even the honeycomb treatment patent of Khalid (ref. 44) (fig. 33(c)), is attempting to provide a recirculation path to move low momentum fluid out of the passage and then reinject in a beneficial manner back into the passage. The patent concepts of Koff, et al. (refs. 41 and 42) and Nolcheff (ref. 43), (fig. 33(a) and (b)), are either using vanes to guide

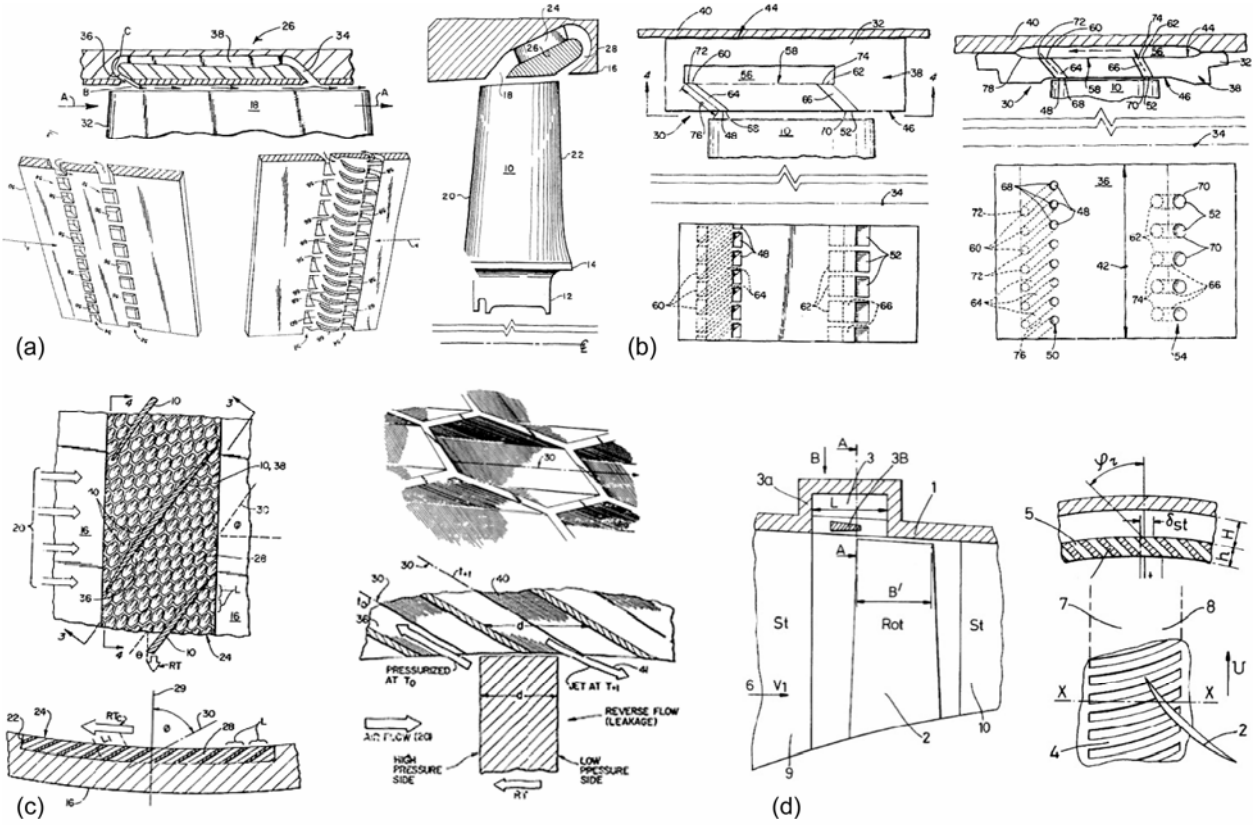

Figure 33.—Examples of patented recirculating casing treatment concepts (refs. 41 to 45). (a) Recirculating casing treatment patents of Koff, et al. (refs. 41 and 42). (b) Casing treatment recirculation patent of Nolcheff (ref. 44). (c) Blade pressure to suction surface recirculation patent of Khalid (ref. 45). (d) Recirculating casing treatment concept of Glemedov, et al. (ref. 36).

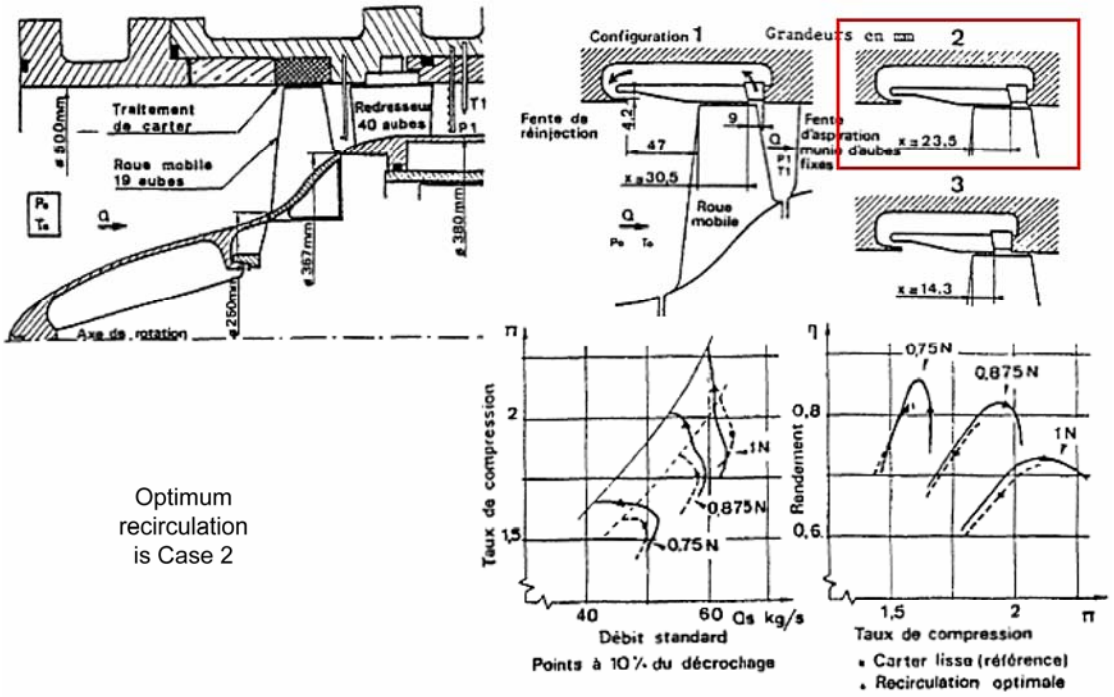

Figure 34.—Measured benefits of different endwall flow recirculation concepts (ref. 46).

the fluid extracted from the flow toward a favorable angle before reintroducing back into the power stream, or providing flow aligned slots or holes to guide the fluid to a plenum before guiding the flow back for reintroduction into the power stream. The patent concept of Gelmedov, et al. (ref. 45), employs a large cavity over the blade leading-edge region, similar to that tested by Azimian, et al. (ref. 34), to allow low momentum fluid from a stall cell to enter and exit the cavity, and for this concept, guided by axially curved, radially skewed slots.

The first reported experimental investigation of the benefits of circumferentially continuous endwall recirculation, as well as independent suction and injection, were reported by Janssens, et al. (ref. 46). The high-speed compressor tested had considerable hub ramp with 1.64 Mach at the rotor tip. They initially tested different recirculation concepts on the transonic rotor, and measured range extension (14 to 16 percent), pressure ratio increase (10 to 18 percent), and efficiency improvement (0.6 to 5 percent), with decreasing benefits as speed increased from 75 to 100 percent, for the optimum recirculation configuration that bled flow from a region just upstream of the rotor trailing edge and reinjected it along the casing endwall upstream of the rotor (fig. 34). Not all recirculation configurations yielded performance benefits, though all provided increased stall range.

The authors also tested different independent suction and injection locations finding that suction provided stall range increase for all cases tested, but efficiency benefit was dependent on the suction location, with the optimum suction location being just aft of about mid rotor tip chord, but not encompassing the rotor trailing edge region (fig. 35). Injection hurt efficiency for both cases investigated, with the best location injecting closer to the rotor leading edge.

The authors concluded that for the mediocre performance of the tested compressor that all treatments were capable of providing range extension, and with careful experimentation it was possible to achieve increased stall range with increased pressure rise and efficiency. They found recirculation to be the best performing, with suction only of less benefit and injection only of even lesser benefit. The authors also concluded that such treatments may be effective only after optimizing via experimentation, and therefore to retain or improve performance while extending the stall range of the compressor would require a tedious systematic (essentially a cut-and-try) experimental approach.

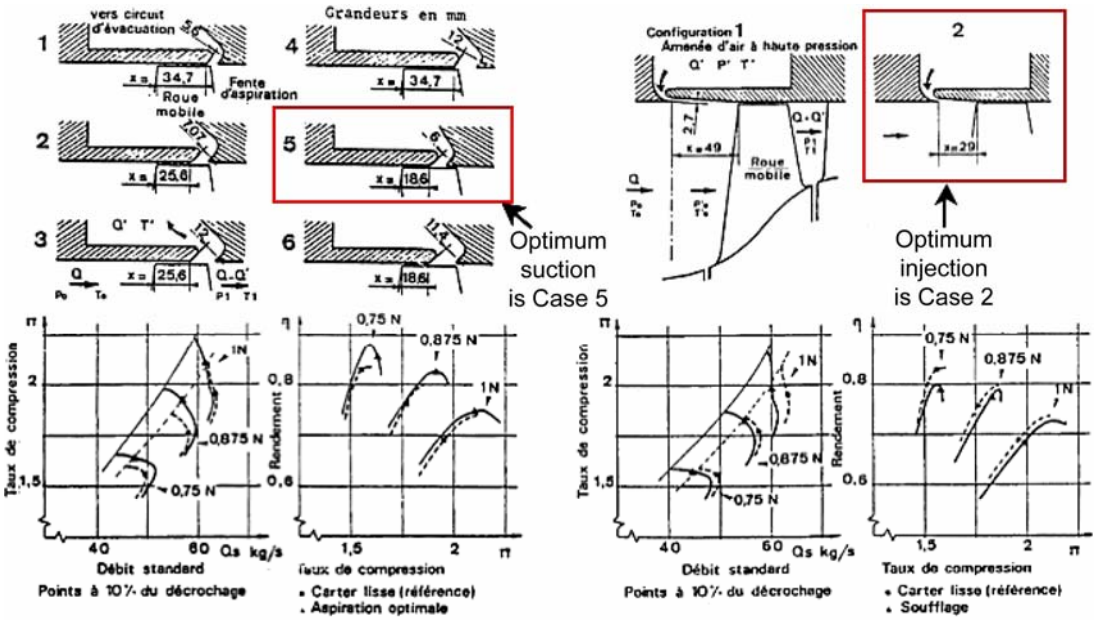

Figure 35.—Measured benefits of different endwall suction or injection locations (ref. 46).

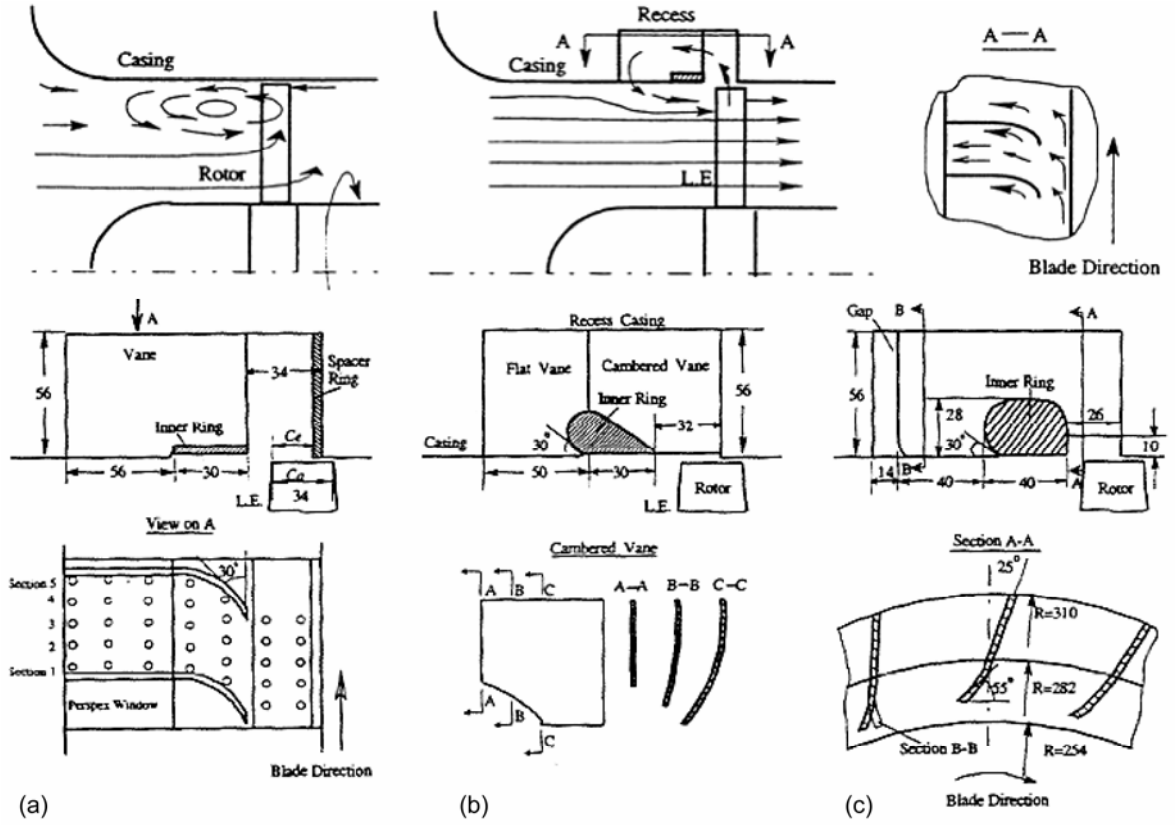

Figure 36.—Recirculating casing treatment concept (refs. 34, 47, and 48) and geometry of tested configurations (ref. 48). (a) Configuration 1. (b) Configuration 2. (c) Configuration 3.

Another recirculating casing treatment concept first proposed in a patent by Ivanov (ref. 47) for performance improvement of ventilation fans, and later tested by Azimian, et al. (ref. 34) in a low speed compressor with representative blade loadings of aero-engine compressors, was also tested by Kang, et al. (ref. 48) with different arrangements of elements of the recirculating casing treatment design (fig. 36).

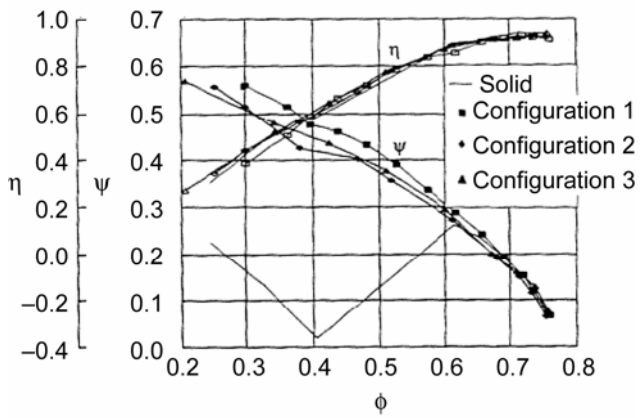

Figure 37.—Measured performance benefits of the recirculating casing treatment concept tested in a low speed compressor by Kang, et al. (ref. 48).

The concept is designed to provide a path for low momentum high swirl fluid from a growing stall cell to be moved out of the power stream and with stationary guide vanes to remove the tangential flow component before the flow is returned back into the flow path. Though there is considerable more work to be done for application to transonic high loaded aero-engine compressors this recirculation concept has shown promise for range extension, with minimal or no loss in performance, in low speed compressor tests employing blades with loading typical of aero-engine compressors (fig. 37). The principal mechanism for range extension was attributed to removal of the low momentum flow from the rotor tip region into the recess provided, and elimination of the swirl by the recess vanes before returning the flow to the main flow path.

3. Recent Advancements

This section provides an overview of some of the recent advancements in endwall stall control technologies and what has been learned from these investigations. The primary concepts to be discussed are from the investigations reported by researchers at the NASA Glenn Research Center (GRC), and co-located therein, the Army Vehicle Technology Directorate (VDC); Insight into the flow mechanism of circumferential grooves, development of discrete tip injection stall control technology, advancements in understanding of recirculating casing treatment concepts, and recent results of a stage recirculation concept. Other related research investigations will be presented and discussed where appropriate. The recent related recirculating casing treatment investigations of Wilke and Kau (ref. 49) is the subject of the following lecture in this series and will be discussed in detail by the authors themselves.

3.1 Circumferential Grooves

The recent reported results of Shabbir, et al. (ref. 50) provide further insight into the flow mechanism of circumferential groove casing treatments. To my knowledge circumferential grooves is the only endwall treatment for compressor stability enhancement ever employed in a production engine (e.g., the JT9D). A set of design rules for circumferential groove casing treatments were summarized and reported by Prince, et al. (ref. 20) (pages 7 and 8) of these notes, and were followed for the circumferential groove casing treatment employed over the first blade row of a low speed multistage compressor. For computational expediency Shabbir, et al. simulated the first rotor in isolation both with and without casing treatment. The overall performance predictions for three different groove aspect ratios (3-groove depths at constant width) are shown in figure 38. The insensitivity of stall margin improvement with increasing aspect ratio beyond 2.0 is consistent with unpublished experimental measurements by Prahst (ref. 51).

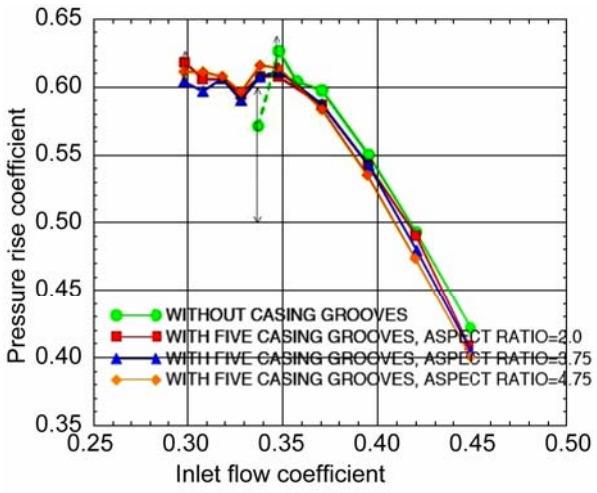

Figure 38.—Predicted operating characteristic of low speed rotor with and without circumferential groove casing treatment (ref. 50).

Shabbir, et al. (ref. 50) hypothesized that the "circumferential groove casing treatment reduces the growth rate of flow blockage relative to a smooth casing," and that the growth rate is "controlled by the near casing flow field over the rotor tip". To prove the hypothesis they analyzed the near casing flow field to quantitatively assess the relevant flow mechanism of circumferential grooves relative to the smooth wall casing. They utilized the equations of motion to analyze the contributions of various terms in the axial momentum equation. Since the focus of their hypothesis was that circumferential grooves controlled blockage growth in the near wall flow field over the rotor tip they considered a control volume circumferentially bounded by the rotor tip blade pitch, axially extending just upstream and downstream of the rotor blade tip, and radially bounded by the wall and first grid cell from the wall. The stresses include both viscous and Reynolds stresses as approximated by an eddy viscosity model (ref. 52).

Summing the various terms of the axial momentum equation on all axial and tangential surfaces bounding the control volumes illustrated in figure 39 yields the following equation:

$$\sum_{\theta,z}\Delta\left(\rho V_z V_r A_r\right)+\sum_{\theta,z}\Delta\left(\rho V_z V_\theta A_\theta\right)+\sum_{\theta,z}\Delta\left(\rho V_z V_z A_z\right)+\sum_{\theta,z}\Delta\left(PA_z\right)=$$
$$\sum_{\theta,z}\Delta\left(\tau_{rz}A_r\right)+\sum_{\theta,z}\Delta\left(\tau_{\theta z}A_\theta\right)+\sum_{\theta,z}\Delta\left(\tau_{zz}Az\right) \qquad \text{(1) (ref. 50)}$$

In the limit as of the radial thickness of the control volume goes to zero, most of the terms of equation (1) go to zero, with the exception of the axial pressure force which is balanced by the wall shear force (fig. 39(a)). For the grooved casing the remaining terms of equation (1) are the same as for the smooth wall case with the exception of an additional term which accounts for the radial transport of axial momentum across the grooves, as indicated in figure 39(b). Using the results of the isolated rotor predictions with and without casing grooves, Shabbir, et al. analyzed the various terms of the axial momentum equation for the control volumes indicated in figure 39. For the smooth wall casing the results of the various terms which contribute to the axial momentum balance are indicated in figure 40 for two operating conditions, one away from stall and the other at the near stall. As can be clearly seen from the results of the analysis of the magnitude of the terms of equation (1), shown in figure 40, the main terms balancing the axial momentum equation are the axial pressure force and the net axial shear force on the radial faces of the control volume, all other terms are zero expect for a small contribution from the radial transport of axial momentum due to the finite radial thickness of the control volume. A Δr goes to zero the radial transport of axialmomentum goes to zero, and the net axial pressure force is completely balanced by the net axial shear force.

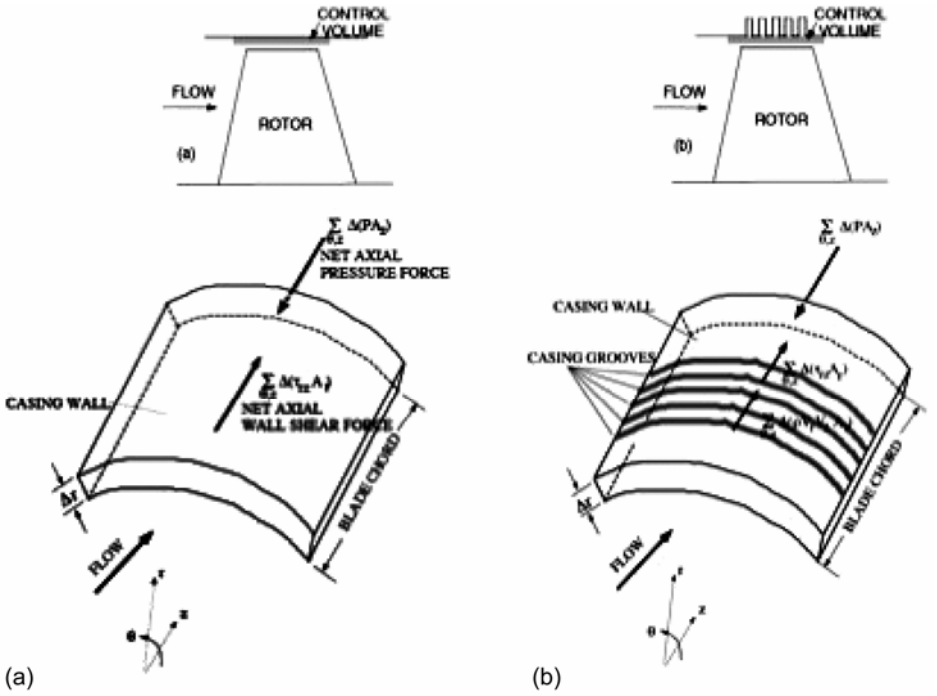

Figure 39.—Sketch illustrating control volume and balance of axial momentum equation for the smooth and grooved casing walls (ref. 50). (a) Smooth wall casing. (b) Grooved wall casing.

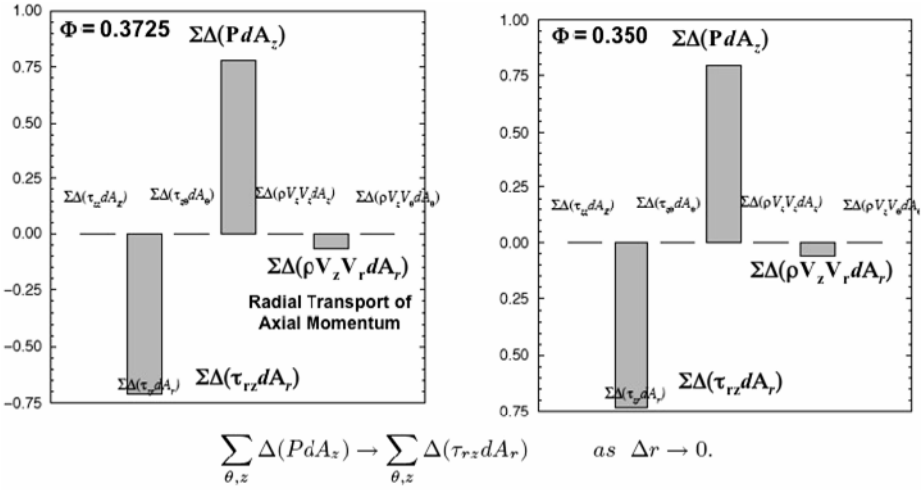

$$\sum_{\theta,z} \Delta(P dA_z) \rightarrow \sum_{\theta,z} \Delta(\tau_{rz} dA_r) \qquad as \quad \Delta r \rightarrow 0.$$

Figure 40.—The balance of the terms of the axial momentum equation for the smooth wall casing at two operating conditions, away from stall, Φ = 0.3725, and near stall, Φ = 0.350. The symbol Σ denotes summation over the axial and tangential surfaces bounding the control volume indicated in figure 39(a) (ref. 50).

However, unlike the smooth casing the grooved casing has regions along the wall, the groove gap, where there is provision for radial transport of flow, as indicated by the predicted results shown in figure 41. The predictions clearly show fluid moving into and out of the circumferential groove slots, which can thus be expected to contribute additional terms to balance the axial pressure force (fig. 42). As can be seen from the results of the analysis of the magnitude of the terms of equation (1) for the control volume of figure 39(b) (fig. 42), the circumferential grooves contribute radial transport of axial

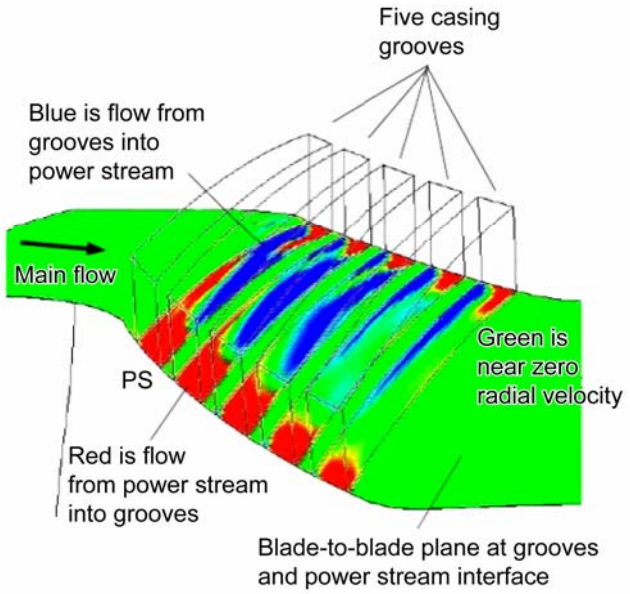

Figure 41.—Radial velocities in the circumferential grooves transport of momentum across groove openings (ref. 50).

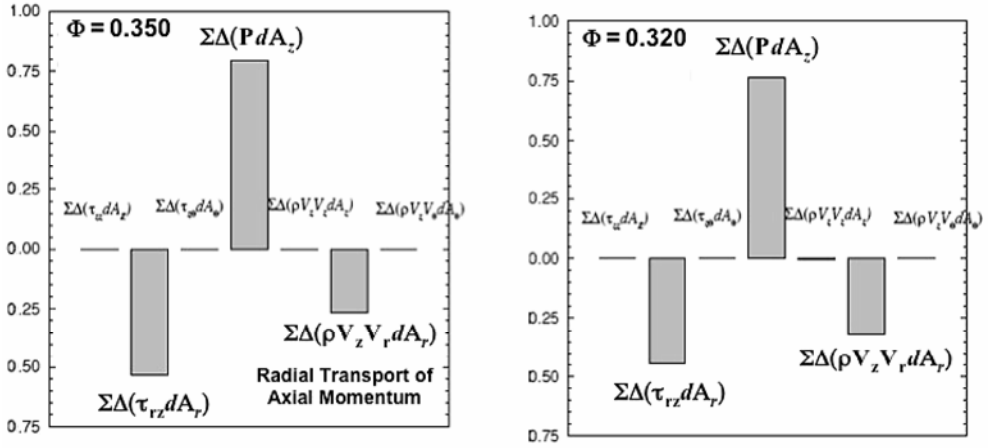

$$\sum_{\theta,z} \Delta(P dA_z) \rightarrow \sum_{\theta,z} \Delta(\tau_{rz} dA_r) - \sum_{\theta,z} \Delta(\rho V_r V_z dA_r) \qquad as \quad \Delta r \rightarrow 0.$$

Figure 42.—The balance of the terms of the axial momentum equation for the grooved casing at two operating conditions, a the smooth wall stall point, Φ = 0.350, and near the groove casing stall point, Φ = 0.320. The symbol Σ denotes summation over the axial and tangential surfaces bounding the control volume indicated in figure 39(b) (ref. 50).

momentum as well as the axial shear force to balance the axial pressure force. The magnitude of the axial shear force has decreased commensurate with the increase in the term associated with the radial transport of axial momentum. As the compressor is then throttle lower in flow than was possible for the smooth wall case we can clearly see that in order to maintain the axial momentum balance the term corresponding to the radial transport of axial momentum is increasing as the axial shear force is decreasing, together balancing the axial pressure force and maintaining the compressor stability.

Shabbir, et al. then further analyzed the simulation results with the aid of equation (1) to assess the contributions of the various terms to the axial momentum balance as a function of the rotor axial chord distance from the rotor leading edge. The results for the smooth wall case are shown in figure 43.

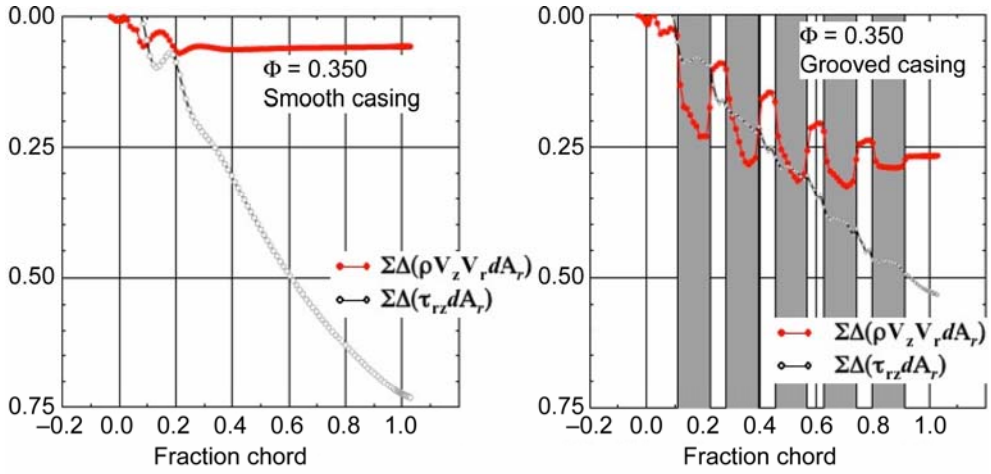

Figure 43.—Evaluation at the smooth wall stall point, Φ = 0.350, of the cumulative sum in the axial direction of the axial shear force and the radial transport of axial momentum for the respective control volumes of the smooth and grooved casings shown in figure 39 (ref. 50).

For the smooth wall casing, the axial pressure force is balanced by the axial shear force on the radial faces of the control volume shown in figure 39(a), and increases in magnitude with axial distance, commensurate with the increasing pressure rise across the rotor. The small contribution of the radial transport of axial momentum is due to the finite radial thickness of the control volume and remains essentially constant with axial distance. For the grooved casing the contribution of axial shear force has decreased and is being replaced now by the radial transport of axial momentum across each groove. The radial transport of axial momentum does not completely return to zero on the lands between the grooves due to the small radial extent of the control volume. It is clear though that each groove is contributing axial momentum force, which along with the axial shear force balances the axial pressure force. Figure 43 provides evidence that the flow mechanism of circumferential grooves is to provide radial transport of axial momentum, which can thus contribute to the axial momentum balance to support the axial pressure gradient, and thus extend the stable operating range of the compressor.

To support the author's hypothesis that the circumferential grooves reduce the growth of endwall blockage to provide range increase contour plots of normalized axial velocity are shown in figure 44 for two operating conditions both with and without circumferential grooves. The simulation results for the condition away from stall, Φ = 0.3725, show comparable flow blockage (ref. 29) predictions of 7.68 and 7.30 percent for the smooth and grooved casing, respectively. However, as the rotor simulation is throttled towards the stall point of the smooth wall, Φ = 0.350, the flow blockage for the smooth wall grows to 12.27 percent while for the same operating condition the grooved casing flow blockage grows to only 9.57 percent. Figure 45 shows the predicted growth in flow blockage as a function of inlet flow coefficient. These results clearly show a predicted rapid growth in flow blockage as the rotor is throttled to the stall point and beyond. The grooved casing, however, maintains a reduced rate of flow blockage with reductions in inlet flow coefficient, thereby enabling a lower mass flow rate to be achieved that was possible for the smooth casing. These results lend support to the author's hypothesis that circumferential grooved casing treatment reduces the growth of endwall flow blockage as a result of the flow mechanism of radial transport of axial momentum.

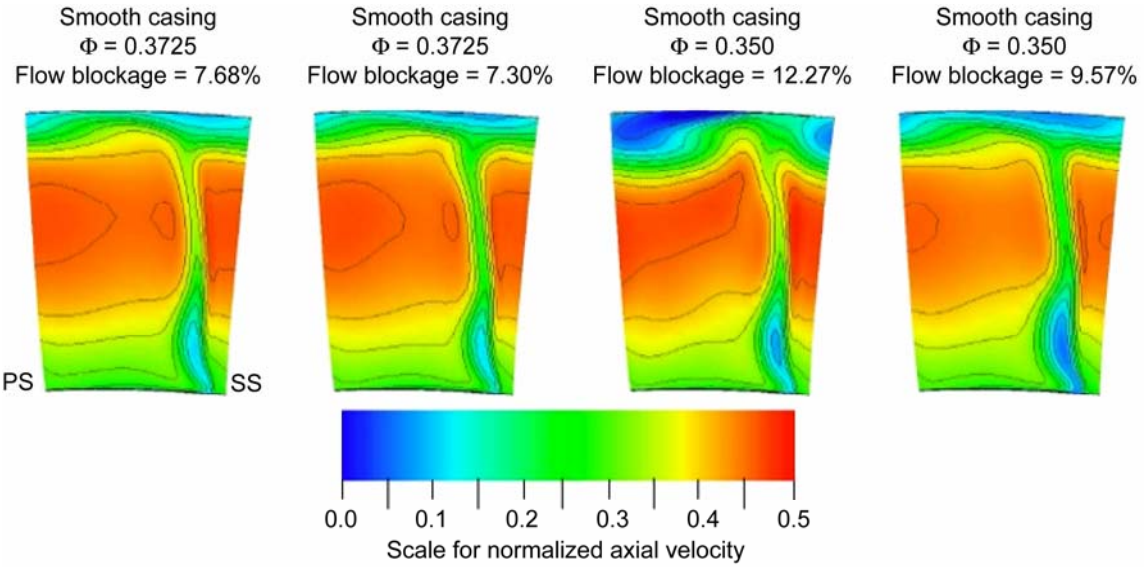

Figure 44.—Normalized axial velocity contours in an axial plane just downstream of the rotor trailing edge for smooth and grooved casings at two flow condition, a flow condition away from stall, Φ = 0.3725, and at the smooth wall stall point, Φ = 0.350 (ref. 50).

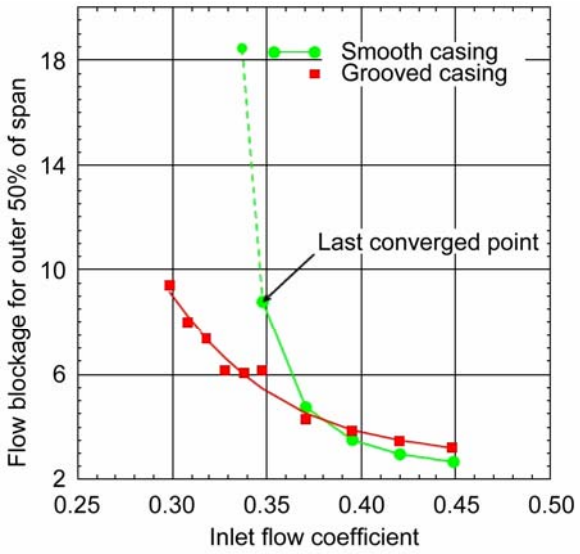

Figure 45.—Predicted growth of flow blockage (ref. 29) as function of flow coefficient for smooth and grooved casings (ref. 50).

Examining the results of the predicted cumulative sum in the axial direction of the axial shear force and the radial transport of axial momentum for the grooved casing control volume (fig. 39(b)), at the near stall condition for the grooved casing, the authors noted that the last groove contributed very little to the axial momentum balance (fig. 46(a)). As a result they removed the last groove from the simulation and reconverged the results to predict if the compressor would remain stable with only the first four grooves. A comparison of the predicted operating characteristics for five grooves and for just the first four grooves is provided in figure 46(b). The predictions confirm that the last groove contributed little to the stability of the rotor, as both characteristics are essentially the same for the five and four groove cases. This adds credibility to the author's analyses of the near wall flow field over the rotor and the contributions of the axial shear force and radial transport of axial momentum across the grooves in supporting the axial pressure gradient.

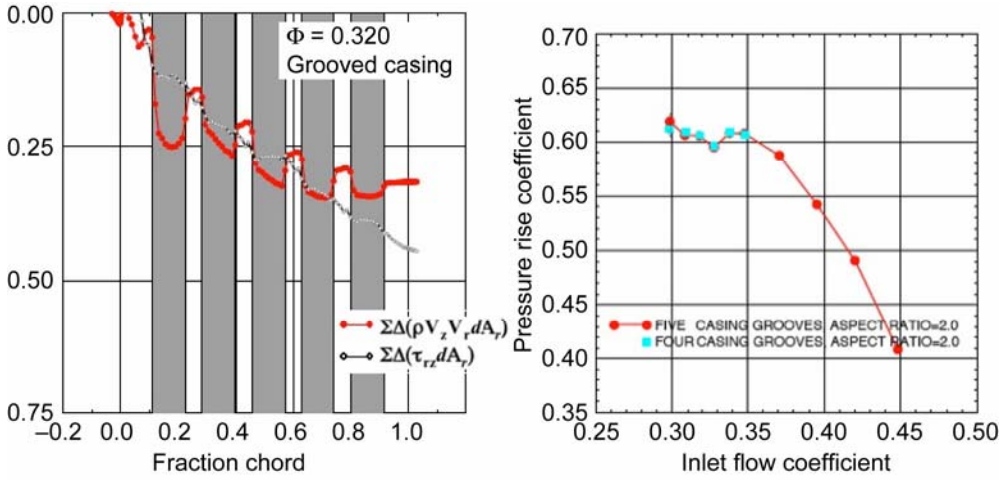

Figure 46.—Evaluation at the smooth wall stall point, Φ = 0.350, of the cumulative sum in the axial direction of the axial shear force and the radial transport of axial momentum for the respective control volumes of the smooth and grooved casings shown in figure 39 (ref. 50). (a) Cummulative contribution of axial momentum terms. (b) Comparison of predicted operating chacteristic with five and four grooves.

3.2 Development of Discrete Tip Injection Stall Control Technology

The development of discrete tip injection stall control technology grew out of research on active stall control technology led by researchers from the Massachusetts Institute of Technology (MIT) (refs. 53 to 57) in collaboration with researchers from the NASA Glenn Research Center's Controls and Dynamics and Compressor branches who provided controls and compressor expertise and test support to demonstrate the MIT active stall control technology. The MIT stall control technology was based on the hypothesis that cancellation or prevention of the growth of stall precursor waves indicative of the onset of stall would stabilize the compression system thereby enabling stall range extension. The active stall control technology was demonstrated on a transonic compressor which included high response static pressure transducers located around the periphery of the annulus to sense modal "precursor" waves, and via a feedback control loop connected to multiple discrete injectors equally spaced around the periphery of the casing upstream of the rotor which were sequentially pulsed to generate a wave out of phase with the modal waves to suppress or cancel the growth of the modal instability waves. This was expected to stabilize the compressor and provide increased stall range. A schematic of the active stall control concept is shown in figure 47. The injectors were setup to allow dual sided control capability by allowing a steady mean flow from the injectors from which the actuators would provide superimpose an alternating pressure wave to cancel the modal waves. The steady flow itself was found to provide significant stall range increase (fig. 48), which led to further investigations of the steady benefits of discrete tip injection by the compressor research personnel from the NASA Glenn Research Center (refs. 58 and 59) while the MIT research team in collaboration with the NASA team continued to pursue active feed-back control technology compressor stability enhancement.

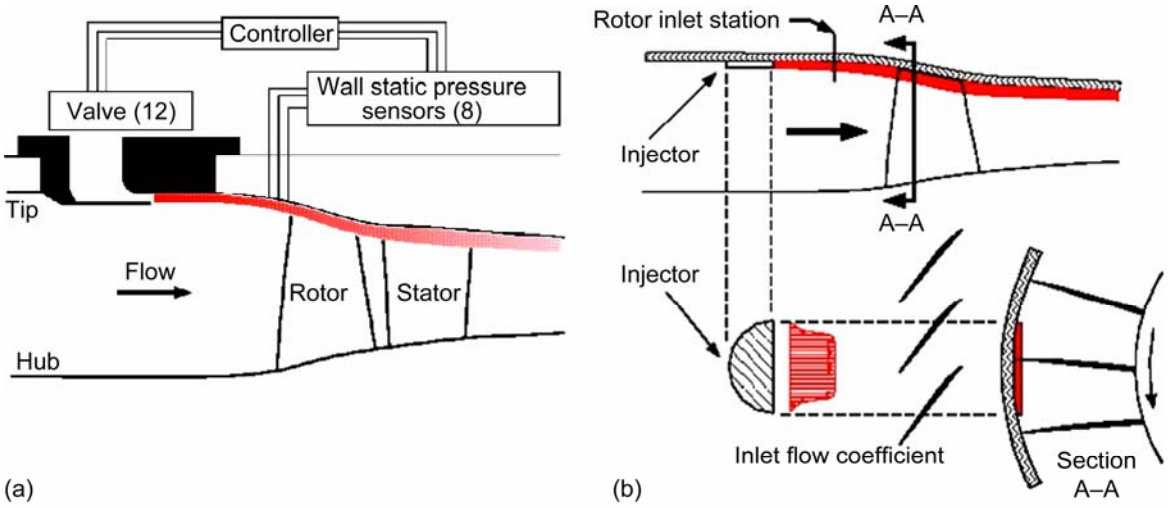

Figure 47.—Schematic of setup for active control technology (refs. 53 to 57) that led to the development of discrete steady tip injection stall control technology (refs. 58 and 59). (a) Feedback control setup for discrete tip injection. (b) Circumferential layout for 12 equally spaced discrete tip injectors.

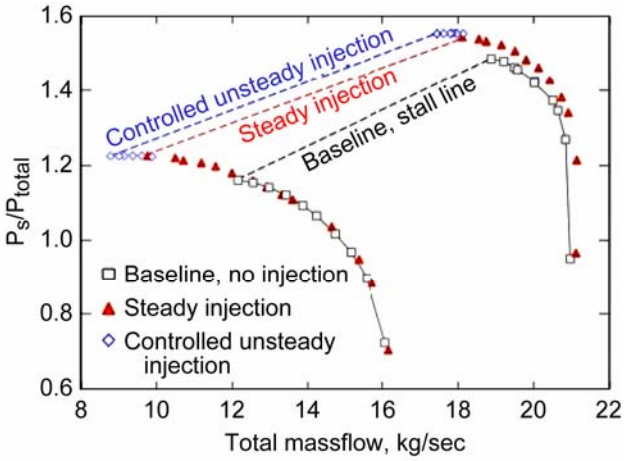

Figure 48.—Measured range extension of a transonic compressor stage due to discrete steady tip injection compared to controlled unsteady injection (ref. 59).

To study the fluid mechanic process by which tip injection increases the stable operating range of a compressor, time-averaged CFD simulations were conducted (ref. 58) which modeled the tip-injection using a source term model (ref. 60). The simulation results predicted range extension with steady discrete tip injection commensurate with the experimentally measured range extension (fig. 49(a)). Furthermore, the predictions indicated that the effectiveness of the steady discrete tip injection increased when the circumferential extent of the injectors was reduced by 50 percent (half versus full). For the same injected flow rate reducing the injector width by 50 percent essentially doubled the injected velocity and momentum and thereby increased the stall range extent and max pressure ratio beyond what was available with the full width injectors. The predictions indicate that at the near stall condition for the no-injection case, operating point 1 in figure 49(b), discrete tip injection, operating point 2, decreases the incidence angle and diffusion factor near the rotor endwall, with the remainder of the span essentially unaffected by the tip injection. The diffusion factor is based on two-dimensional cascade thinking and therefore is only an approximate indicator that tip injection may be reducing the diffusion near the rotor casing endwall.

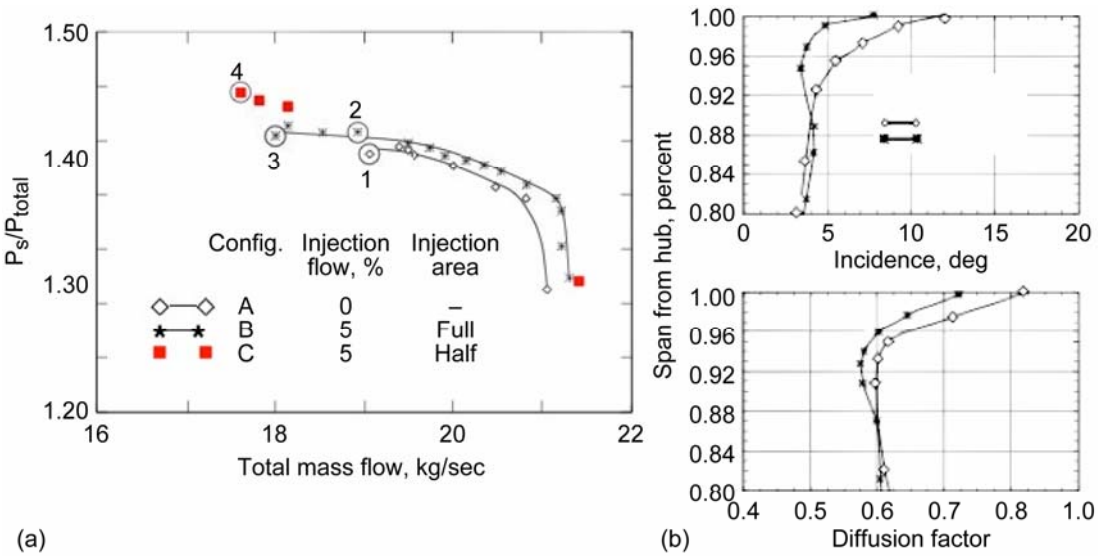

Figure 49.—Predicted design speed lines and rotor tip incidence and diffusion factor with and without steady discrete tip injection (ref. 58). (a) Predicted design speed characteristic with and without steady discrete tip injection. (b) Predicted impast of steady discrete tip injection on rotor tip flow.

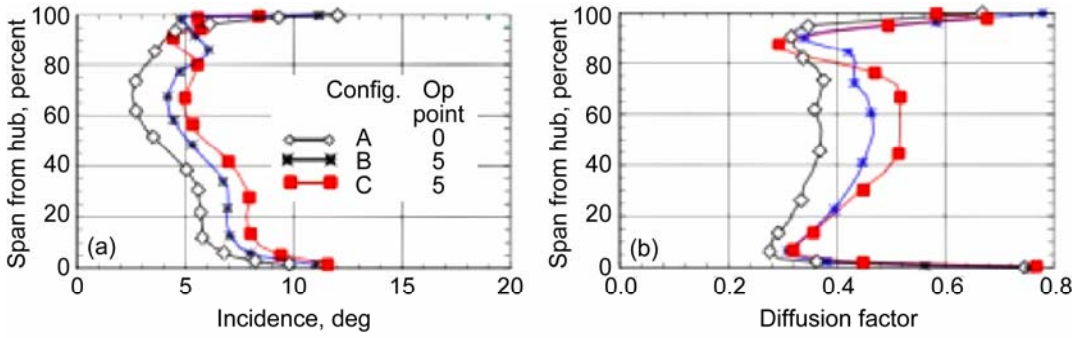

Figure 50.—Predicted spanwise distribution of rotor (a) incidence angle and (b) diffusion factor for the near stall operating points (1, 3, and 4) of configurations A, B, and C, respectively, as indicated in figure 49 (ref. 58).

A comparison of the spanwise distributions of incidence angle and diffusion factor for operating points 1, 3, and 4, corresponding to the near stall points for the no-injection, full injection, and half injection cases, respectively, are shown is figure 50. The configurations with injection are operating at substantially lower mass flow rates than the baseline case, as evidenced by the increased incidence and diffusion factors below 90 percent span. At the baseline stalling mass flow rate the lower portion of the blade span is evidently not close to stall, and therefore with steady discrete tip injection stabilizing the rotor endwall flow the remainder of the span is able to throttle to much lower flow rates than was achievable for the baseline case without tip injection.

Experimental confirmation of the predictions is provided in figures 51 and 52, which show the experimentally measured performance at 70 and 100 percent speed with and without tip injection, figure 51, and the measured spanwise distribution of diffusion factor at 70 percent speed for operating conditions 1 and 2 (fig. 52(a)), and 1 and 3 (fig. 52(b)) (fig. 51). In this case range extension is provided from 3, 4, and 6 injectors where the injectors are operating at their maximum (choking) flow rate. To test the predicted behavior that steady discrete tip injection provides stall range extension by unloading the rotor tip, Suder, et al. (ref. 59) grouped six injectors together so that one half of the circumference consisted of 6 injectors spaced 30° apart and the other half had no injectors. The experimentally measured stall range extension, $\phi_{stall} = ((\phi_{stall})_b - (\phi_{stall}))/(\phi_{stall})_b$ where $((\phi_{stall})_b$ is the baseline (no injection) stalling flow coefficient, was found to be independent of the circumferential arrangement of injectors (fig. 53).

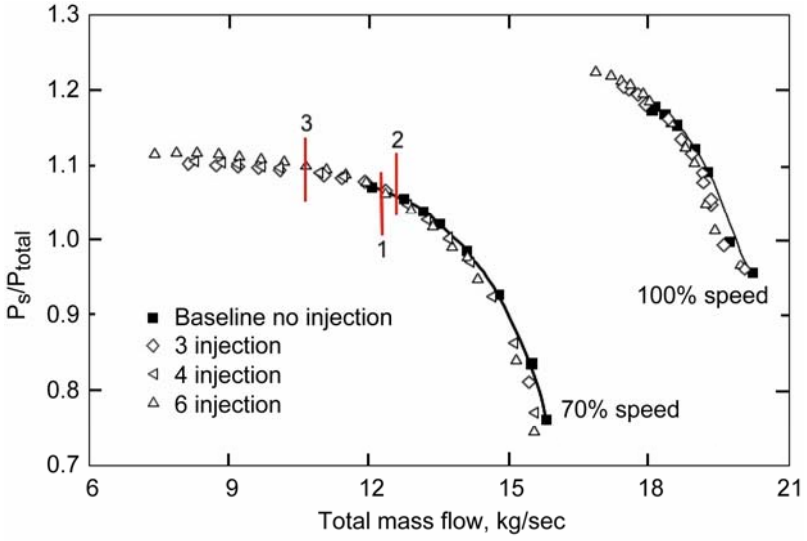

Figure 51.—Experimentally measured 70 and 100 percent speed operating characteristics of a transonic compressor stage with and without steady discrete tip injection (ref. 59).

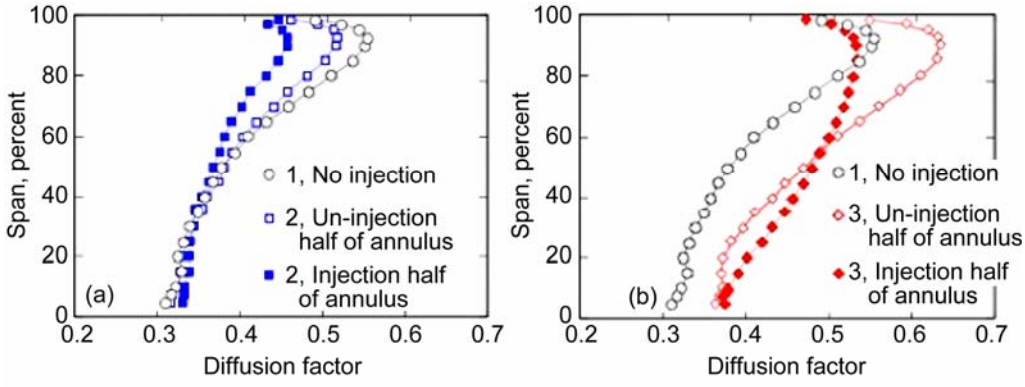

Figure 52.—Comparison of spanwise distributions of diffusion factor at different operating conditions, see figure 51, determined experimentally at locations within the injected and uninjected half of the annulus, and without injection (ref. 59). (a) Comparison at baseline stall condition, points 1 and 2. (b) Comparison at operating points 1 and 2.

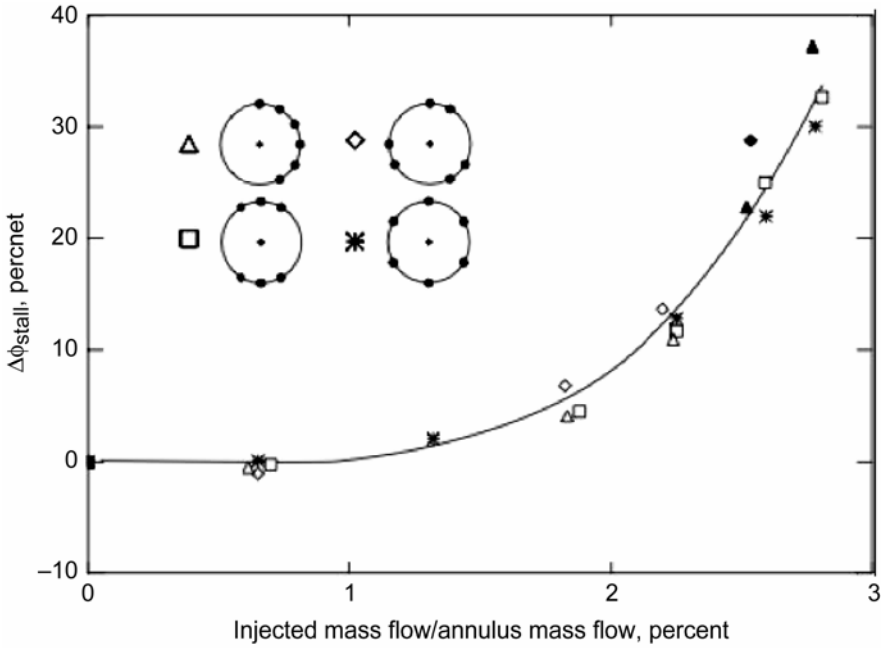

Figure 53.—Stall range increased measured to be independent of circumferential arrangement of injectors (ref. 59).

Spanwise surveys of total pressure, total temperature and flow angle were then acquired at two locations downstream of the rotor, one in the injected half of the circumference and the other in the uninjected half. The surveys were conducted at the operating conditions (1, 2, and 3) indicated in figure 51. With the injectors choked the total injected massflow rate was 2.8 percent of the annulus flow. From a comparison of the experimentally determined spanwise distribution of diffusion factor at operating points 1 and 2 of figure 51, corresponding to the baseline stall point, the diffusion factor peaks at 90 percent span, indicating the rotor is tip critical, with the no-injection case having the highest diffusion factor and the case in the uninjected half of the circumference being of similar magnitude (fig. 52(a)). For the results within the injected half of the circumference the diffusion factor has been reduced significantly (fig. 52(a)), as was indicated by the predictions shown in figure 49(b), confirming that steady tip injection unloads the rotor tip.

As the compressor is then throttled to flow rates below the baseline stall point the diffusion factor across the span would be expected to then increase as was predicted (fig. 50). Figure 52(b) shows a comparison of the spanwise distribution of experimentally determined diffusion factor at the baseline stall point and at a mass flow operating condition below the baseline stall point, operating points 1 and 3, respectively (fig. 51). The diffusion factor for the no injection and uninjected half of the circumference is the same at the hub, and increases across the span towards the rotor tip. The peak diffusion factor in the injected half of the circumference remains below the peak diffusion factor for the no injection case even though the peak diffusion factor for the uninjected case considerably exceeds the peak diffusion factor for the no injection case. This indicates that the stability of the compressor is controlled by the peak diffusion factor in the injected half of the circumference where the diffusion factor remains below the peak diffusion factor for the no injection case. It is clear that injection reduces the tip loading thereby increasing the stall range of the compressor.

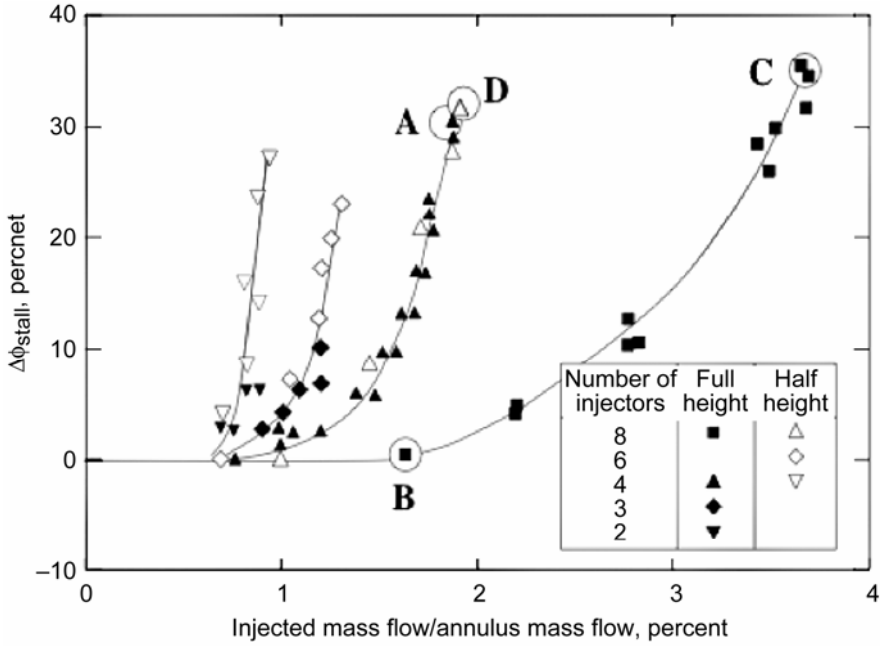

Figure 54.—Measured range extension at 70 percent speed for various number of full- and half-height injectors (ref. 59).

Suder, et al. tested various number of full and half height injectors in attempt to determine if there were a correlation of stall range increase with total injected mass flow rate, total injected momentum, mass flow rate per injector, momentum per injector, or injector exit velocity (fig. 54) and table 1. The results of comparisons of parameters indicated in table 1 against the measured range extension shown in figure 54 indicates that stall range extension may correlate with injector exit velocity. The results of figure 54 also indicate that high injector exit velocity is a key attribute for increased effectiveness. Injecting flow through a few injectors at high velocity (e.g., 4 half height injectors) is almost as effective as using many injectors at low velocity (e.g., 8 full height injectors), and requires only about 1/4 the total injected mass flow rate. For all injector configurations tested the maximum stall range extension was limited by the choke flow rate of the injectors.

TABLE 1.—SUMMARY OF PARAMETERS COMPARED FOR CORRELATION WITH STALL RANGE INCREASE (FIG. 54) FOR IDENTIFICATION OF COMPARISON CASES. STALL RANGE INCREASE APPEARS TO CORRELATE WITH INJECTOR EXIT VELOCITY

Injected parameter	Comparisons	Range increase
Total massflow	A = B = C	B<<A or C
Total momentum	C = 2*A	C = A
Massflow per injector	B = D	B<<D
Momentum per injector	A = 2*D	A = D
Injector exit velocity	**A = C = D** **B<<A,C or D**	**A = C = D** **B<<A,C or D**

In order to verify that the injector exit velocity correlates to range extension, the data shown in figure 54 are analyzed in terms of the axial velocity mass averaged over the radial extent of the injectors (the outer 6 percent of the annulus height). The mass averaged axial velocity is defined as:

$$\overline{V_z} = \frac{\left[\rho_i\left(N*W*V_i^2\right)+\rho_c\left(\pi D - N*W*V_c^2\right)\right]}{\rho_i\left(N*W*V_i\right)+\rho_c\left(\pi D - N*W\right)*V_c\right)} \qquad (2)\ (\text{ref. 59})$$

where N is the number of injectors, W is the injector width, and D is the annulus diameter. V_i and ρ_i are the injected flow velocity and density, respectively, and V_c and ρc are the annulus flow velocity and density at 9 percent span (the center of the injector height). This is a rather simple approximate analysis that does not account for mixing of the injector with the core flow, but acknowledges that with decreasing injector count the fraction of time the rotor is bathed in injected flow decreases, and vice versa. Results of figure 54 are replotted in figure 55 as a function of $\overline{V_z}/U_{\text{tip}}$ for the 70 percent speed cases (fig. 55(a)), and the 100 percent speed cases (fig. 55(b)). These results lend credence to the assessment from the cases analyzed in figures 49 to 52 and 54 and table 1 that stability enhancement is directly related to the increase in the mass averaged axial velocity at the rotor tip, which acts to unload the rotor tip and reduce the flow blockage buildup therein. Since the tested rotor is tip critical, all of these effects allow increased blade tip loading before the blade stalls, thereby enabling a reduction in the stalling mass flow.

Suder, et al. (ref. 59) also investigated the applicability of steady discrete tip injection stall control technology for stall recovery, and for stage matching at part speed operating conditions. The stall recovery potential of steady discrete tip injection stall control technology was investigated for both 70 and 100 percent design speed conditions in two different scenarios: 1) with the injectors turned off, throttling the compressor into stall, and then activating the injectors with no change in throttle setting, and 2) with the injectors turned on, throttling the compressor to a mass flow rate below the baseline (non-injected) stall point, and then with no change in throttle setting turning the injectors off, and then turning them back on again. The results of a stall recovery test of type 1) is indicated in figure 56 which shows the steady-state 100 percent speed operating characteristic for the tested transonic rotor, in black, superimposed on which is an unsteady characteristic as the compressor is throttled into stall with the injectors turned off, blue line, and while operating in fully developed stall during 1200 rotor revolutions, gray traces, what happens after the injectors are then turned on from a fully developed stalled condition, red line. The recovery from stall, red line, occurred during 90 rotor revolutions after the injectors were activated by opening a fast-acting valve, which pressurized the injector supply torus. Steady discrete tip injection not only recovers from stall, but also restores the compressor to its pre-stall level of pumping.

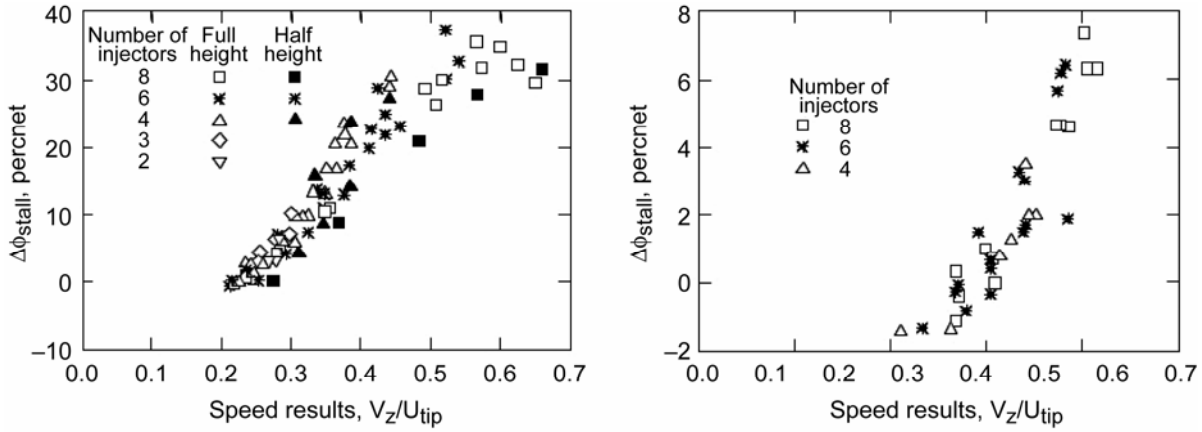

Figure 55.—Stall range increase as a function of mass averaged axial velocity over the injector height (outer 6 percent span) normalized by tip speed for (a) 70 percent and (b) 100 percent rotor speed results (ref. 59).

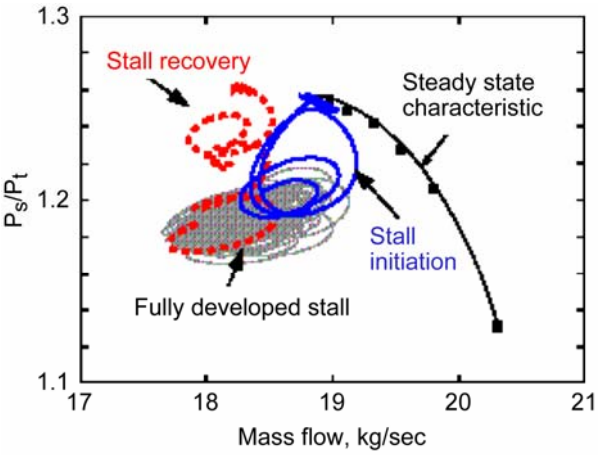

Figure 56.—Unsteady operating characteristic at design speed during stall inception and recovery with tip injection (ref. 59).

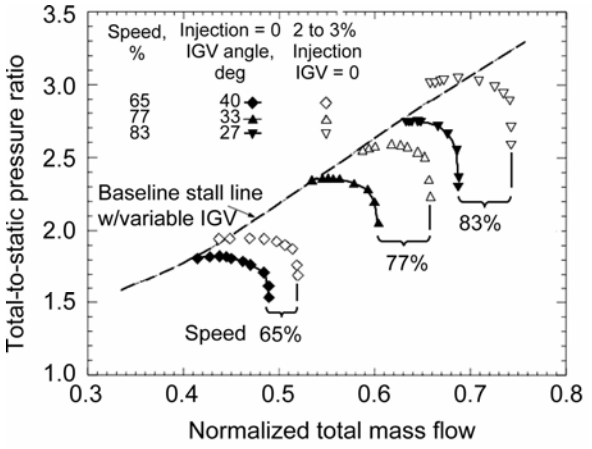

Figure 57.—Part-speed performance of a twostage high-speed fan with nominal IGV schedule without injection, and with IGV fixed at 0° (axial) with injection (ref. 59).

A test of the potential of steady discrete tip injection to be used as an alternative to variable geometry for stabilizing multistage compressor part speed performance is indicated in figure 57. The results are from testes of steady discrete tip injection on a two-stage low-aspect-ratio fan with a design tip speed of 490 m/sec. The two-stage fan included variable IGV and first stage stator for matching at part-speed conditions. Fourteen injectors were located around the circumference between the IGV and first stage rotor. Air was injected from an external source, with the injectors operating at their choke conditions providing a total injected flow of 2 to 3 percent of the annulus flow. With the first stage stator fixed at it's design-speed setting angle the IGV setting angles were set according to speed as the compressor operating characteristics were measured for three constant speed conditions, solid symbols in figure 57. The speed characteristics were remapped with steady air injection turned on, and with the IGV's set to the axial (IGV = 0° setting) direction, open symbols in figure 57. At part speed the compressor stalls when the IGV is opened from it's nominal setting to the axial (IGV = 0° setting) direction with air injection turned off. The results show that air injection enabled the nominal surge line to be met or exceeded without the need for variable geometry. For actual implementation in an engine the injected flow would be supplied from a higher pressure and temperature location within the engine, which would penalize the efficiency. To minimize the efficiency penalty a valve would need to be installed to turn on the injectors only when needed. For optimum stage matching the removal and reinjection of air would have to be properly managed, and account for the injected air, which at higher pressure and temperature would alter the corrected flow conditions into the rotor tip.

Unsteady three-dimenstional full-annulus Navier-Stokes simulations of the transonic compressor stage used for the development of the discrete tip injection stall control technology have been completed both with and without modeling of the discrete tip injectors (refs. 61 to 65). The simulations show evidence of the development of stall precursors leading to stall inception and into fully developed stall as the simulation was throttled into stall (refs. 63 to 65). The simulations with modeled discrete tip injection predicted stall range extension comparable to measured results and clearly show the stabilizing effect of the tip injection (fig. 58). The results are currently being analyzed to better understand the flow mechanisms in the tip clearance region leading to stall inception, and how the tip injection stall control technology mitigates stall inception.

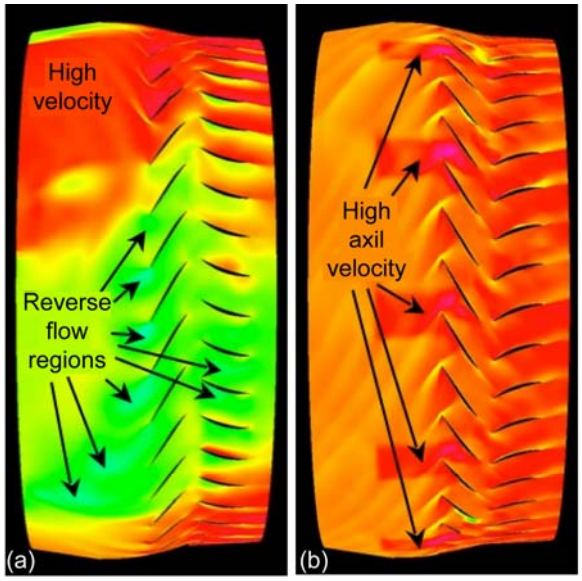

Figure 58.—Unsteady full-annulus simulations predict stall range extension with steady discrete tip injection (refs. 63 to 65). (a) Without tip injection. (b) Stable lower flow rate with tip injection.

Based on the results of these investigations of **steady discrete tip injection** from an externally supplied air source the following **characteristics or conclusions** are summarized:

- Tip injection can be an effective means for enabling stall range extension for tip critical rotors.
  - Tip injection unloads the rotor tip reducing the tip diffusion rate.
  - For the compressor to be throttled to lower flow rates the remainder of the blade span, or blade rows, must be able to accommodate increased blade loading levels.
- Effectiveness of tip injection does not depend on the circumferential arrangement of injectors.
- Effectiveness of tip injection correlates with the mass averaged axial velocity around the annulus over the injector height.
  - Fewer injectors with higher injector exit velocity are more effective than many injectors with lower injector exit velocity.
  - Injector effectiveness is limited by the choke flow of the injectors.
- Tip injectors can be used to recover from a stalled condition.
- Tip injection have potential for enabling multistage matching at part speed conditions.
  - Must account for introduction of injected mass flow at different corrected conditions than where the flow is injected.
- Important to minimize the injected air to reduce the efficiency penalty.
- Injection has the potential to be turned on when needed, or if desired modulated for active control capability.

Further developments of the steady discrete tip injection technology for stall control enhancement will be discussed in a subsequent section.

3.3 Self Recirculating Endwall Treatments

A natural and intended follow on to the development of the steady discrete tip injection stall control technology is to couple the injectors to a high pressure bleed source within the compression system rather than providing injection by an external air source. Recognizing the detrimental impact on performance of bleeding expensive air from within the compression system it is important to minimize the amount of injected air, and to improve on the injectors by developing a non-intrusive injector more suitable for application in real engine compressors with typically close-coupled blade rows. Recirculation of bleed air to supply the injectors brings with it concerns with injector effectiveness and impact of high pressure, high temperature air on stage matching. Where to bleed air is an important consideration. The bleed air has to have sufficient pressure to maximize the injector effectiveness (i.e., choke the injectors) while being accessible given the limited access via the casing endwall, and the limitations of injector circumferential placement to avoid exciting blade harmonics. The previous results have indicated the flexibility of the steady discrete tip injection has potential for managing these concerns.

The idea of endwall recirculation is certainly not new as has been briefly outlined in the historical overview section of these notes. Both casing recirculation, defined herein to be confined to the rotor tip region, and stage recirculation, that can encompass one or multiple stages (fig. 59), have been investigated by Strazisar, et al. (ref. 66) and Hathaway (refs. 67 and 68), and are discussed in the following sections. Some advantages and disadvantages of these two endwall recirculation concepts in terms of design trades are also indicated in figure 59. Some advantages of the stage recirculation concept (fig. 59(a)), are the potential for a higher pressure source to drive the injectors to their maximum effectiveness, and using the stator rather than the casing treatment to remove swirl in a more efficient manner. A disadvantage of stage recirculation is finding an appropriate recirculation path to circumvent the casing hardware, such as stator synch rings, and potential excess injector velocities that would erode efficiency as it mixes with the core stream. The main advantage of the recirculating casing treatment concept is that it can be more easily integrated with the case. It's biggest disadvantages are that the injector supply pressure is limited by the rotor tip pressure rise, and that it must remove the high rotor exit swirl in an efficient compact flow path while also turning the flow 360° in the meridional direction. An additional tradeoff relevant to either concept, but categorized under one due to the manner in which each was developed, is the location of where the air is reinjected. The flow can be injected upstream of the rotor tip thereby reducing the rotor tip incidence, loading, and diffusion as discussed in the previous section, or it can be directly targeted at the rotor tip leakage flow, or other fluid dynamic flow feature, that has been identified as most responsible for generating the endwall blockage, as will be discussed in the following section. The design choices will be dependent on the application and the identified flow mechanism of the instability.

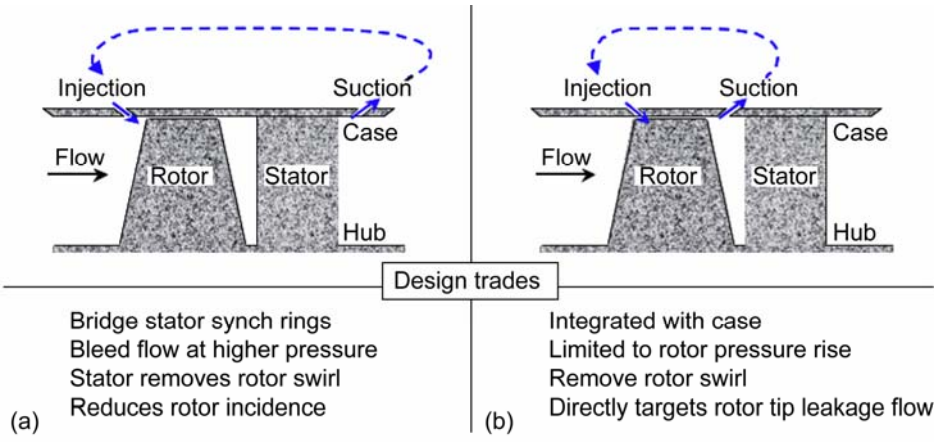

Figure 59.—Comparison of (a) stage recirculation, and (b) recirculating casing treatment.

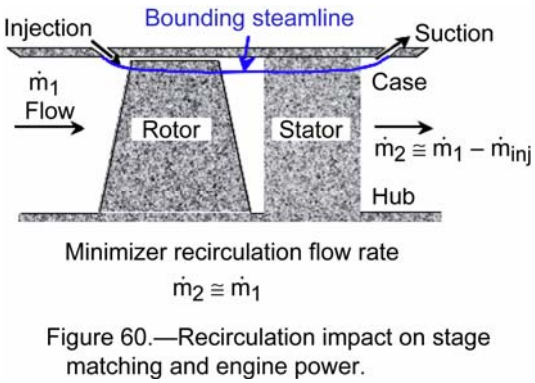

Figure 60.—Recirculation impact on stage matching and engine power.

Another important characteristic of recirculation concepts is that they take flow from a downstream higher-pressure source to be reinjected upstream to a lower pressure region and as such are removing air from the power stream, thereby preventing it from passing through the combustor and turbine where it would otherwise produce power or thrust. It is therefore evermore important to reduce the mass flow rate of the recirculated air as it can adversely impact compressor efficiency and reduce power output (fig. 60). As previously mentioned it also impacts stage matching, both due to removal and reinjection of air from different locations as well as altering the corrected flow conditions in the vicinity of the rotor tip due to injection of air at higher pressure and temperature than usual. The next two sections will discuss the development of both casing recirculation and stage recirculation concepts that were developed somewhat concurrently, but via different paths. Subsequently a discussion of application of steady discrete tip injection, and stage recirculation concepts to multistage turbomachinery and in actual engines will be presented.

3.3.1 Casing recirculation (i.e., over a rotor)

The impetus for the investigation of casing recirculation by the NASA Glenn Research Center and U.S. Army Vehicle Technology Directorate research team was from a suggestion of Prof. Ed Greitzer that state-of-the-art CFD codes could be an effective tool for understanding the effective flow mechanism of stall control technologies. Past computational investigations provided some insight into characteristic flow features of various casing treatments (refs. 31 to 33 and 50), such as flow recirculation into and out of cavities, but little understanding as to their effective flow mechanism for stall range extension. Hall, et al. (refs. 32 and 33) used an advanced CFD code to simulate a number of different casing treatments with steady and unsteady analyses, comparing to experimental data for validation of the predictions. These results were analyzed in detail (ref. 35) to provide an initial basis of understanding from which to guide the subsequent computational investigations of endwall suction and injection by the NASA GRC/Army VTD research team (refs. 67 and 68). However, after considerable analysis of the computational results it was concluded that, due to various inconsistencies, the computational results provided limited understanding (ref. 35). A significant aspect learned from analysis of the computational investigations of Hall, et al. was recognition of the limitations of the employed boundary conditions coupling the endwall treatment to the compressor flow field, and the computational intensive effort of meshing the complex treatment geometries. As such, it was decided early in the computational investigations of endwall suction and injection that *a priori* description of any specific endwall geometry was not essential for understanding the impact of endwall suction or injection on the rotor tip flow field. It was considered sufficient to provide an endwall boundary condition for injecting or bleeding flow from the endwall for purpose of understanding where best to bleed and inject flow for effective management of the endwall flow field features that limit stability of a tip critical compressor.

The computational code selected for the investigations of Hathaway (refs. 67 and 68) was the APNASA code (ref. 69) that had been developed specifically for support of multistage turbomachinery design. The code had been successfully used for understanding and guiding the development of the steady

discrete tip injection stall control technology and included provision for a bleed boundary condition that was deemed suitable for modeling the effects of endwall injection and bleed (suction). The subsequent computationally based parametric investigations of the effects of endwall suction and blowing was guided by understanding of the endwall flow physics. Low momentum flow that was believed to contribute to the instability of the rotor tip flow field (e.g.,) was independently bled off or energized via flow injection. The locations for suction or injection were commensurate with the identified flow feature most responsible for the low momentum flow. The intent of investigating the benefits of independent bleed or injection was to eventually identify the "best" bleed and injection locations for coupling as a recirculating casing treatment. The objective was to improve on the current capability for stall margin improvement with minimal or no efficiency penalty. To understand the flow mechanism of endwall recirculation for the purpose of changing the current historical trend of decreased efficiency with increasing stall range improvement (fig. 10(a)).

The author (refs. 67 and 68) hypothesized that control of endwall blockage producing flow mechanisms via suction and blowing would reduce the accumulation of endwall blockage, and thereby increase the compressor stall range. With the aid of a state-of-the-art CFD code the author simulated the flow field of a moderate speed (258 m/s, 846 ft/s) fan rotor for which the tip clearance was increased by 3Xdesign clearance to assure the fan rotor was tip critical. The low speed fan was used to investigate the benefits of endwall suction and blowing targeted at those flow features identified from the CFD simulations as most responsible for contributing to the endwall blockage. The author considered that if the computational investigations provide sufficient understanding of the flow mechanisms that contribute to the endwall blockage and how best to manage the blockage by suction and injection then such understanding should be equally applicable to any other tip critical rotor in guiding an effective casing recirculation configuration for stall range enhancement. As had been shown by previous investigations compressibility effects were not essential for understanding endwall treatments. Though the presence of a strong shock has a profound impact on the rotor tip blockage development it was not considered germane to "testing" the author's hypothesis. The moderate speed fan with 3Xdesign tip clearance was therefore considered adequate for the intended purpose, and sufficient for guiding a suitable recirculating casing configuration for subsequent application on a low aspect ratio transonic fan rotor to further "test" the author's hypothesis.

Figure 61 illustrates the selected suction and injection locations for the physics guided computationally based parametric investigations. The injection and suction flow rates were varied from 0.1 to 3.5 percent of the predicted choke flow rate of the rotor. The predicted moderate speed fan-rotor performance for various suction and injection locations, compared to the smooth wall case, are provided in figures 62 and 63, respectively. The performance results are based on a control volume analysis that accounts for the injected or bleed flow crossing the rotor casing. The flow range extension indicated in the figures is relative to the baseline flow range from choke to stall and does not include the increased pressure rise capability. As can be readily seen from the predicted results presented in figures 62 and 63, both injection and suction can either help or hurt the rotor performance. Suction of the blockage associate with the leakage vortex always helped performance, providing increased flow range, pressure rise, and efficiency, but decreasing as the suction location was moved downstream of the location of where the leakage first forms. Obviously it is important to remove the blockage as soon as possible as additional performance loss is incurred as the low momentum flow commensurate with the blockage is allowed to mix with the core flow. With the original intent of coupling suction and injection for developing an improved casing recirculation concept it is desirable that injection contribute to the performance as well as the bleed. The results of figure 64 show evidence that injection provides range extension and with an increase in pressure ration and efficiency. It should be remembered though that for these simulations the tip clearance had been tripled from the design clearance, and thus there was considerable blockage generated in the rotor tip.

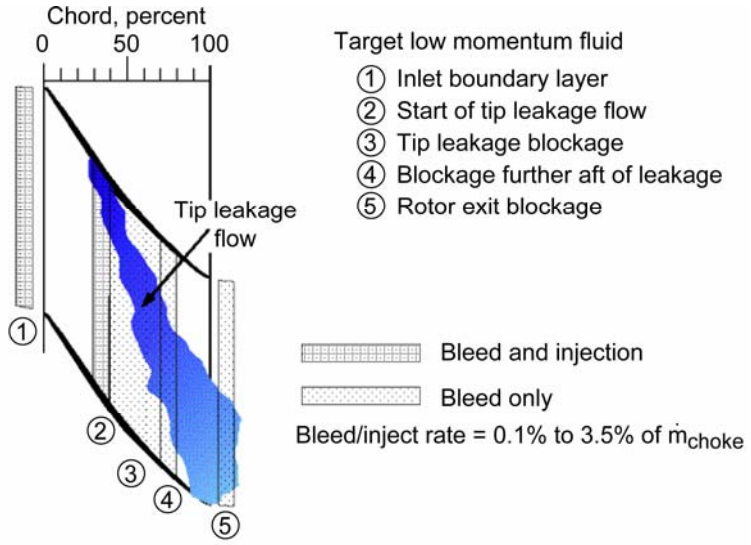

Figure 61.—Illustration of injection and suction sites selected for the computationally based parametric investigations (refs. 67 and 68).

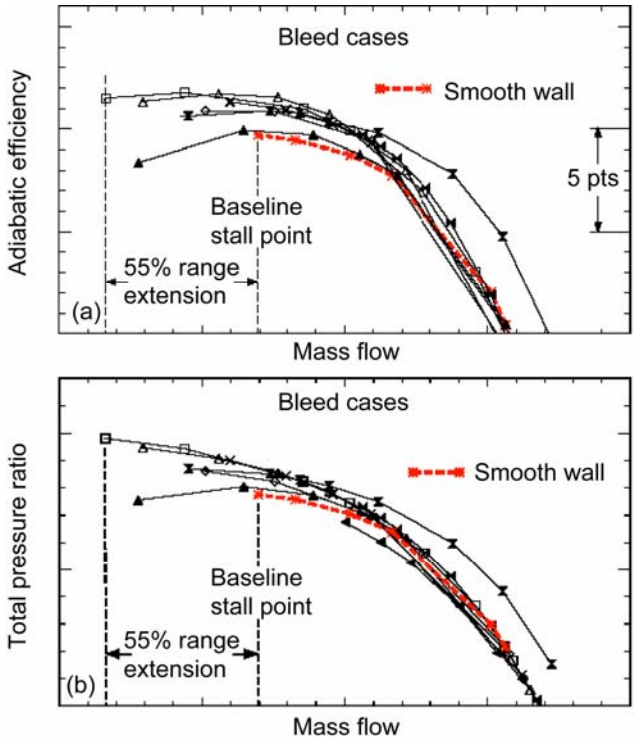

Figure 62.—Predicted performance of bleed (suction) cases (refs. 67 and 68). (a) Adiabatic efficiency. (b) Total pressure ratio.

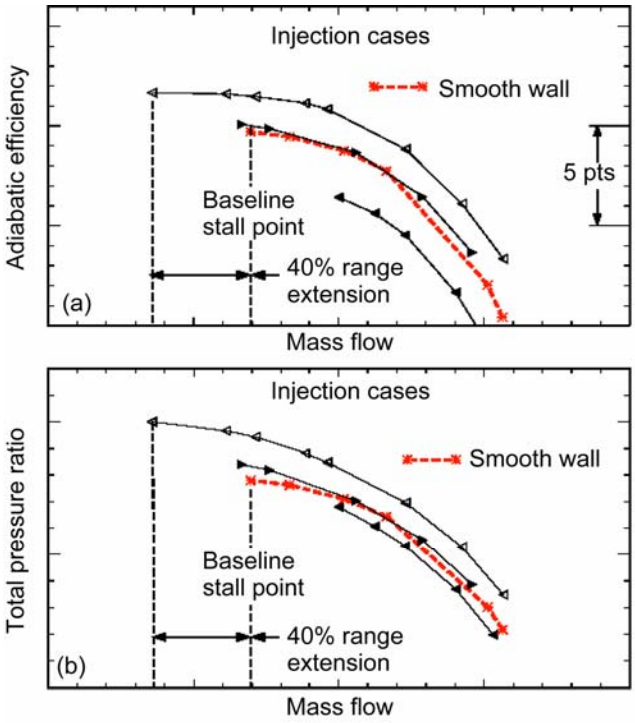

Figure 63.—Predicted performance of injection cases (refs. 67 and 68). (a) Adiabatic efficiency. (b) Total pressure ratio.

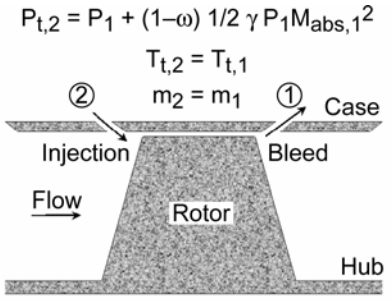

Figure 64.—Self-recirculating casing treatment model (refs. 67 and 68).

Based on the results of the independent parametric studies of casing bleed and injection additional simulations were performed which coupled the best bleed and injection cases to model a self-recirculating casing treatment. The best injection location corresponded to injecting high total pressure fluid at the location of where the tip leakage flow originates. The suction location was selected to be just downstream of the rotor trailing edge with the intent of allowing sufficient distance to recirculate flow to the injection site with the rotor swirl removed while not being so far downstream of the rotor that additional mixing loss would be incurred. The coupled self-recirculating casing treatment model employed in the simulations is illustrated in figure 64. The model requires the injected and bled mass flow rates (m_2 and m_1) to be the same, and the total temperature of the injected fluid ($T_{t,2}$) to be that of the mass averaged total temperature of the fluid bled from the rotor flow field ($T_{t,1}$). The total pressure of the injected fluid ($P_{t,2}$) is derived from the average static pressure of the bled fluid (P_1) plus the mass averaged dynamic pressure of the bled fluid ($1/2gP_1M_{abs,1}^2$) with an assumed loss (ω) in dynamic pressure due to bleed cavity entrance losses and loss incurred within the re-circulated casing treatment flow path.

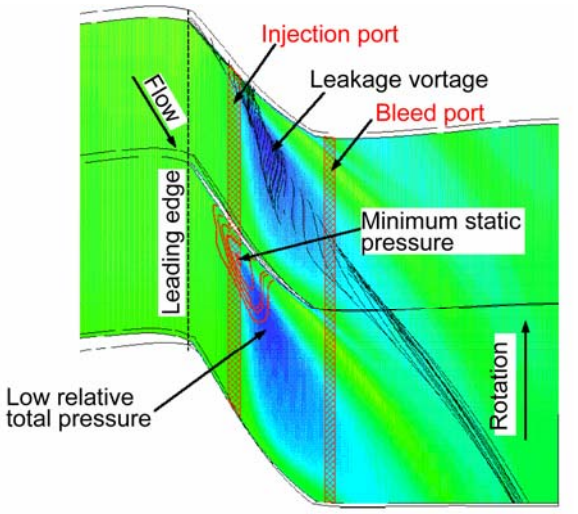

Figure 65.—Relative total pressure surface contours at tip section of low speed fan rotor identifies blockage producing mechanism to control (refs. 67 and 68).

The injected fluid should be directed to lie along the casing endwall to energize the low momentum fluid most responsible for contributing to the blockage in the vicinity of the casing endwall. The injection port should be located just upstream of the region of low momentum fluid (identified by the region of low relative total pressure) to be energized, typically the tip-leakage flow, figure 65. The pitchwise angle of injection should be such that the fluid is aligned with the rotor blade suction surface in the frame of reference relative to the rotor. The mass flow recirculated through the casing treatment should initially be sized commensurate with the mass flow deficit in the rotor blade tip-clearance gap (eq. (3)). The velocity of the injected fluid in the frame of reference of the casing, V_2, will be that dictated by the pressure ratio between the bleed and injection ports and the pressure losses associated with the casing treatment (fig. 64 and eq. (4)). To the extent possible by the available pressure rise across the rotor and the absolute angle of injection, it is desirable to attempt to achieve a relative velocity for the injected fluid commensurate with the free stream velocity away from the influence of the tip clearance flow. With the initially established mass flow rate through the casing treatment, the prescribed injection angles, and the pressure ratio set by the location of the bleed and injection ports the area of the injection port is established (eq. (5)). The bleed port area should be sized to accommodate the injection mass flow rate and to insure that the flow will not choke at the bleed port.

$$m_{2=}\rho_t V_{x,t}\pi\left(r_c^2 - r_t^2\right) - 2\pi\int_{r_t}^{r_c}\rho_2 V_{x,2} r dr \qquad (3)\ \text{(ref. 63)}$$

$$V_2 = \sqrt{\frac{2\gamma R g_c}{\gamma - 1} T_{t,2}\left[1 - \left(P_{2/P_{t,2}}\right)^{(\gamma-1)/\gamma}\right]} \qquad (4)\ \text{(ref. 63)}$$

$$V_{n,2} = V_2 \sin\alpha_2 \qquad (5)\ \text{(ref. 63)}$$

$$a_2 = m_2 / \left(\rho_2 V_{n,2}\right) \qquad (6)\ \text{(ref. 63)}$$

The effectiveness of the modeled self-recirculating casing treatment for the moderate speed rotor is shown in figure 66. Evidence that the stall range improvement was a direct result of targeting the endwall blockage, in this case primarily associated with the tip leakage flow, is shown in figure 67, which lends

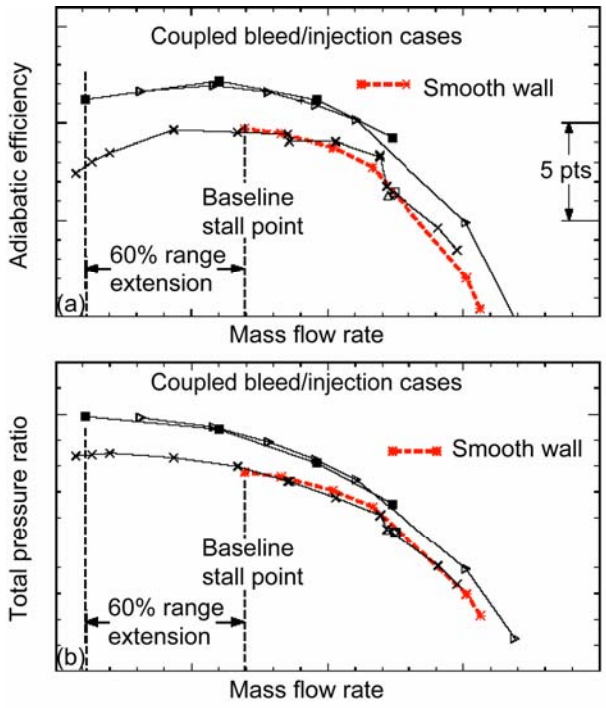

Figure 66.—Coupled bleed/injection cases applied to low speed fan cases, (refs. 67 and 68). (a) Adiabatic efficiency. (b) Total pressure ratio.

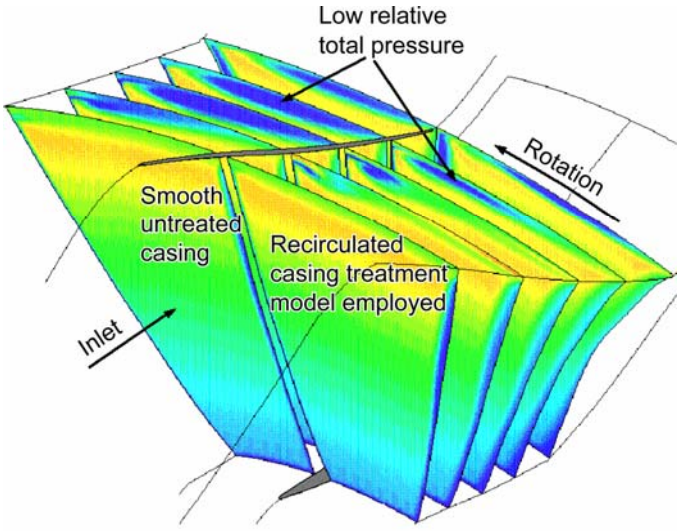

Figure 67.—comparison of relative total pressure contours for smooth and treated casing end walls of low speed fan rotor (refs. 67 and 68).

credence to the author's original hypothesis. The impact of the recirculating casing treatment has improved the efficiency of the rotor in the outer 25 percent of span relative to the smooth wall case, with the efficiency decreasing towards the smooth wall case as the rotor with recirculating casing treatment is throttled towards stall (fig. 68).

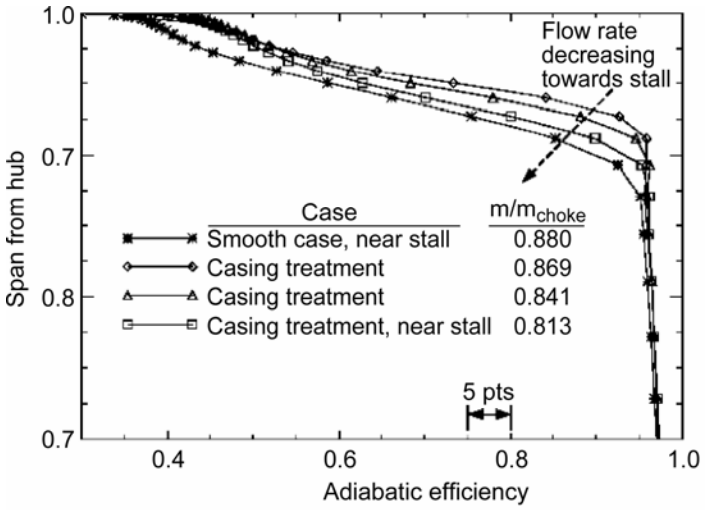

Figure 68.—Spanwise distributions of adiabatic efficiency for the moderate speed rotor with and without recirculating casing treatment (refs. 67 and 68).

The understanding gleaned from the moderate speed rotor simulations was then applied to a low aspect ratio transonic compressor for which the major contributor to the endwall blockage was also due to the leakage flow, but for the transonic rotor, unlike the moderate speed rotor, the leakage flow moved forward towards the leading edge as the transonic fan rotor was throttled towards stall. As a result, the injection site was located just downstream of the rotor leading edge so that it might continue to be effective in energizing the leakage vortex as it moved upstream with rotor throttling. The predicted design speed performance of the low aspect ratio transonic fan rotor with and without modeling of recirculating casing treatment is shown in figures 69 and 70 for clean and distorted inlet flow conditions, respectively. The performance of this low aspect ratio fan rotor with modeled recirculated casing treatment was predicted to provide considerable range increase with increasing pressure rise capability, both with and without inlet distortion, and without a loss in efficiency. The effectiveness of the recirculating casing treatment with inlet distortion suggests its potential usefulness for reducing the design margins typically incurred for tolerance to inlet distortion.

An unsuccessful attempt to experimentally verify the predicted benefits of the recirculating casing treatment concept indicated stall range increase, relative to the baseline smooth wall performance, for the tested 60 to 100 percent speed operating conditions without a reduction in efficiency. However, on disassembly it was discovered that the casing treatment had melted in the vicinity of the rotor tip chord, but not in the casing treatment passages above the casing endwall. For reasons of cost and manufacturing simplicity the casing treatment had been fabricated with a high temperature plastic. Since it was not clear when the melting occurred or if there were appreciable expansion to decrease rotor tip clearance we were unable to confirm the effectiveness of the measured performance. The recirculating casing treatment implemented for this test was an expected improvement from previous tested recirculating casing treatments, some of which had failed due to excess heating from reworking the air as it recirculated through the rotor tip (ref. 70).

All previous casing treatments reported in the literature have always provided essentially continuous full annular coverage around the casing annulus, even if “discretely” implemented. The casing treatment implemented in this investigation followed the lessons learned from the development of the steady discrete tip injection discussed in the previous section and the potential failure due to excess heating from recirculating fluid across the rotor tip. With few injection sites required for stall range improvement (refs. 53 to 59) the author considered that each discrete injection site could be coupled to a discrete suction site, and with proper circumferential placement of the couple injection and suction sites relative to

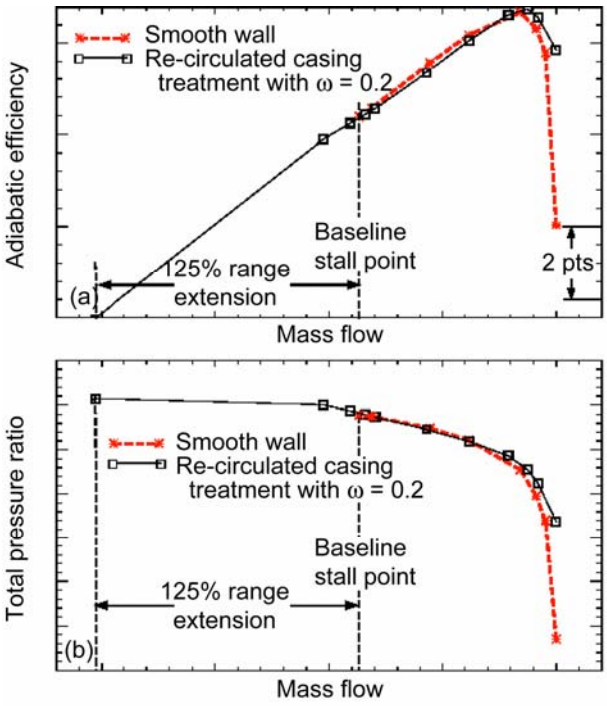

Figure 69.—Re-circulated casing treatment model applied to transonic fan rotor 67 without inlet distortion (refs. 67 and 68). (a) Adiabatic efficiency. (b) Total pressure ratio.

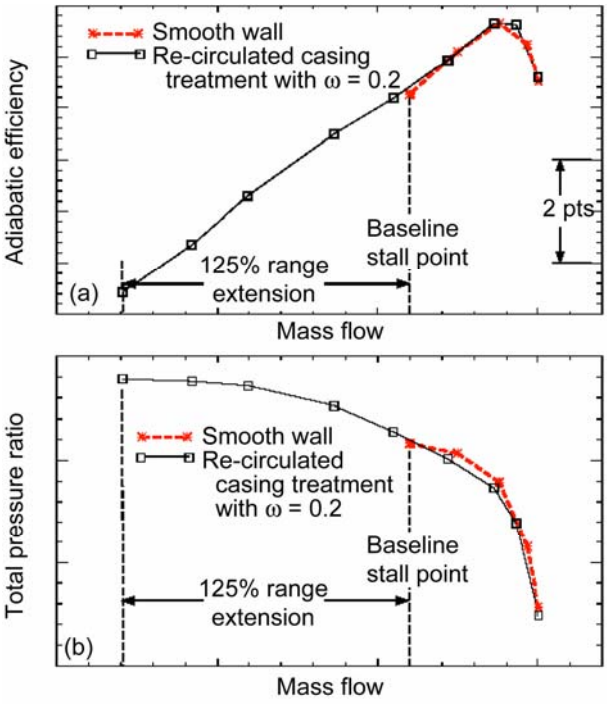

Figure 70.—Re-circulated casing treatment model applied to transonic fan rotor 67 without inlet distortion (refs. 67 and 68). (a) Adiabatic efficiency. (b) Total pressure ratio.

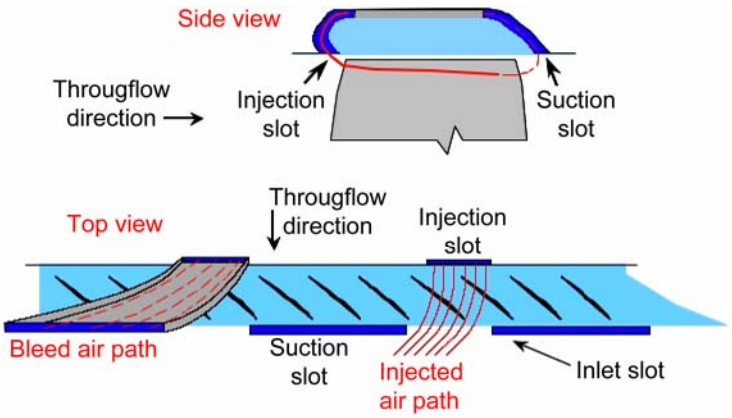

Figure 71.—Single-pass discrete self-recirculating casing treatment concept (ref. 68).

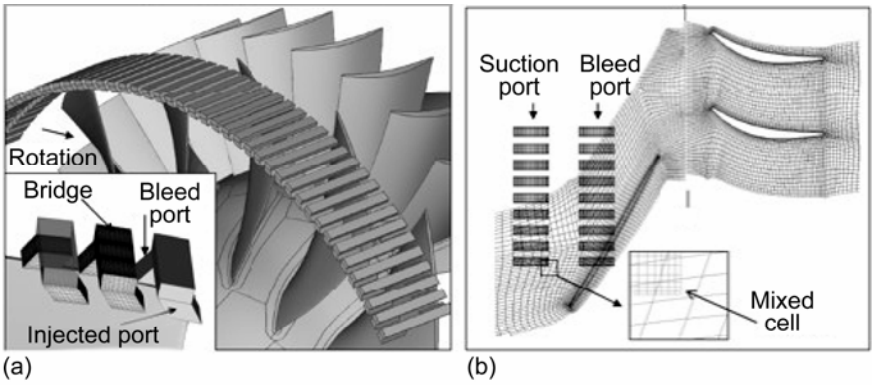

Figure 72.—Self-recirculating casing treatment with forward injection sites (refs. 73 and 74). (a) Configuration of self-recirculating casing treatment. (b) Block structured grid showing location of bleed and injection ports reative to the rotor.

each other and between subsequent coupled injection/suction pairs the injected fluid could be prevented from entering the downstream suction locations (fig. 71). Determination of the expected rotor turning would be sufficient for such guidance. Of course, the high rotor exit swirl would have to be efficiently ingested through each bleed port and guided to the coupled injector port with minimal loss. This is a major challenge of recirculating casing treatment concepts relative to stage recirculation that allow the stator to remove the rotor exit swirl, therefore greatly simplifying the casing treatment flow path design. Due to program constraints the author was unable to provide experimental evidence of the recirculating casing treatment concept, but subsequent tests of a stage recirculation concept to be discussed in the next section clearly show the potential benefits of endwall recirculation, if properly managed.

Other investigators have attempted computational simulations of similar self-recirculating casing treatment concepts (refs. 71 to 75), also predicting range increase, endwall blockage reduction, and with minimal to no efficiency decrements as was presented in this section. The concepts include both recirculation with flow bled from the rotor exit to be reinjected at the origin of the leakage vortex, as proposed for the recirculating casing treatment described in this section (refs. 67 to 68 and 71), as well as bleeding from the site of the leakage vortex and injecting upstream (refs. 72 to 78). Figure 72 shows an example of a recirculating casing treatment which bleeds from the leakage vortex site and recirculates the air foward to inject upstream of the rotor for the purpose of reducing the tip incidence angle (refs. 73 and 74), as was done with the steady discrete tip injection presented in the previous section. The predicted performance with and without the self-recirculated casing treatment is shown in figure 73, which predicts minimal impact on efficiency. Figure 74 shows that the self-recirculating casing treatment of Yang (refs. 73 and 74) has reduced the extent of the low momentum flow associated with the interaction of the

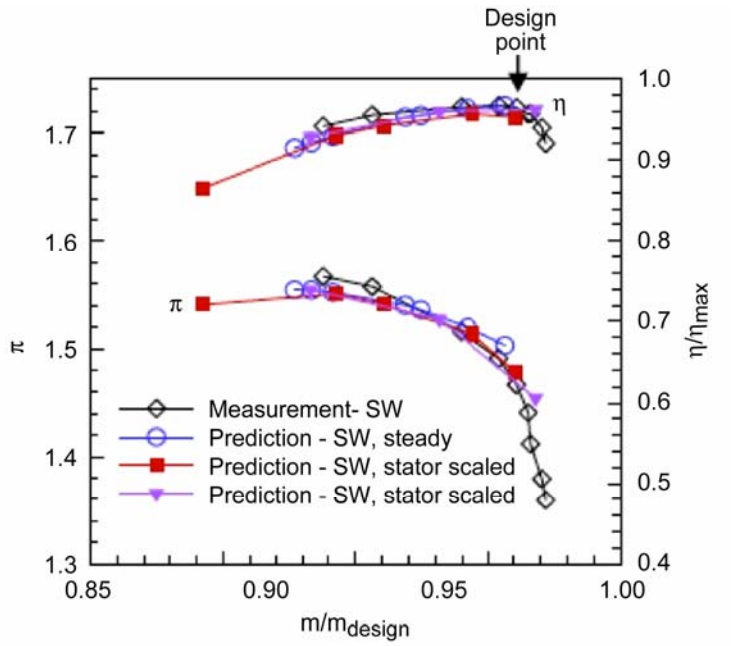

Figure 73.—Predicted pressure ratio, π, and efficiency characteristic, η, at 100 percent design speed with and without the self-recirculating casing treatment concept of Yang (refs. 73 and 74).

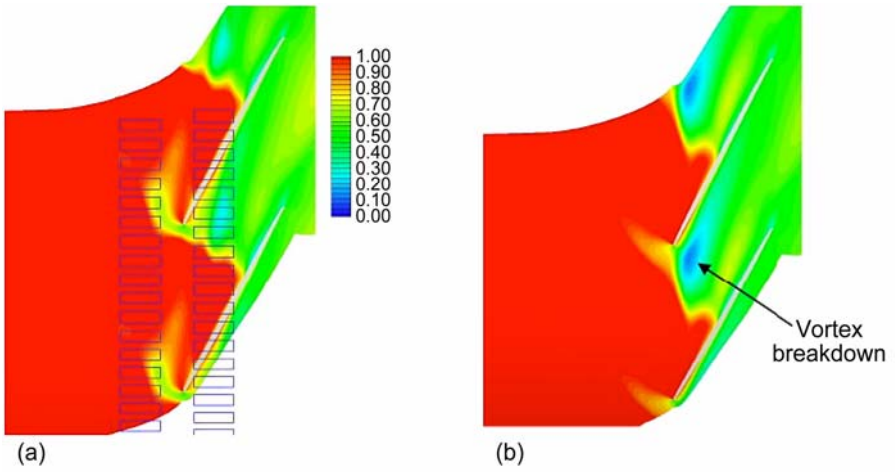

Figure 74.—Time mean relative Mach contours at the rotor tip for the smooth wall near stall point (refs. 73 and 74). (a) With casing treatment. (b) With smooth wall.

leakage vortex with the rotor shock. The next lecture of this series presented by Dr. Kau will provide an extensive presentation of yet another variant of a self-recirculating casing treatment concept proposed by Wilke, et al. (refs. 75 to 78).

Fite (ref. 66) recently reported acoustic and rake based performance tests of a 1.294 pressure ratio, 725 ft/sec tip speed low noise fan with various configurations of vaned passage casing treatment, designed following the philosophy of Koff, et al. (ref. 42). The vaned passage casing treatment was employed as a result of concerns of having inadequate operating range due to the low fan tip speed, especially when operating with inlet flow distortion. The configurations of vaned passage casing treatments tested included different injection and suction locations, either entirely within or outside the rotor tip chord, or with injection inside and bleed from outside the rotor tip chord, or vice versa. In addition, the recirculation flow rates were measured to vary from 0.15 to 3.07 percent of the fan corrected

flow rate. All of the vaned passage casing treatments tested provided stall range improvement. In addition, in some cases there was a slight noise penalty measured and in other cases a noise benefit. However, for all vaned passage casing treatments tested there was a measured reduction in efficiency. The author concluded that it might be possible to design a treatment that provides stall range improvement with a noise reduction benefit, albeit with an efficiency penalty. He also concluded that an optimal design would have to balance the impacts of each of these performance metrics as required for the intended application, but that such optimization was not completed for any of the vaned passage casing treatment designs that were tested.

Based on the results of these computational investigations of endwall suction and blowing as coupled in a **self-recirculating casing treatment** concept the following **characteristics or conclusions** are summarized:

- It's critical to properly manage the amount and location of endwall suction and blowing to provide stall range increase without the usual reduction in efficiency.
  - Suction or blowing can be beneficial or detrimental to performance.
    - Excess or improper injection/bleed can detrimentally impact performance of blade elements outside the region affected by the endwall blockage flow mechanism (typically the leakage vortex) that the treatment is attempting to alleviate.
  - Must know where and how much to bleed and inject.
    - Injection flow rate is approximately commensurate with filling the mass flow deficit in the blade tip clearance gap where the tip leakage vortex originates.
  - Stall range enhancement with minimal efficiency decrement is dependent on proper balance of design parameters.
    - Stall range increases with injector exit velocity magnitude
      - Injector exit velocity must be greater than the velocity of the low momentum fluid (typically the origin of the tip leakage vortex) targeted by the injectors to energize the blockage producing flow mechanism.
    - Efficiency decreases with excess injector exit velocity magnitude.
      - Loss production from mixing of high stream jet with surrounding lower velocity fluid outside the blockage producing flow mechanism targeted by the injected flow.
    - Stall range increases with injector circumferential coverage.
      - Continuous recirculation is detrimental to performance and can result in treatment failure due to excess heating.
    - Optimum injection flow angle
      - High velocity jet along endwall
      - Relative flow angle aligned to the local blade angle at the injection site.
    - Minimize losses associated with recirculating the flow from the bleed site to the injection site.
      - Minimize bleed slot entrance losses.
      - Efficiently reduce and reorient high swirl flow for subsequent injection.
      - Minimize ducting losses.
  - Efficient removal of the high rotor exit swirl in a short axial distance is a major challenge.
  - Excess mass recirculation is detrimental to performance.

    - All casing treatments are loss-producing mechanisms and must therefore eliminate or reduce a larger loss mechanism to prevent reductions in rotor performance.
- Concepts that rely on recirculating high pressure fluid from downstream of a rotor to be reinject upstream or within a rotor will potentially entail greater that one pass through the rotor, and thus increase the recirculated fluid temperature accordingly. The “single pass” single-recirculating casing treatment discussed in this section has a single pass through the treatment, but two passes through the rotor, each of which adds work (i.e., pressure and temperature rise) to the recirculated fluid.
- Recirculated casing treatments can effectively reduce casing endwall blockage.
- Recirculated casing treatments have greater potential benefit in the presence of inlet distortions, which is consistent with past reported casing treatments.
- Recirculating casing treatments have the potential to be self-regulating driven by the changing rotor pressure rise with operating condition.
- Recirculating casing treatment can provide a noise benefit or penalty, which should be considered in the casing treatment design as required for the application.

3.3.2 Stage recirculation

The development of stage recirculation (ref. 67) followed somewhat in tandem with the development of the self-recirculating casing treatment concept proposed by Hathaway (refs. 68 and 69), both of which were advantaged from the prior investigations of steady discrete tip injection. The two different approaches were adopted merely for convenience of the respective research leads to facilitate division of their separate, though related, investigations. Both concepts as well as the discrete tip injection concept capitalized on the various understanding gleaned from each during the course of their development. As previously mentioned in the introduction to section 3.3, stage recirculation considers similar ideas to that discussed in the previous two subsections on discrete tip injection and stage recirculation, but continues the development of non-intrusive injectors for application in the close coupled blade rows of real multistage compressors, by taking advantage of the stator for removal of the high rotor exit swirl which challenges recirculating casing treatment design. Both stage recirculation and casing recirculation have advantages and disadvantages and will likely have unique applications depending on requirements and tradeoffs.

The first important advancement was to develop a compact non-intrusive injector that would be more amendable for application in multistage compressors with typically close-coupled blade rows. Two concepts computationally explored to assess their ability to provide a wall jet along the compressor casing are shown in figure 75(a). The first injector style evaluated featured a slot aligned at a shallow angle relative to the casing meridional contour, as shown in the upper half of figure 75(a). A three-dimensional Navier-Stokes prediction of the injector indicates a small separation just upstream of where the rotor leading edge would be located, followed by a larger region of low momentum fluid occupying about 3 to 5 times the rotor tip clearance. Since the design objective is to increase the axial momentum near the rotor tip the slot injector was deemed not suitable. The second coanda injector design, bottom half of figure 75(a), relied on the coanda effect, wherein the static pressure gradient across the curved streamlines within the injector acts to keep the flow attached to the compressor casing wall. The predictions indicate a wall jet with high axial velocity in the region that would be occupied by the rotor blade tip. The predictions indicate the injector is choked which is required for maximum effectiveness, and that the wall jet thickness is approximately equal to the injector throat height with little mixing taking place in the region that would be occupied by the rotor blade tip. Based on these results a set of prototype coanda injectors was fabricated for testing in the NASA GRC single stage compressor facility. To facilitate comparison with the sheet injectors the prototype coanda injectors, shown installed in a transonic compressor in figure 75(b), were designed with similar circumferential extent and aspect ratio as was used for the sheet injectors. A high aspect ratio, $w/h = 18$, where w is the injector width, and h the injector

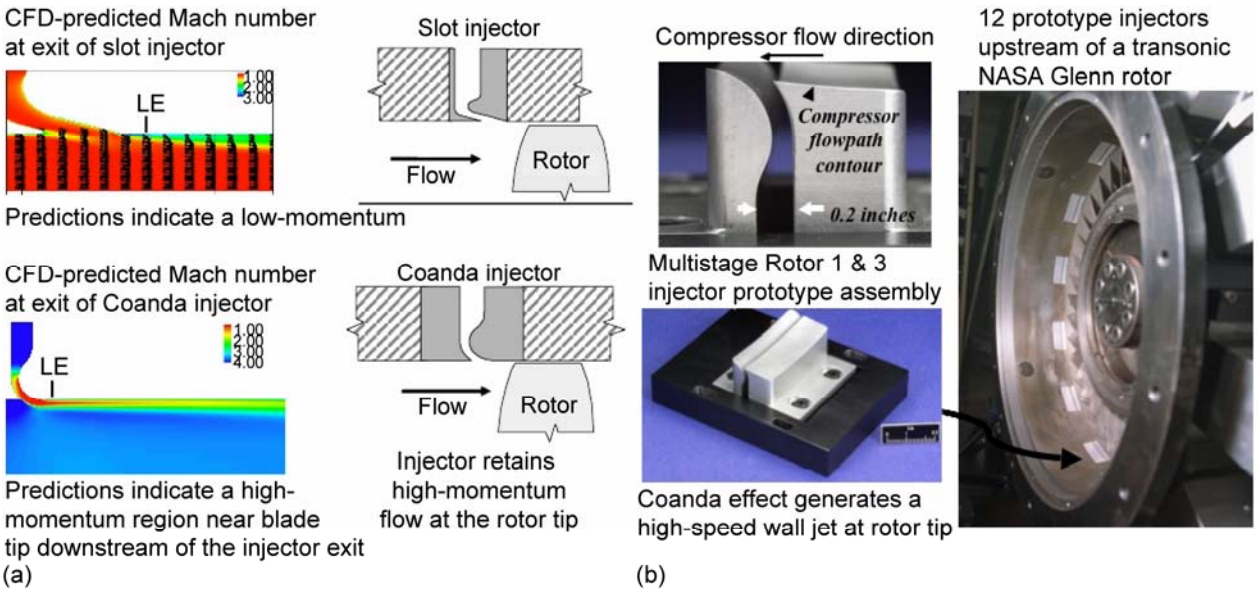

Figure 75.—Coanda injector development and prototype injectors installed in a transonic compressor (ref. 67). (a) CFD prediction of injector effectiveness. (b) Prototype injectors installed in transonic rotor.

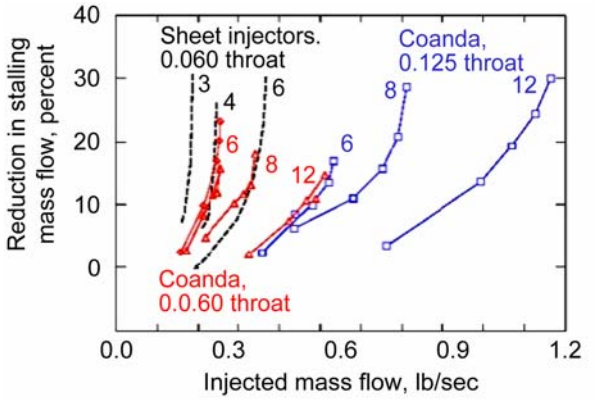

Figure 76.—Measured effectiveness of compact non-intrusive coanda injectors compared to intrusive sheet injectors as tested in a isolated rotor at U_{tip} = 314 m/s (1030 ft/sec) (ref. 67).

height, was used to minimize the tendency for streamwise vorticity generated at the injector edges to lift the injected flow away from the wall. Test results of the effectiveness of the compact non-intrusive coanda injectors compared to the original intrusive sheet injectors in an isolated transonic rotor are shown in figure 76. As with the sheet injectors (ref. 59) the coanda injectors also showed correlation of stall range increase with mass averaged injector exit velocity (ref. 67). Based on these results the coanda design injector was found to be effective and most feasible for multistage compressor application and subsequently adopted for all future testing.

For implementation in an actual engine application the injectors would necessarily be fed from high-pressure fluid bled from aft stages. A test of a “stage recirculation” system was therefore designed for the NASA GRC compressor facility to assess this concept (fig. 77). The system consists of a coanda style bleed slot located downstream of the stator and connected via a “bridge” to a coanda style injector located upstream of the rotor. The upper half of figure 77 shows a meridional view of the bridge flow path and the lower half shows a view looking radially inward at the plane of the rotor and stator blade tips. Since this is expensive air from a thermodynamic point of view it is desirable to achieve maximum stability

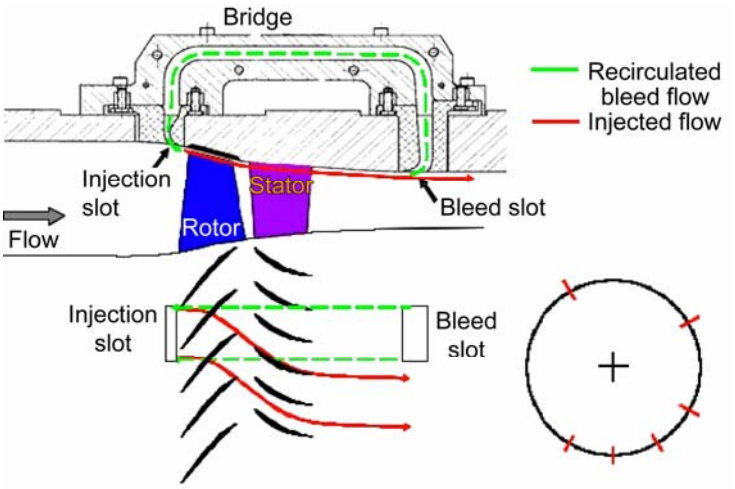

Figure 77.—Scale drawing of the stage recirculation system (ref. 66).

augmentation with minimum flow recirculation and to assess the effectiveness of injectors supplied by air extracted from within the compressor. Maximizing the mass averaged injector exit velocity has been shown to be the important parameter for minimizing the amount of flow recirculation, as well as utilizing the coanda injector design to assure that the recirculated fluid is injected along the compressor casing with high axial momemtum. The bleed slots incorporated the coanda design features with 4 times the slot width, and the bridge channel was set to five times the injector throat. These features coupled with the large radius turns in the bridge channel served to reduce the flow velocity and total pressure loss within the recirculation system.

Based on the results of the previous injector studies (ref. 67), six recirculating bridges were installed on the test compressor using half-height injectors to minimize the amount of recirculated air. Due to existing hardware on the compressor the bridges were not uniformly spaced around the circumference, as shown in figure 77. This limitation was considered acceptable as it is consistent with expected constraints of implementation on actual engines, including reducing aeromechanical excitations of the injectors, and would further demonstrate that uniform spacing is not essential to effectiveness of steady discrete tip injection (refs. 67 and 80) even when fed by an internal air source. A comparison of measured performance of the transonic stage with and without stage recirculation at 70 and 100 percent design speed is shown in figure 78. Early measurements with and without the injectors flowing indicated no measurable difference in compressor performance or stalling mass flow rate.

Measurements indicate the bleed slot recovers about 30 percent of the dynamic head in the annulus flow exiting the stage. The calculated injector flow rates show that the flow through the injectors increases as the rotor pressure-rise increases with the maximum injector flow rate occurring at the stall point. The total flow through the injectors at 70 and 100 percent speed at the lowest pressure rise points shown in figure 78 is 0.3 and 0.6 percent, respectively, of the annulus flow. At the stall point the total injected flow is 0.9 percent of the annulus flow at both operating speeds. With recirculation activated, the change in stalling flow coefficient is 6 and 2 percent for 70 and 100 percent speed, respectively.

To assess the difference in use of ambient temperature air versus recirculated warm air the bridges were removed and the injectors instead fed from a plenum supplied from an external source at the compressor inlet air temperature. The results are presented in figure 79 for 70 and 100 percent design speed. At the design speed stall point this compressor generated enough pressure rise to choke the injectors and the recirculation system was operating at a temperature ratio of $T_{bleed}/T_{inlet} = 1.31$. Since the choke condition is the upper limit set for injector operating pressure, the results of figure 79(b) indicate there is no effect on injector performance over this operating range. For lower speeds where there may be insufficient pressure rise across a single stage to choke the injectors (fig. 79(a)), as might be expected in

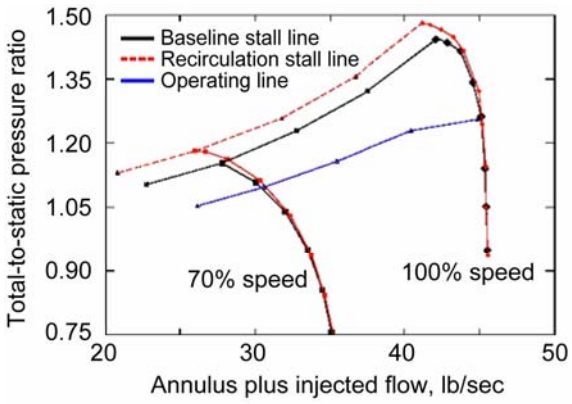

Figure 78.—Measured pressure rise characteristics of a transonic rotor with and without stage recirculation (ref. 66).

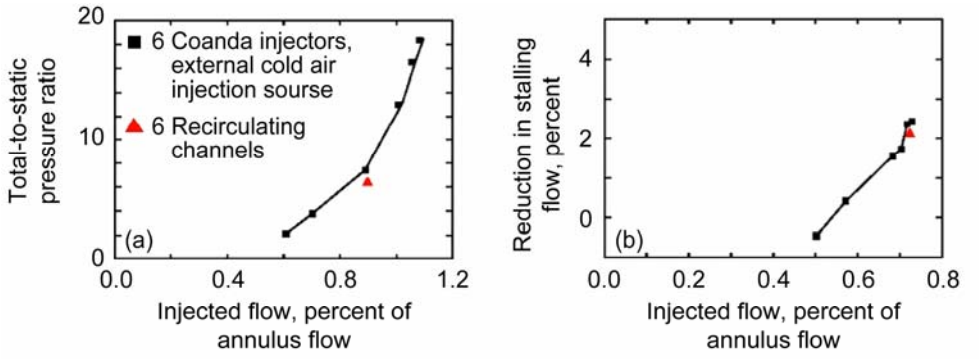

Figure 79.—Measured reduction in stalling mass flow rate for recirculating bridges compared to external air injection (ref. 67). (a) 70 percent speed where injectors are operating below choke condition. (b) 100 percent speed where injectors are operating below choke condition.

the aft stages of a multistage compressor, it may therefore be necessary for maximum injector effectiveness (i.e., choked injectors) to bleed and recirculate air from more than one stage downstream of the injection location. These results indicate that such is possible if recirculating across no more than one to two stages. If the injectors are pressurized beyond their choked condition the jet will expand as it issues from the injector, thus decreasing the injector effectiveness.

A subsequent test of the stage recirculation concept was tested on a transonic low aspect ratio fan stage that included a torque meter to measure the efficiency penalty associated with stage recirculation. The fan stage tested was the same fan stage used for preliminary testing of the casing recirculation concept and included provisions in the recirculating bridges to relocate the injection site from upstream of the rotor leading edge plane to just within the rotor leading edge plane commensurate with that deemed to be most efficient for the self-recirculated casing treatment concept (i.e., to direct the injected flow to target the leakage vortex at its inception point for expected maximum effectiveness with minimal performance penalty). The measured stage pressure rise efficiency characteristics with and without stage recirculation for speeds ranging from 70 to 100 percent speed are shown in figure 80. The measurements indicate significant stall range increase with no measurable loss in efficiency, and in some cases a slight efficiency increase. The maximum amount of total flow injected was 0.3 percent of the compressor mass flow rate.

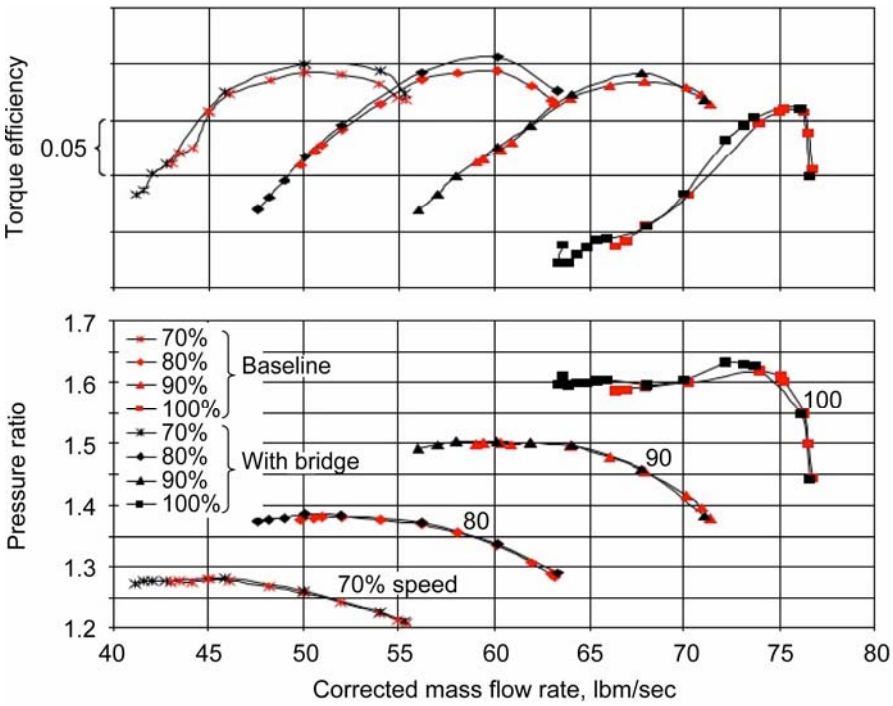

Figure 80.—Measured performance of transonic low aspect ratio fan stage with and without stage recirculation, injecting 0.3 percent of compressor 100 percent speed choke flow rate (ref. 81).

Based on the **stage recirculation** results the following **characteristics or conclusions** are summarized:

- Coanda injectors effectively generate a high momentum jet along the casing.
- The stall range effectiveness of coanda injectors is dependent on the mass average injector exit velocity, as was also found to be true for sheet injectors.
- Coanda injectors are well suited for multistage applications.
  - Non-intrusive
  - Compact footprint
- Recirculation of air bled from within the compressor is as effective as supplying air from an external source.
  - The increased temperature of the injected flow does not adversely affect injector effectiveness, at least for pressure rises sufficient to choke the injectors.
- For maximum effectiveness the injectors should be choked.
  - Can recirculate across multiple stages for part speed conditions where there is insufficient pressure rise across a stage to choke the injectors.
  - Excess supply pressure will over expand the jet, thus reducing the jet effectiveness.
  - Should assure that the injector throat is the choke point of the recirculation system.
- Range increase is independent on the circumferential arrangement recirculation bridges, as was also found for steady discrete tip injectors.
- Stage recirculation has the potential for minimal to no efficiency penalty.

- Must assure that inherent inefficiencies of stall control technology is less than or equal to the loss associated with the endwall fluid that the injected flow is energizing.
- Very little recirculated mass flow is required for effective stall range increase of tip critical rotors, on the order of ~0.3 percent. The additional loss associated with recirculating such a small amount of high loss, low momentum air contributes little to the overall loss of the rotor.
- Work done on endwall fluid by rotor provides sufficient pressure rise to provide high momentum fluid at the upstream injection site, thereby reducing the endwall blockage and increasing the efficiency of the outer blade elements.

- Stage recirculaton has the potential to be self-regulating driven by the changing stage pressure rise with operating condition.

3.3.3 Multistage and engine applications

Several researcher teams have tested steady discrete tip injection or stage recirculating stall control technologies on multistage compressor or engine applications (refs. 67, 80, 82 to 86). Due to the close coupling between blade rows and the typically smaller blade pitches in the aft stages of multistage compressors the injector sizes are necessarily much smaller than for the front stages. The application of the steady discrete tip injection concept to an aggressive high stage loading multistage compressor required coanda design injector plugs for the aft stage that were about 1 cm in diameter to fit within the blade pitch of the upstream stator row such that a jet of high momentum fluid could be injected upstream of the adjacent downstream rotor leading edge plane. Together with the extensive hardware and instrumentation external to the casing there was limited access to the flow path, none-the-less injectors were designed and fitted to an advanced high pressure ratio multistage which included external provisions to match the customer or compressor discharge bleed to the required flow rates for the injectors ahead of rotor 1, 3, and 5, respectively (fig. 81). However, due to injector temperature limitations for injectors in front of stages 1 and 3 the injected air was at ambient conditions for all stages. A separate air injection supply circuit was provided for each set of injectors (with 8, 12, and 12 injectors upstream of rotors 1, 3 and 5, respectively covering 22, 23, and 2 percent of the circumference), and injector flow rates measured

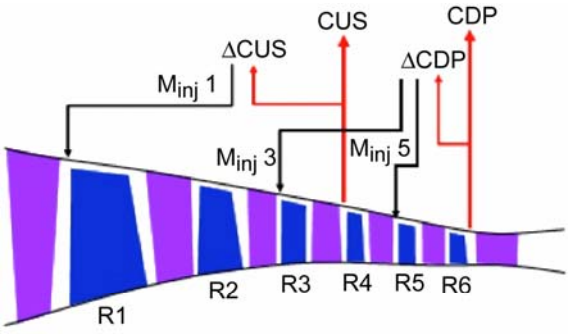

Figure 81.—Schematic representation of simulated recirculation in an advanced multistage compressor. Customer bleed, CUS is incremented by an amount ΔCUS to account for the mass flow M_{inj} 1 injected into R1, and compressor discharge bleed, CDP, is incremented by and amount ΔCDP to account for mass flow M_{inj} 3 + M_{inj} 5 injected into Rotors 3 and 5 (ref. 67).

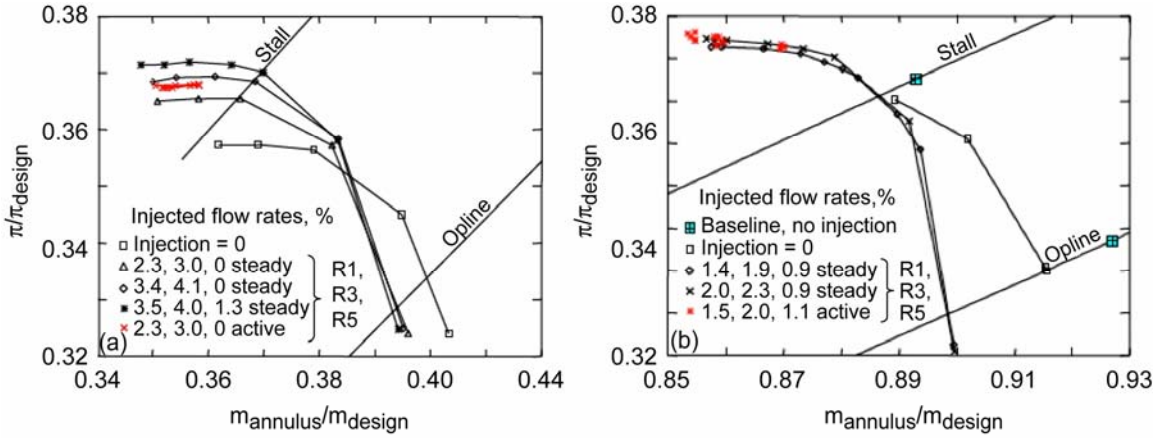

Figure 82.—Measured pressure rise (π/π_{design}) versus flow ($m_{annulus}/m_{design}$) characteristic at 78 and 97 percent design speed in an advanced multistage compressor with and without injection with simulated recirculation (ref. 67). (a) 78 percent design speed. (b) 97 percent design speed.

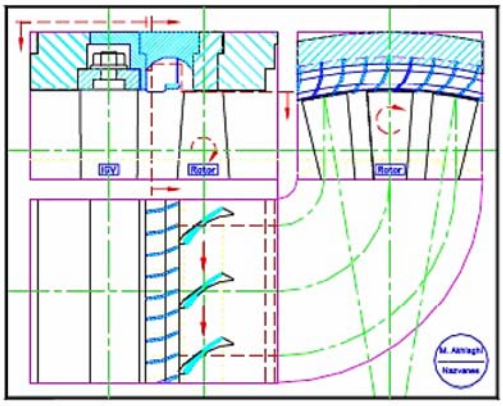

Figure 83.—Vane-recessed tubular-passage casing treatment, 23.2 percent rotor-tip exposure (ref. 73).

to assure proper balancing of the bleed flow rates to simulate recirculation within the compressor. The injectors provided significant stall range extension and increased pressure-rise capability at all speeds (fig. 82). A follow on test of the tip injection stall control technology on a redesigned build of the multistage compressor failed to increase the compressor stall range, perhaps due to limitations on injector locations or greatly improved stage matching thereby precluding the potential for increased stall range without stall control being implemented on all stages.

The multistage compressor was also tested for tolerance to increased design clearance with the tip injection stall control technology. The measurements demonstrated the ability of the tip injection stall control technology to provide greater than the design clearance stall range even with the degraded pressure rise due to the increased rotor tip clearances.

Akhlaghi, et al. (ref. 73) tested various configurations of rotor tip exposure and shape of a vane-recessed tubular-passage stall control technology on a low speed multistage axial compressor (fig. 83), which due to spacing between blade rows had limited access for implementing the stall control technology.

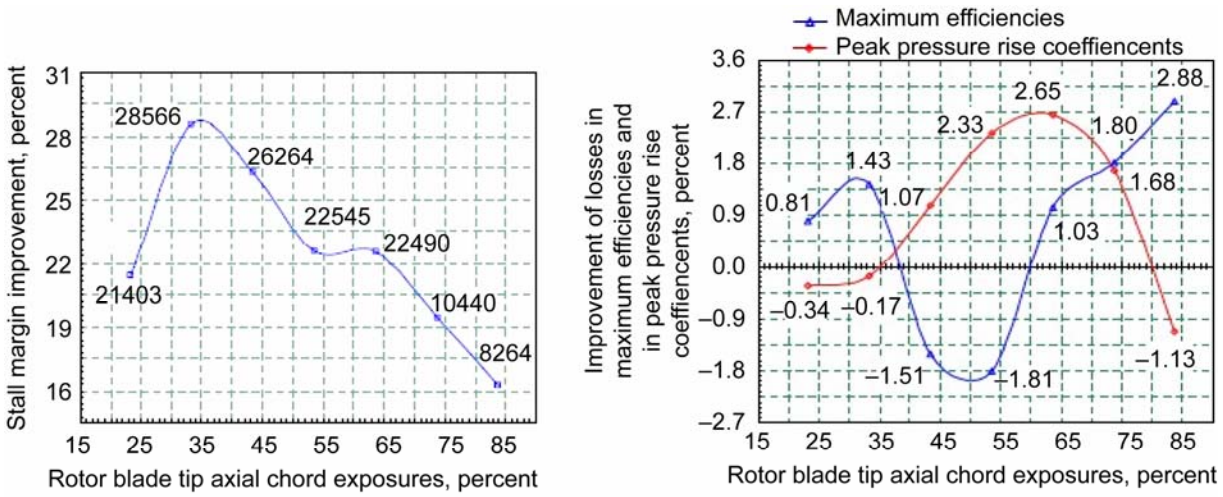

Figure 84.—Relative performance improvements as a function of rotor tip axial chord exposure of vane-recessed tubular-passage stall control technology in a low speed multistage axial compressor (ref. 73). (a) Stall margin improvement. (b) Improvements in maximum efficiency and peak pressure rise coefficient.

Akhlaghi, et al. measured improvements in stall range, peak efficiency, and peak pressure rise capability, dependent on extent of rotor tip exposure to the casing treatment (fig. 84). This stall control technology though showing promise on low speed compressors has yet to be tested on a transonic compressor. As previously discussed in section 2.4 with regard to tests of a similar casing treatment by Kang, et al. (ref. 48), this stall control technology is designed to provide a path for low momentum high swirl fluid from a growing stall cell to be removed from the power stream, and via stationary guide vanes to remove the tangential flow component, the flow is subsequently returned to the compressor flow path upstream of the rotor.

Lienhos, et al. (refs. 82 and 83) and Scheidler and Fottner (ref. 84) have investigated steady discrete tip injection into the first rotor of the LP spool of a twin-spool turbofan engine with and without distortion (ref. 84) using both external air (refs. 82 and 83) and recirculating air bled from the aft stage of the HPC (ref. 84). Scheidler, et al. (ref. 85) also investigated the same stall control technology but with unsteady actuation via a feedback control loop. The injector installation and engine setup with provision for recirculation is shown in figure 85. Also shown in figure 85 is the installation of a delta wing at the LPC inlet to generate swirl. The inlet distortion is generated by distortion screens, which are not shown in the figure. The measured LPC performance with and without externally supplied steady tip injection and with and without inlet distortion is shown in figure 86. The results clearly demonstrate the ability of steady discrete tip injection to provide significant range extension in an actual engine environment, and to almost eliminate the detrimental impact of the inlet distortion. Attempts to provide stall range extension with recirculation of air from the HPC last stage bleed proved unsuccessful due to improper sizing of the injectors for the high pressure, high temperature air. The authors plan to redesign the injectors for a subsequent test with recirculation (ref. 84).

A test of steady discrete tip injection on a production engine using coanda design injectors, with air recirculated from within the compression system, was recently completed by Skoch, et al. (ref. 86). The engine compression system consisted of a multi-stage axial plus centrifugal compressor with discrete tip injection stall control technology on the 1st, 2nd, and 5th stages, and a different form of stall control technology, “control rods,” on the centrifugal compressor (ref. 87). The preliminary results indicate range extension was provided with the recirculation stall control technology during tests with the stators locked in position as the engine was decelerated to lower speeds (i.e., unable to vary setting angle with speed).

Tests of air injection supplied from air within the engine while the compression system was throttled along a constant speed line by in-bleed at the compressor exit showed negligible stall range improvement. However, when the plumbing lines connecting the injectors to a common supply plenum were

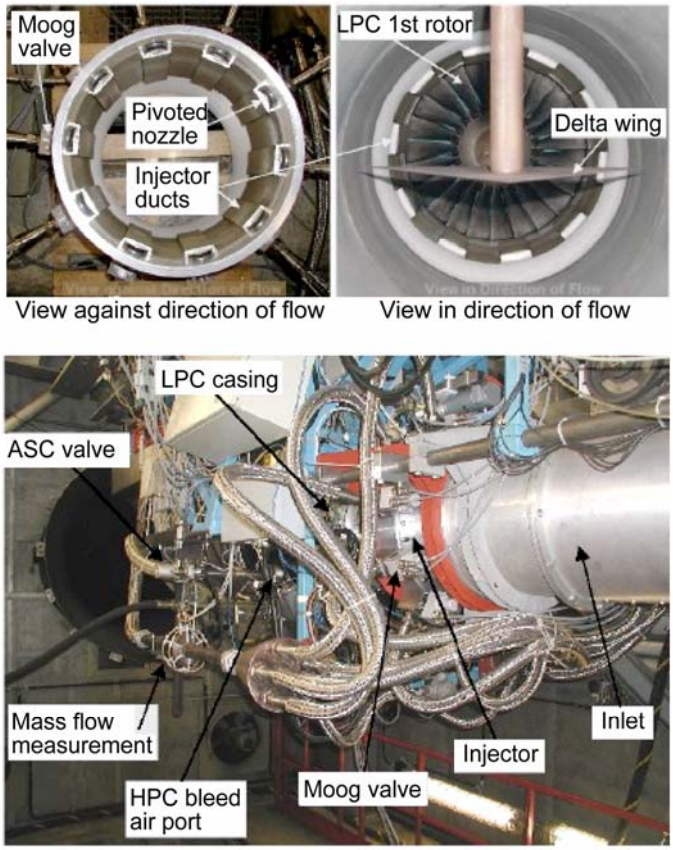

Figure 85.—Discrete tip injection stall control technology implemented on the first stage LPC rotor of a twin-spool turbofan engine (refs. 81 to 84).

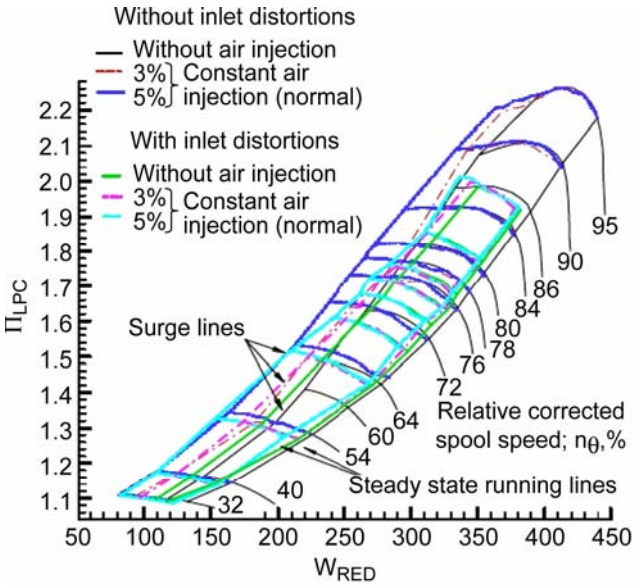

Figure 86.—Comparison of measured performance with and without inlet distortion and with and without externally supplied steady tip injection of 3 and 5 percent of the compressor flow rate (ref. 83).

disconnected and capped off with about 1ft of tubing remaining connected to the injectors the stall range decreased considerably. This indicated that circumferential communication between the injectors connected via a common plenum was perhaps itself stabilizing the compressor, thereby preventing additional stall range extension with air injection. It was also apparent from additional measurements with in-bleed at the exit of the multistage axial compressor to isolate the centrifugal compressor from controlling stall that the centrifugal compressor was the critical component limiting the stall range. With in-bleed at the exit of the multistage compressor and upstream of the centrifugal compressor the multistage compressor stall range increased without tip injection. These tests underscore the importance of clearly understanding where stability is being limited within the compression system and assuring that sufficient range increase is available from the remaining components or stages if the critical stage(s) are improved with stall control technology. A very well matched multistage compressor may not be able to realize stall range improvement with stall control technology unless perhaps incorporated on all stages.

4. Summary

The lecture notes provided herein provide an overview of the development of passive endwall technologies for increasing the stable operating range of compressors. Though fairly complete these lecture notes have not attempted to be inclusive of all reported research, but rather to provide the reader an appreciation of the extensive efforts of numerous investigators to develop technologies that may extend the stall range of fans and compressors. Furthermore, where deemed suitable throughout the lecture notes I've deviated from following the actual historical order of development in order to better communicate the lessons learned by the various investigations. In the remainder of this section I've summarized my perspective as to the important general lessons learned with regard to the development and future application of passive endwall stall control technologies in production engines, and also recommended some future needs for further development. A more complete summary of lessons learned and conclusions with regard to specific passive endwall stall control concepts are provided at the end of each section.

4.1 General Observations and Conclusions

Based on the information gleaned from preparing the material for this overview and personal experience with the development of passive endwall stall control technologies the following general observations and conclusions are provided:

- Stall control technologies have clearly demonstrated the potential for providing significant stall-range increase with minimal or no loss in performance, however fundamental understanding and design guidance are essential. The designer must:
    - Clearly and accurately understand and identify the flow mechanism limiting the compressor stability relative to the applicable operating range desired for stall range extension.
    - Clearly and accurately understand and assess the potential of the remainder of the blade span, rows, stages, or components to tolerate reduced flow rates given the critical stall limiting region of the flow is stabilized.
    - Clearly and accurately understand and predict the design and performance attributes of the intended stall control technology relative to its impact on the compressor performance.
    - Maximize the benefits while minimizing the penalties such that the technology can "buy" it's way onto an engine.
- Inherent in technologies for extending the stable operating range of compressors is the fact that they either generate loss and/or penalize system performance, for example:
    - Loss generation due to energy exchange between low and high momentum flows.

    - "Plumbing" loss generated due to recirculating flow, fore and aft, blade-to-blade, pumping in and out of cavities or slots, etc.
    - Entrance losses associated with flow extraction.
    - Mixing loss within or external to casing treatment.
    - Incidence loss due to improper alignment of injected fluid with relevant blade angle.
    - Performance detriment due to excess control amount, or extent, thus spoiling the performance of previously well performing blade elements.
    - Performance detriment due to adversely impacting stage matching.
    - System performance penalty due to extracting fluid from the power stream or recirculating flow that would otherwise generate power or thrust if allowed to continue through the combustor and turbine.
    - System penalty due to added weight.
    - System penalty from energy expenditure required to "power" stall control mechanism.
- It is essential that stall control technologies are able to "buy" their way onto an engine, by balancing benefit against:
    - Performance penalties
    - Weight
    - Cost
    - Manufacturability
    - Durability
    - Reliability
    - Acoustic impact
    - Aeromechanical impact
    - Complexity and facility of implementation, particularly for multistage application.
    - Availability of reliable design guidance to provide a "guaranteed" benefit.
- State-of-the-art steady and unsteady Navier-Stokes codes coupled with compressor testing using conventional and advanced experimental techniques are invaluable tools that if properly employed can provide valuable insight into the compressor flow physics limiting the compressor stall range and the fundamental fluid mechanism for effectiveness of stall control technologies. Such tools are essential for developing or providing proper design guidance.

4.2 Future Needs

- Improved understanding through computational and experimental investigations of:
    - Fundamental stall inception mechanism.
    - Fluid mechanics of tip clearance flow field.
    - Flow mechanism of casing treatment effectiveness.
- Develop reliable and accurate rules for design guidance.
- Incorporate relevant impact of stall control technology in compressor design system where appropriate:
    - Design velocity diagrams should accurately reflect impact of stall control technology on power stream.
    - Impact of stall control technology should be adequately reflected in blade and endwall design features.
    - Aeromechanical impact must be considered.
    - Assess the system impact of stall control technology.

References

1. Cumpsty, N.A., *Compressor Aerodynamics*, Longman Scientific & Technical, England (co-published in the U.S. with John Wiley and Sons), 1989.
2. Lakshminarayana, B.G., *Fluid Dynamics and Heat Transfer of Turbomachinery*, John Wiley and Sons, 1996.
3. Wilde, G.L., "Improvements in or Relating to Gas Turbines," British Patent (701,576), filed June 28, 1950.
4. Turner, R.C., "Improvements in or Relating to Gas Turbines," British Patent (826,669), filed July 18, 1955.
5. Erwin, J.R., and Emery, James, C., "Effect of Tunnel Configuration and Testing Technique on Cascade Performance," NASA Report 1016, 1951.
6. Nichols, M.R., and Pierpont, P.K., "Preliminary Investigation of a Submerged Air Scoop Utilizing Boundary-Layer Suction to Obtain Increased Pressure Recovery," NACA TN 3437, 1955.
7. Campbell, R.C., "Performance of Supersonic Ramp-Type Side Inlet with Combinations of Fuselage and Inlet Throat Boundary-Layer Removal," NASA E56A17, 1956.
8. Griffin, R.G., Smith, L.H., Jr., "Experimental Evaluation of Outer Case Blowing or Bleeding of a Single Stage Axial Flow Compressor, Part I—Design of Rotor Blowing and Bleeding Configurations," NASA CR–54587, 1966.
9. Koch, C.C., Smith, L.H., Jr., "Experimental Evaluation of Outer Case Blowing or Bleeding of a Single Stage Axial Flow Compressor, Part II—Performance of Plain Casing Insert Configuration with Undistorted Inlet Flow and Boundary Layer Trip," NASA CR–54588, 1968.
10. Koch, C.C., Smith, L.H., Jr., "Experimental Evaluation of Outer Case Blowing or Bleeding of a Single Stage Axial Flow Compressor, Part III—Performance of Blowing Insert Configuration no. 1," NASA CR–54589, 1968.
11. Koch, C.C., Smith, L.H., Jr., "Experimental Evaluation of Outer Case Blowing or Bleeding of a Single Stage Axial Flow Compressor, Part IV—Performance of Plain Bleed Insert Configuration no. 3," NASA CR–54590, 1968.
12. Koch, C.C., Smith, L.H., Jr., "Experimental Evaluation of Outer Case Blowing or Bleeding of a Single Stage Axial Flow Compressor, Part V—Performance of Plain Casing Insert Configuration with Distorted Inlet Flow," NASA CR–54591, 1969.
13. Koch, C.C., Smith, L.H., Jr., "Experimental Evaluation of Outer Case Blowing or Bleeding of a Single Stage Axial Flow Compressor, Part VI—Final Report," NASA CR–54592, 1970.
14. Bailey, E.E., Voit, C.H., "Some Observations of Effects of Porous Casings on Operating Range of a Single Axial-Flow Compressor Rotor," NASA TM X–2120, 1970.
15. Osborn, W.M., Lewis, G.W., Jr., Heidelberg, L.J., "Effect of Several Porous Casing Treatments on Stall Lmit and Overall Performance of an Axial-Flow Compressor Rotor," NASA TN D–6537, Nov. 1971.
16. Moore, R.D., Kovish, G., Blade, R.J., "Effect of Casing Treatment on Overall and Blade-Element Performance of a Compressor Rotor," NASA TN D–6538, Nov. 1971.
17. Tesch, W.A., "Evaluation of Range and Distortion Tolerance for High Mach Number Transonic Fan Stages: Task I Stage Data and Performance Report for Casing Treatment Investigations," NASA CR–72862, Nov. 1971.
18. Bailey, E.E., "Effect of Grooved Casing Treatment on the Flow Range Capability of a Single-Stage Axial-Flow Compressor," NASA TM X–2459, 1972.
19. Mikolajczak, A.A., Pfeffer, A.M., "Methods to Increase Engine Stability and Tolerance to Distortions," Distortion Induced Engine Instabilities, AGARD Lecture Series 72, 1974.
20. Prince, D.C., Wisler, D.D., Hilvers, D.E., "Study of Casing Treatment Stall Margin Improvement Phenomena," NASA CR–134552, March, 1974.
21. Wisler, D.C., Hilvers, D.E., "Stator Hub Treatment Study," NASA CR–134729, December, 1974.

22. Wenzel, L.M., Moss, J.E., Mehalic, C.M., “Effect of Casing Treatment on Performance of a Multistage Compressor,” NASA TM X–3175, January 1975.
23. Fujita, H., Takata, H., “A Study of Configurations of Casing Treatment for Axial Flow Compressors,” Bulletin of JSME, 1984, vol. 27, pp. 1675–1681.
24. Greitzer, E.M., Nikkanen, J.P., Haddad, D.E., Mazzawy, R.S., Joslyn, H.D., “A Fundamental Criterion for the Application of Rotor Casing Treatment,” Transactions of the ASME, Journal of Fluids Engineering, vol. 101, June 1979, pp. 237–243.
25. Takata, H., Tsukuda, Y., “Stall Margin Improvement by Casing Treatment—Its Mechanism and Effectiveness,” ASME Journal of Engineering for Power, Jan. 1977, pp. 121–133.
26. Cheng, P., Prell, M.E., Greitzer, E.M., Tan, C.S., “Effects of Compressor Hub Treatment on Stator Stall and Pressure Rise,” AIAA Journal of Aircraft, vol. 21, pp. 469–475, 1984.
27. Smith, G.D.J., Cumpsty, N.A., “Flow Phenomena in Compressor Casing Treatment,” ASME Journal of Engineering for Gas Turbines and Power, 1984, vol. 106, pp. 532–541.
28. Johnson, M.C., Greitzer, E.M., “Effects of Slotted Hub and Casing Treatments on Compressor Endwall Flow Fields,” ASME Journal of Turbomachinery, vol. 108, pp. 380–387, July 1987.
29. Khalid, S.A., Khalsa, A.S., Waitz, I.A., Greitzer, E.M., Tan, C.S., Cumptsy, N.A. Adamczyk, J.J., Marble, F.E., “Endwall Blockage in Axial Compressors,” SME Paper 98–GT–188, 1998.
30. Lee, N.K.W., Greitzer, E.M., “Effects of Endwall Suction and Blowing on Compressor Stability Enhancement,” ASME Journal of Turbomachinery, vol. 112, pp. 133–144, January 1990.
31. Crook, A.J., Greitzer, E.M., Tan, C.S., Adamczyk, J.J., “Numerical Simulation of Compressor Endwall and Casing Treatment Flow Phenomena,” ASME Journal of Turbomachinery, vol. 115, pp. 501–512, July 1993.
32. Hall, Edward J. Delaney, Robert A., “Aerodynamic analysis of compressor casing treatment with a 3-D Navier-Stokes solver,” AIAA–1994–2796, ASME, SAE, and ASEE, Joint Propulsion Conference and Exhibit, 30th, Indianapolis, IN, June 27–29, 1994.
33. Hall, E.J., Topp, D.A., Heidegger, N.J., Delaney, R.A., “Investigation of Advanced Counterrotation Blade Configuration Concepts for High Spped Turoprop Systems: Task VII—Endwall Treatment Inlet Flow Distortion Analysis Final Report,” NASA Contract NAS3–25270, NASA CR–195468, July, 1995.
34. Azimian, A.R., McKenzie, A.B., Elder, R.L., “A Tip Treatment for Axial Flow Fans and Compressors,” IMechE, April, 1987.
35. Ensenat, S., private communication and memo’s while pursuing Ph.D. research from MIT while at NASA, 1997.
36. Cumptsy, N.A., “Part-Circumference Casing Treatment and the Effect on Compressor Stall,” ASME Gas Turbine and Aeroengine Congress and Exposition, Toronto, Canada, June 4–8, 1989.
37. Robideau, B.A., Njiler, J., “Blade Tip Seal for an Axial Flow Rotary Machine,” U.S. Patent (4,238,170), December, 1980.
38. Wisler, D.C., “Compressor Casing Recess,” U.S. Patent (464,541,417), Feb. 1987.
39. Wisler, D.C., Beacher, B.F., “Improved Compressor Performance Using Recessed Clearance (Trenches),” AIAA Journal of Propulsion, vol. 5, no. 4, pp. 469–475, July-August 1989.
40. Thompson, D.W., King, P.I., Rabe, D.C., “Experimental Investigation of Stepped Tip Gap Effects on the Performance of a Transonic Axial-Flow Compressor Rotor,” ASME Journal of Turbomachinery, vol. 120, pp. 477–483, July 1998.
41. Koff, S.G., Mazzawy, R.S., Nikkanen, J.P., Nolcheff, A., “Case Treatment for Compressor Blades,” U.S. Patent (5,282,718), Feb. 1, 1994.
42. Koff, S.G., Nikkanen, J.P., Massawy, R.S., “Rotor Case Treatment,” U.S. Patent (5,308,225), May 3, 1994.
43. Nolcheff, N.A., “Flow Aligned Plenum Endwall Treatment for Compressor Blades,” U.S. Patent (5,586,859), December 24, 1996.
44. Kahlid, S.J., “Compressor Endwall Treatment,” U.S. Patent (5,520,508), May 28, 1996.
45. Gelmedov, F.S., Lokshtanov, E.A., Olstain, L. E-M., Sidorkin, M.A., “Anti-Stall Tip Treatment

Means," U.S. Patent (5,762,470), June 9, 1998.
46. Janssens, G., Chedozeau, M., "Controle du Decollement Parietal dans les Compresseurs Axiaux par Aspiration ou Soufflage de la Couche Limite," Communication presentee au XVI Colloque d'Aerodynamique Appliquee (AAAF), Lille, November 13–15, 1979.
47. Ivanov, S.K., "Axial Flow Ventilation Fan," British Patent (112,124,303A), 1984.
48. Kang, C.S., McKenzie, A.B., Elder, R.L., "Recessed Casing Treatment Effects on Fan Performance and Flow Field," Proceedings of the ASME Turbo Expo 1995, Houston, Texas, June 5–8, 1995.
49. Wilke, I., Kau, H.-P., "A Numerical Investigation of the Flow Mechanisms in a HPC Front Stage with Axial Slots," ASME Paper No. GT2003–38481, Proceedings of ASME TURBO EXPO 2003, Atlanta, Georgia, June 16–19, 2003.
50. Shabbir, A., Adamczyk, J.J., "Flow Mechanism for Stall Margin Improvement due to Circumferential Casing Grooves on Axial Compressors," ASME Journal of Turbomachinery, vol., 127, pp. 708–717, October, 2005.
51. Prahst, P.S., 1999, Private Communication.
52. Shabbir, A., Zhu, J., Celestina, M.L., "Assessment of Three Turbulence Models in a Compressor Rotor," ASME Paper no. 96–GT–198, 1996.
53. Weigl, H.J., "Active Stabilization of Rotating Stall and Surge in a Transonic Single Stage Axial Compressor," Ph.D. Dissertation, Massachusetts Institute of Technology, Cambridge, Massachusetts, June 1997.
54. Weigl, H.J., Paduano, J.D., Frechette, L.G., Epstein, A.H., Greitzer, E.M., Bright, M.M., and Strazisar, A.J., "Active Stabilization of Rotating Stall and Surge in a Transonic Single Stage Axial Compressor," *ASME Journal of Turbomachinery*, vol. 120, no. 4, pp. 625–636, 1998.
55. Spakovsky, Z.S., "Active Control of Rotating Stall in a Transonic Compressor Stage with Inlet Distortion," M.S. Thesis, Massachusetts Institute of Technology, Cambridge, Massachusetts, February 1999.
56. Spakovszky, Z.S., Weigl, H.J., Paduano, J.J., van Schalkwyk, C.M., Suder, K.L., Bright, M.M., "Rotating Stall Control in a High-Speed Stage with Inlet Distortion: Part I—Radial Distortion," *ASME Journal of Turbomachinery*, vol. 121, pp. 510–516, July 1999.
57. Spakovszky, Z.S., J.J., van Schalkwyk, C.M., Weigl, H.J., Paduano, Suder, K.L., Bright, M.M., "Rotating Stall Control in a High-Speed Stage with Inlet Distortion: Part II—Circumferential Distortion," *ASME Journal of Turbomachinery*, vol. 121, pp. 517–524, July 1999.
58. Hathaway, M.D., Strazisar, A.J., "Impact of Discrete Tip Injection on Stabilization of a Transonic Compressor Rotor," 21st Army Science Conference, Norfolk, Virginia, June 15–17, 1998.
59. Suder, K.L., Hathaway, M.D., Thorp, S.A., Strazisar, A.J., and Bright, M.M., "Compressor Stability Enhancement Using Discrete Tip Injection," *ASME Journal of Turbomachinery*, vol. 123, pp. 14–23, January 2001.
60. Turner, M.G., Saeidi, S., "Average Passage Code Development and Validation," NASA Contract NAS3–26617, Task Order No. 57, December 1997.
61. Hathaway, M.D., Chen, J., Webster, R., "Time Accurate Unsteady Simulations of the Stall Inception Process in the Compression System of a U.S. Army Helicopter Gas Turbine Engine," 2003 DoD High Performance Computing Modernization Program User's Group Conference, Bellevue, WA, June 9–13, 2003.
62. Hathaway, M.D., Chen, J., Webster, R., Herrick, G.P. "Time Accurate Unsteady Simulations of the Stall Inception Process in the Compression System of a U.S. Army Helicopter Gas Turbine Engine," 2004 DoD High Performance Computing Modernization Program User's Group Conference, Williamsburg, VA, June 7–10, 2004.
63. Chen, J., Webster, R., Skoch, G.J., Herrick, G.P., Hathaway, M.D., "Technology for Stabilizing the Compression System of a U.S. Army Helicopter Gas Turbine Engine: Validation of Unsteady Simulations" American Helicopter Society 61st Annual Forum, Grapevine, TX, June 1–3, 2005.
64. Hathaway, M.D., Chen, J., Webster, R., Herrick, G.P. "Time Accurate Unsteady Simulations of the Stall Inception Process in the Compression System of a U.S. Army Helicopter Gas Turbine Engine,

Final Year Progress" 2005 DoD High Performance Computing Modernization Program User's Group Conference, Nashville, TN, June 27–30, 2005.
65. Chen, J.P., Webster, R.S., Hathaway, M.D., Herrick, G.P., Skoch, G.J., "Numerical Simulation of Stall and Stall Control in Axial and Centrifugal Compressors," AIAA–2006–0418, 44th AIAA Aerospace Sciences Meeting and Exhibit, Reno, NV, January 9–12, 2006.
66. Fite, E.B., "Fan Performance from Duct Rake Instrumentation on a 1.294 Pressure Ratio, 725 ft/sec Tip Speed Turbofan Simulator Using Vaned Passage Casing Treatment," NASA/TM—2006-214241, April 2006.
67. Strazisar, A.J., Bright, M.M., Thorp, S., Culley, D.E., Suder, K.L., "Compressor Stall Control Through Endwall Recirculation," ASME Paper No. GT2004–54295, June 2004.
68. Hathaway, M.D., "An Improved Self-Recirculating Casing Treatment Concept for Enhanced Compressor Performance," 22nd Army Science Conference, Baltimore, Maryland, December 11–13, 2000.
69. Hathaway, M.D., "Self-Recirculating Casing Treatment Concept for Enhance Compressor Performance," Proceedings of the ASME Turbo Expo 2002, Amsterdam, The Netherlands, June 3–6, 2002.
70. Adamczyk, J.J., "Model Equation for Simulating Flows in Multistage Turbomachinery," ASME Paper No. 85–GT–226, 1985.
71. Kerney, P. "Recirculating Cavity Casing Treatment Failure, "Wright Laboratories Report WL–TR–94–2092, 1994.
72. Iyenar, V., Sankar, L.N., Niazi, S., "Assessment of the Self-Recirculating Casing Treatment Concept to Axial Compressors," AIAA–2005–0632, 3rd AIAA Aerospace Sciences Meeting and Exhibit, Reno, NV, January 10–13, 2005.
73. Akhlaghi, M., Elder, R.L., Ramsden, K.W., "Effects of a Vane-Recessed Tubular-Passage Passive Stall Control Technique on a Multistage Axial-Flow Compressor," ASME Paper No. GT2003–38301, 48th ASME IGTI Turbo/Expo, Atlanta, Georgia, June 16–19, 2003.
74. Yang, H., "Unsteady Simulation of a Transonic Compressor Coupled with Casing Treatment," 11th Annual Conference of the Computational Fluid Dynamics Society of Canada," CFD2003, Paper no. 75, Vancouver, B.C., Canada, May 28–30, 2003.
75. Yang, H., Neumberger, D., Nicke, E., Weber, A., "Numerical Investigation of Casing Treatment Mechanisms with a Conservative Mixed-Cell Approach," Proceedings of the ASME Turbo Expo 2003, Atlanta, Georgia, June 16–19, 2003.
76. Wilke, I., Kau, H.-P., "A Numerical Investigation of the Influence of Casing Treatments on the Tip Leakage Flow in a HPC Front Stage," ASME GT–2002–30642, 2002.
77. Wilke, I., Kau, H.-P., "Stall Margin Enhancing Flow Mechanisms in a Transonic Compressor Stage with Axial Slots," ISROMAC10–2003–006, 2003.
78. Wilke, I., Kau, H.-P., "A Numerical Investigation of the Flow Mechanisms in a HPC Front Stage with Axial Slots," ASME Journal of Turbomachinery, vol. 126, pp. 339, 2004.
79. Wilke, I., Kau, H.-P., Brignole, G., "Numerically Aided Design of a High-Efficient Casing Treatment for A Transonic Compressor," ASME Paper No. GT2005–68993, ASME Turbo Expo 2005, Reno-Tahoe, NV, June 6–9, 2005.
80. Freeman, C., Wilson, A.G., Day, I.J., Swinbanks, M.A., "Experiments in Active Control of Stall on an Aeroengine Gas Turbine," ASME Journal of Turbomachinery, vol. 120, pp. 393–401, 1998.
81. Prahst, P.S., Strazisar, A.J., Hathaway, M.D., unpublished data, August, 2004.
82. Leinhos, D.C., Scheidler, S.G., Fottner, L, "Active Stabilization of a Low Pressure Compressor in a Turbofan Engine with Constant Air Injection," AIAA–2001–3312, 37th AIAA/ASME/SAE/AESS Joint Propulsion Conference, Salt Lake City, Utah, July 8–11, 2001.
83. Leinhos, D.C., Scheidler, S.G., Fottner, L, Grauer, F., Hermann, J., Mettenleiter, M., Orthmann, A., "Experiments in Active Stall Control of a Twin-Spool Turbofan Engine," ASME GT–2002–30002, Proceedings of the ASME TURBO EXPO 2002, Amsterdam, The Netherlands, June 3–6, 2002.

84. Scheidler, S.G., Fottner, L., “Active Stabilization of the Compression System in a Twin-Spool Turbofan Engine at Inlet Distortions,” ISABE–2003–1083, Proceedings of the XVI International Symposium on Air Breathing Engines (ISABE), Cleveland, OH, August 31–September 5, 2003.
85. Scheidler, S.G., Mundt, C., Mettenleiter M., Hermann, J., Hiller, S.-J., “Active Stability Control of the Compression System in a Twin-Spool Turbofan Engine by Air Injection,” Paper ID No. 073, The 10th International Symposium on Transport Phenomena and Dynamics of Rotating Machinery, Honolulu, Hawaii, March 7–11, 2004.
86. Skoch, G.J., Griffin, T.A, Stevens, M.A., Hathaway, M.D., unpublished data, Sept. 2005.
87. Skoch, G.J., “Experimental Investigation of Centrifugal Compressor Stabilization Techniques,” ASME Journal of Turbomachinery, October 2003, pp. 705–713.

REPORT DOCUMENTATION PAGE	Form Approved OMB No. 0704-0188

1. REPORT DATE *(DD-MM-YYYY)*	2. REPORT TYPE	3. DATES COVERED *(From - To)*
01-07-2007	Technical Memorandum	

4. TITLE AND SUBTITLE
Passive Endwall Treatments for Enhancing Stability

5a. CONTRACT NUMBER

5b. GRANT NUMBER

5c. PROGRAM ELEMENT NUMBER

6. AUTHOR(S)
Hathaway, Michael, D.

5d. PROJECT NUMBER

5e. TASK NUMBER

5f. WORK UNIT NUMBER
WBS 861726.01.03.0420.01

7. PERFORMING ORGANIZATION NAME(S) AND ADDRESS(ES)
National Aeronautics and Space Administration
John H. Glenn Research Center at Lewis Field
Cleveland, Ohio 44135-3191

8. PERFORMING ORGANIZATION REPORT NUMBER
E-15688

9. SPONSORING/MONITORING AGENCY NAME(S) AND ADDRESS(ES)
National Aeronautics and Space Administration
Washington, DC 20546-0001
and
U.S. Army Research Laboratory
Adelphi, Maryland 20783-1145

10. SPONSORING/MONITORS ACRONYM(S)
NASA, ARL

11. SPONSORING/MONITORING REPORT NUMBER
NASA/TM-2007-214409; ARL-TR-3878

12. DISTRIBUTION/AVAILABILITY STATEMENT
Unclassified-Unlimited
Subject Categories: 02 and 07
Available electronically at http://gltrs.grc.nasa.gov
This publication is available from the NASA Center for AeroSpace Information, 301-621-0390

13. SUPPLEMENTARY NOTES

14. ABSTRACT
These lecture notes were presented at the von Karman Institutes lecture series on Advances in Axial Compressor Aerodynamics, May 2006. They provide a fairly extensive overview of what's been learned from numerous investigations of various passive casing endwall technologies that have been proposed for alleviating the stall limiting physics associated with the compressor endwall flow field. The lecture notes are organized to give an appreciation for the inventiveness and understanding of the earliest compressor technologists and to provide a coherent thread of understanding that has arisen out of the early investigations. As such the lecture notes begin with a historical overview of casing treatments from their infancy through the earliest proposed concepts involving blowing, suction and flow recirculation. A summary of “lessons learned” from these early investigations is provided at the end of this section. The lecture notes then provide a somewhat more in-depth overview of recent advancements in the development of passive casing treatments from the late 1990’s through 2006, including advancements in understanding the flow mechanism of circumferential groove casing treatments, and the development of discrete tip injection and self-recirculating casing treatments. At the conclusion of the lecture notes a final summary of “lessons learned” throughout the history of the development of passive casing treatments is provided. Finally, a list of future needs is given. It is hoped that these lecture notes will be a useful reference for future research endeavors to improve our understanding of the fluid physics of passive casing treatments and how they act to enhance compressor stability, and that they will perhaps provide a springboard for future research activities in this area of interest.

15. SUBJECT TERMS
Compressor; Axial stability

16. SECURITY CLASSIFICATION OF:			17. LIMITATION OF ABSTRACT	18. NUMBER OF PAGES	19a. NAME OF RESPONSIBLE PERSON
a. REPORT	b. ABSTRACT	c. THIS PAGE			Michael D. Hathaway
U	U	U		77	19b. TELEPHONE NUMBER *(include area code)* 216-433-6250